NEW IDEAS IN OCEANOLOGY

In two volumes

MOSCOW NAUKA 2004

NEW IDEAS IN CEANOLOGY

Volume 1

Physics
Chemistry
Biology

MOSCOW NAUKA 2004

УДК 551.46
ББК 28.082
Н76

Executive editors:
academician of the RAS
M.E.Vinogradov
correspondent member of the RAS
S.S.Lappo

Referees:

academician of the RAS *M.V.Ivanov*
D.S. *I.I.Volkov*

New **ideas** in **Oceanology** / P.P. Shirshov Institute of Oceanology - Moscow: Nauka. -ISBN 5-02-033069-8
V. 1: Physics. Chemistry. Biology / Ed. by M.E. Vinogradov, S.S. Lappo. - 2004. - 351 p.: il. - ISBN 5-02-033070-1

Elaborated at the end of twentieth century - beginning of twenty first century new approaches in the field of oceanography, marine geology and geochemistry arc considered in this book. Paper for this monograph have been written by leading Russian marine scientists focused their studies on the most important aspects of modern earth sciences. New approaches in the sphere of physical oceanography arc considered in six papers. These arc new studies of the World Ocean governing role in the Earth climate, long-term observation on density stratification in the Ocean, new direction in the fields of hydrooptical and aerocosmic techniques, circulation system simulations (by the example of White Sea). New approaches in the field of marine chemistry are given in two papers. One paper is dedicated to comparative marine hydrochemislry, the other one sup up hydrochemical studies and outlines prospects for XXI century. Four important papers consider new approaches in marine biology.

For occanographcrs, biologists, geographers, teachers and students.

ISBN 5-02-033069-8 (общ.)
ISBN 5-02-033070-1 (Т. 1)

AEROSPACE METHODS IN MODERN OCEANOLOGY

V.G. Bondur

INTRODUCTION

The development of modern oceanology is dependant upon the application of the most recent aerospace methods, technologies, and systems. These possess numerous advantages, the most important of which include the following:

wide area coverage of aerospace sensors, which enhances the capability to conduct regional and global studies of seas and oceans over their entire extent;

real time monitoring of information on various processes and phenomena in the ocean;

capable of working in any areas of seas or oceans difficult to access;

capability to acquire data on processes and phenomena in the ocean with various spatial and temporal resolutions, on practically any scale and over wide areas of the electromagnetic wave spectrum;

high accuracy of received data, especially when combined with traditional methods *in situ* measurements (ship based and buoy sensor systems);

measurement of a wide spectrum of ocean parameters, which contributes to the solution of both scientific and applied oceanological problems;

capability to network aerospace information, as well as retransmit data received from monitoring by airplane, helicopter, ships and buoy stations to customers with various requirements.

Remote aerospace sensing methods for oceans and seas had already proven their effectiveness by the end of the millennium. However, to improve these capabilities, there should be continuous development of new methods, and expansion of the areas in which these methods can be applied.

In recent times, there has been intensive development of methods and tools for remote sensing of the ocean. There has been also parallel development of methods for processing and interpretation of these remote sensing data. In the 21st century, these improved techniques will become critical for the study of oceans and seas.

In recent years, new methods and tools have been developed for remote sensing of the ocean the usage of which will allow significant broadening of the spectrum of data acquired, and allow the study of key ocean processes and phenomena [Alpers et al., 1994; Bondur, 1993; 1995; 2001; Bondur, Grebenuk, 2001; Bondur, Zubkov, 2001; Bondur, Savin, 2000; Bunkin et al., 1987; Viter et al., 1994; *Remote Sensing in meteorology, oceanography, and hydrology*, 1984; *Remote Sensing of the Earth, vol. 1 Gydrometeoizdat* 2000; Koptev, 1994; Melentiev, Bobilev, 2001; Melentiev, Chernook, 2002; *Methods, procedures, and means of computer radiotomography*, Nauchni Mir 1996; Mitnik et al., 2003; Moore, 2003; Raizer, 1994; Savinih, Solomatin, 1995; *Satellite system of communication transmission*, addendum 1, 2001; Shamaev, 1994; Pfeiffer, 2002; Bondur, 1995; Ducet, 2000; *ERS-1, ERS-2*, 1995; MODIS, 2002; NOAA, 1998; *Remote Sensing of environment,* Elsevier, 2002]. Significant success has been achieved in the problems of validation and calibration of remote sensing data. This has increased the reliability of aerospace methods in defining important characteristics of the water environment [see for example Bukin et al., 2003; Burenkov et al., 2000; 2001; 2001; 2002 Kopelevich et al., 2002; Remote sensing, 2002].

Significant success has also been achieved in the development of effective methods for analyzing and interpreting high volume data streams, including large amounts of remote sensing data used for critical modeling of various ocean processes inside the ocean [Belchanski 2000; Bondur, 1991; 1995; 2000; Bondur et al.,1986; 1990; 2003; Bondur, Grebenuk, 2001; Bondur,

Savin, 1995; 2000; Bondur, Starchenkov, 2001; Ibraev, 2001; Kozoderov et al., 1998; 2000; Kopelevich et al., 2002; Marchuk et al., 1984, 1992; Pozdniakov, 2000; Sarkisian, 2003; Sarkisian, Zunderman, 1995].

Application of these new capabilities in the area of remote sensing makes possible the solution of a series of problems related to the study of various fields inside the ocean depths through their manifestations on the surface and in the near-surface layer. It also permits more in-depth studies of various processes and phenomena in the oceans and seas, significantly widening the spheres of practical application, and setting out developmental directions for the future.

Aerospace methods and techniques can be used for the solution of many applied problems. These include global exploitation of resources, protection of the environment and various aspects of national security. These means have already been quite effective for conducting purely scientific studies regarding the physics, chemistry, biology, and geology of oceans [Bondur, 1998; 1995; Bondur, Savin, 1992; 2000; Brehovskih, 1974; Vinogradov, 1971; 1983; 1994; 1998; Gramberg, 2002; Israel, 1984; 2002; Kondratiev, 1992; 2003; Lappo, 1979; in this book; Lisitsin, 1986; 1988; 2001; Matishov, 1992; 1997; 2000; 2001; Matishov, Matishov, 2001; Monin, 1992; 1998; Monin, Krasitski, 1982; *Experience of systematic oceanological research in the arctic*, Nauchni Mir, 2001; Romankevich, Vetrov, 2001; Fedorov, Ginzburg, 1988; Hain, 2001; *Remote Sensing of Environment,* Elsevier, 2002].

Many previously unsolved problems of modern oceanology which can be solved by remote sensing methods, have been described in the fundamental works of Academician A.L. Lisitsin [Lisitsin, 1974; 1978; 1983; 1986; 1988; 1991; 1994; 2001 *Experience of systematic oceanological research in the arctic*, Nauchni Mir, 2001].

Other examples of aerospace techniques are cited in [Avanesova et al., 1984; Arumov et al., 1981; Bondur, 1987; 1991; 1993; 1995; 2001; Bondur, Voliak, 1984; Bondur, Grebenuk, 2001; Bondur, Zubkov, 2001; Bondur, Savin, 2000; Bondur, Sharkov, 1982; 1986; Grankov, 2001; Remote Sensing, 1984; Zidko et al., 1987; Irisov et al., 1987; Kondratiev et al., 2000;1992; 2002; Laverov, Vedeshin, 2002; Lazarev et al., 1993; Mezeris, 1987; Monin, 1992; Monin, Krasitski, 1985; Pokazaev, Filatov, 2002; Filatov, 1991; Atlas, 1986; Bolin, 1996; Merrifield, Holloway, 2002; Viktorov, 1996]. These references discuss the following activities:

study of ocean and littoral sea water dynamics (surface currents, oceanological fronts, turbulence, and circulatory movements of various scales, interactions between internal and surface waves, mechanisms of mass and energy transfer, etc.);

study of various hydrophysical fields in the ocean depths through their effects on the surface and near-surface layers;

study of the interactions between the ocean and the atmosphere, including short term and long term fluctuations in climate;

evaluation of the contribution of the global ocean into the carbon cycle of the Earth;

studies of the bio-productivity of oceans and seas, biodiversity and changes in ecosystems under influence of natural and anthropogenic factors;

monitoring of ocean pollution caused by various sources;

detailed studies of the composition and variability of ocean coastal zones including anthropogenic effects on their ecosystems;

study of ocean upwelling areas;

monitoring of ice conditions;

determination of bottom topography and its variability under the influence of various processes;

study of high and low tide processes and levels of the global ocean on regional and global scales;

monitoring of catastrophic natural processes (tropical cyclones, tsunamis, etc.).

The application of aerospace methods for evaluation of anthropogenic effects on ocean and sea water environments is critically important [Bondur, 1993; 1995; 2001; Bondur, Savin, 2000; Burenkov et al., 2002; Vinogradov, 1998; Israel, 2002; Kondratiev, 1992; Marchuk, Kondratiev, 1992; 2000; 2002; Matishov, 1997; Mor, Bridge, 2003]. At present, the overall volume of polluting substances dumped into the Global Ocean is over 1.2 billion tons [Vladimirov et al., 1991; Dolotov, 1996; Israel, Tsiban, 1989; Neshiba, 1991; Problems, 1985].

This volume is constantly increasing. The coastal zones are subject to the strongest pollution.

The primary sources of anthropogenic effects on the oceans and seas, especially coastal waters are: industrial production and maritime transportation; mining of natural resources and fossil fuels; dumping of industrial and household wastes directly into the ocean or via rivers; inflow from the land of various compounds used in agriculture and forestry; intentional burial in the sea of pollutants, including radioactive compounds; leakage of various compounds during routine maritime operation of sea vessels; accidents involving maritime transportation and military vessels; accidental discharges from ships and underwater pipelines; tourist and recreational activities; transfer of pollutants through the atmosphere, etc [Ibulatov, 2000; Vinogradov, 1998; Vladimirov et al., 1991; Dolotov, 1996; Israel, Tsiban, 1989; Matishov, 1997; 2000; 2001; Matishov, Matishov, 2001; Problems, 1985].

The continuing increase and additive effect of these various pollution sources lead to a progressive eutrophication and microbiological contamination of water, making it substantially more difficult to use for human needs. A substantial concentration of anthropogenic pollutants in the near-surface layer of the ocean leads to a disruption in the ecosystem's balance and a drop in environmental bioproductivity [Vinogradov, 1971; 1983; 1998; Israel, Tsiban, 1989; Matishov, 1997; 2000; 2001; Oceanology, Ocean Biology, Vol. 1 , Nauka 1977].

As a consequence of the increasing threat to our environment, it is important to organize monitoring of the water environment, and create the corresponding systems, including the most recent aerospace platforms. The resolution of this problem is a top priority in Russia and abroad [Bondur, 1993, 1995; 2001; Bondur, Savin, 1992; 2000; Garbuk, Gershenzon, 1997; Remote Sensing, 1984; 2000; Israel, 1984; 2002; Kienko, 1994; Complex Studies, 2002; Kondratiev, 2000; Kondratiev et al., 1992; 1993; Koptev, 1995; Space Methods, 1998; Lazarev et al., 1993; Mishev, 1985; Moiseenko, 1994; Mor, Bridge, 2003; Savin, 1993, 2000; Savinikh, Solomatin, 1995; Atlas et al, 1986; ATSR, 1995; Baldrige et al, 1980; Bondur, 1995; Indian, 1995; Remote Sensing, 2002]

This work describes a perspective on past and current aerospace methods, as well as some results of their application towards the solution of modern oceanological issues.

PHYSICAL BACKGROUND OF OCEAN REMOTE SENSING

The possibilities of using aerospace methods for remote sensing of water bodies are due to both direct and indirect effects of the various processes taking place in the water environment; these are changes in the parameters of physico-chemical and biological fields of the ocean. Some of these are the various hydrodynamic parameters; current velocity and direction; turbidity; temperature; color; dielectric permittivity; salinity; concentrations of primary biogenic elements (nitrogen, oxygen, phosphorous); acidity; concentrations of heavy metals; condition of phytoplankton that cause changes in the characteristics of signals registered by various types of aerospace equipment [Bondur, 1991; 1993; 1995; 2001; Bondur, Grebenuk, 2001; Remote Sensing, 1984; Israel, Tsiban, 1989; Kondratiev et al., 1992; Bondur, 1995; Remote Sensing, 2002].

The observable properties of the water environment that allow remote sensing of various processes and phenomena in the seas and oceans can be divided into the following main types:

1. Changes in the optical characteristics of the water column, which manifest themselves through changes in sea water color, increases or decreases in turbidity due to changes in light

scattering caused by the variability in the concentrations of suspended material with depth, as well as changes in light absorption due to variations in concentrations of organic material [Bondur, 1993; 2001; Remote Sensing, 1984; Ivanov, 1975; Monin, and Krasitski, 1985; Oceanology, 1978; Remote Sensing, 2002].

The most viable method for identifying such phenomena is based on the observation of changes in light scattering by ocean water. Here, it is possible to use passive multispectral and hyperspectral optical methods [Bondur, 1993; 2001; Burenkov et al., 2001; 2001; 2002; Advanced, 1996; Remote Sensing, 2002; MODIS, 2002].

However, it is important to note that in these passive methods the main contribution to the observed radiation comes from near-surface layers, because of the exponential decay with depth in solar light entering through the air sea interface [Ivanov, 1975; Oceanology, 1978]. Therefore, if changes in water properties take place in relatively deep areas, then the changes in light scattering for this area will not have a strong effect on the registered radiation. In this case it is necessary to use active lidar methods.

In using lidar methods for sensing of the water depths, pulsed lasers are the preferred source because of their high pulse power and the ability to gate the pulse return with depth. Application of strobing by depth is also possible, where short-pulsed lasers are used as the illuminating light source [Bondur, Zubkov, 2001; Bunkin et al., 1987; Mezeris, 1987]. Here, the receiver sensitivity is also a major factor, as is the acceptance bandwidth of the filters used [Bunkin et al., 1978; Mezeris, 1978; Lutomirsky, 1994].

2. Changes in hydrodynamic parameters of the water environment due to its transition to turbulent flow, formation of vortexes of various scales, current fields, and due to the perturbation of internal waves in a stratified medium under the influence of many factors (variations in current field flow around the uneven bottom, deep outfalls, fluctuation of atmospheric pressure, etc.) [Basovich et al., 1987; Bondur, 1987; 1991; 1993; 1995; 2000; 2001; Bondur, Savin, 2000; Vedenkov et al., 1999; Dynamics, 1999; Karbishev et al., 2003; Monin, Krasitski, 1985; Ozmidov, 1986; Oceanology, 1978; Fedorov, Ginzburg, 1988].

The turbulence causes changes in the spatial structure of surface waving and the hydro-optical characteristics of the water, which can be found using remote optical and radio-physical methods [Bondur, 1987; 1991; 1993; 1995; 2001; Bondur, Savin, 2000; Ivanov, 1975; Monin, Krasitski, 1985; Oceanology, 1978; Fedorov, Ginzburg, 1988]. These phenomena can be registered using radio-physical or optical methods, and by their appearance on the surface. The presence of internal waves of various origins results in local changes to current speed. Internal wave modulation of the spectra of surface waves, which can be registered using optical (active and passive) as well as radar methods [Basovich et al., 1987; Bondur, 1986; 1987; 1991; 1993; 1995; 2000; 2001; Bondur, Savin, 2000; Dynamics, 1999; Monin, Krasitski, 1985].

The propagating internal waves also lead to periodic deformation of the vertical profile of hydro-optical characteristics [Bondur, 1991; 1993; 2001; Bondur, Grebenuk, 2001; Bondur, Zubkov, 2001; Ivanov, 1975; Monin, Krasitski, 1985; Oceanology, 1978, Fedorov, 1978; Fedorov, Ginzburg, 1988]. If the stratification of these characteristics is clearly enough expressed, then changes in their vertical profiles by depth can potentially be registered using lidars, as well as multispectral and hyperspectral optical equipment [Bondur, 1993; 1995; 2001; Bondur, Zubkov, 2001; Ivanov, 1975; Mezeris, 1987].

Changes in hydrodynamic parameters of the water environment under the influence of various factors can also lead to changes in the characteristics of surface foam patches, which is easily measured using optical (visible and IR), radar and passive (UHF) methods [Bondur, 1991; 1993; 2001; Bondur, Sharkov, 1982, 1986; Irisov et al., 1987; Monin, Krasitski, 1985; m Raizer, Cherni, 1994; Shutko, 1986; Sharkov, 2003].

3. Formation of oil films and changes in the characteristics of surface active substance (SAS) films on the ocean surface due to the surfacing of dissolved organics. Such films and changes in their characteristics can lead to changes in the amplitude-and frequency spectrum of

wind driven wave. These changes can be detected using radar as well as passive and active optical methods [Arumov, Bondur, 1981; Bondur, 1986, 1987, 1991, 1993, 1995; 2000; 2001; Bondur et al., 1988; 1999; Bondur, Voliak, 1984; Remote Sensing, 1984; Ermakov et al., 1982; Mezeris, 1987; Methods, 1996; Shamaev, 1994; Bondur, 1995; Zubkov, Bunkin, 1995].

The appearance of various films on the ocean surface causes changes in its color and observed temperature. These changes are effectively detected by multispectral and hyperspectral sensors, as well as by use of infrared and UHF radiometers [Bondur, 1991; 1993; 2001; Raizer, Cherni 1994; Shutko, 1996; National, 1998; Remote Sensing, 2002; Sharkov, 2003].

Also, increases in concentration of dissolved organics in the near-surface water layers can be registered using lidar-induced fluorescence. [Bondur, 1993; Bondur, Zubkov, 2001; Bunkin et al., 1987; Klishko, Fadeev, 1978; Mezeris, 1987].

4. The next type of indicators pertain to the variations of the temperature field in areas of ocean currents, due to local changes in current fields, upwelling zones, influence of turbulence, internal waves on the surface, among others. Measurement of temperature variation is important for studying heat and mass transfer between the ocean and the atmosphere.

For registration of changes in sea surface temperature under the influence of various factors, it is effective to employ infrared sensors and UHF radiometers, installed on board aerospace platforms [Bondur, 1993; 1995; 2001; Bondur, Savin, 2000; Garbuk, Gershenzon, 1997; Grankov, 2001; Remote Sensing, 1984; 2000; Eremeev, 2003; Irisov et al., 1987; Karbishev, 2003; Kondratiev et al., 1992; Koptev, 1995; Lazarev et al., 1993; Mishev, 1985; Moiseenko, 1994; Raizer, Cherni, 1994; Shutko, 1986; Baldrige et al, 1980; Bondur, 1995; Johnson, Rodvald, 1994; Viktorov, 1996, Sharkov, 2003].

5. Changes in the physico-chemical characteristics of the water environment, which are manifested through variations in the concentrations of dissolved organic compounds, phosphorous and nitrogen, heavy metals, dissolved oxygen, temperature and salinity of sea water, and other parameters. For observation of these characteristics, it is effective to use lidar systems.

The concentration of dissolved organic compounds can be measured by analyzing spectra of combinational (Raman) scattering and fluorescence, stimulated by laser radiation [Bondur, Zubkov, 2001; Bunkin et al., 1987; Klishko, Fadeev, 1978; Mezeris, 1987]. The remaining parameters can be measured using: the laser-spark method, laser correlation spectroscopy method, coherent antistokes light refraction, and other methods [Bondur, 1993; Bondur, Zubkov, 2001; Bunkin et al., 1987; Vasilkov et al., 1990; Klishko, Fadeev, 1978; Mezeris, 1987].

6. Indirect indicators, such as changes in the status of phytoplankton living in the water environment. Like any biological system, phytoplankton are quite sensitive to changes in ambient conditions, such as anthropogenic effects [Vinogradov, 1983; 1998; Vladimirov et al., 1991; Remote Sensing, 1984; Dolotov, 1996; Israel, Tsiban, 1989; Neshiba, 1991; Problems, 1985; Oceanology, 1977].Changes in the condition of phytoplankton cause changes in the spectral characteristics and fluorescence signals associated with their presence, which can be detected by remote methods [Bondur, 1993, 2001; Bondur, Zubkov, 2001; Bondur, Savin, 2000; Bunkin et al., 1987; Remote Sensing, 1984; Klishko, Fadeev, 1978; Mezeris, 1987; Bondur, 1995].

7. Changes in ocean levels caused by surface geostrophic currents, large scale and mid-scale circulation movements, meteorological changes, tide movements, underwater earthquakes, etc.

For these measurements, we use altimetry equipment functioning in the radio range (radio altimeters) and in the optical range of the electromagnetic spectrum (laser altimeters) [Ginzburg et al., 2003; Ivanov, 2003; Melentiev, Bobilev, 2001; Korotaev et al., 2002; Atlas, 1986; Crawford, 2000; Ducet, Le Traon, 2000; Gairola, 2001; Iudicone, 1998; Merrifield, Holloway, 2002; National, 1998].

It should be noted, that with the wide spectrum and diversity of water environment parameters, registration through remote sensing of water bodies does not alone allow a complete

resolution of the issues being analyzed. It is critical to expand the set of measurement tools through combination of remote and contact methods, complimenting each other.

SOME EXAMPLES OF TRADITIONAL OCEAN REMOTE SENSING METHODS

At this time, many methods of remote aerospace sensing of the ocean have been developed and successfully applied, the most important of which are:

- photography onto black and white, spectrazonal, and color film; multi-zonal photography [Bondur, 1993; Garbuk, Gershenzon, 1997; Remote Sensing, 1984; Kienko, 1994; Kondratiev et al., 1992; Koptev, 1995; Lazarev et al., 1993; Moiseenko, 1994; Bondur, 1995; Johnson, Rodvald, 1994; Viktorov, 1996];
- optical-electronic multispectral scanning imaging [Bondur, 1993; Garbuk, Gershenzon, 1997; Remote Sensing, 1984; 2000; Kondratiev et al., 1992; 2003; Koptev, 1995; Lazarev et al., 1993; Melentiev, Bobilev, 2001; Mishev, 1985; Moiseenko, 1994; Savinых, Solomatin, 1995; Bondur, 1995; Johnson, Rodvald, 1994; Baldrige et al, 1980; Indian, 1995; MODIS, 2002; National, 1998; Remote Sensing, 2002; Viktorov, 1996];
- spectrometry [Bondur, 1993; Lazarev et al., 1993; Garbuk, Gershenzon, 1997; Moiseenko, 1994; Mishev, 1985; Beliaev et al., 1978; Bondur, 1995; Johnson, Rodvald, 1994];
- radar imaging [Alperis et al., 1994; Bondur, 1993; 1995; Bondur, Savin, 2000; Bulatov et al., 2003; Viter et al., 1994; Garbuk, Gershenzon, 1997; Remote Sensing, 1984; Zidko et al., 1987; Zagorodnikov, 1978; Kondratiev et al., 1992; 2003; Koptev, 1995; Kudriavtsev et al., 2003; Lazarev et al., 1993; Mitnik et al., 2003; Moiseenko, 1994; Radiolocation, 1990; ATSR-2, 1995; Bondur, 1995; ERS-1, 1995; Johnson, Rodvald, 1994; The special issue, 1982; 1983];
- thermal imaging in the infrared range [Bondur, 1993; 1995; 2001; Garbuk, Gershenzon, 1997; Remote Sensing, 2000; Kondratiev et al., 1992; Koptev, 1995; Lazarev et al., 1993; Melentiev, Bobilev, 2001; Moiseenko, 1994; Savinih, Solomatin, 1995; Atlas et al., 1986, Baldrige et al., 1980; Bondur, 1995; Johnson, Rodvald, 1994; Viktorov, 1996];
- UHF-radiometry [Grankov, 2001; Remote Sensing, 2000; Irisov et al., 1987; Kondratiev et al., 1992; Koptev, 1995; Raizer, Cherni, 1994; Shutko, 1986];
- laser sensing [Bondur, 1993; Bondur, Zubkov, 2001; Bunkin et al., 1987; Eremeev, 2003; Klishko, Fadeev, 1978; Mezeris, 1987; Bondur, 1995; Keeler, Ulich, 1997; Lutomirski, 1994];
- laser and radio altimetry [Garbuk, Gershenzon, 1997; Kondratiev et al., 1992; 2003; Lazarev et al., 1993; Atlas, 1996; Bondur, 1995; Ducet, Le Traon, 2000; Gairola, 2001; Johnson, Rodvald, 1994] and others.

For example, satellite measurements of color characteristics have allowed a deeper understanding of regional and global ocean processes, including the study of phytoplankton distributions and estimation of ocean bio-productivity [Vinogradov, 1998; Remote Sensing, 1984; 2000; Space Methods, 1998; Atlas et al., 1986, Baldrige at al., 1980].

Fig. 1a shows, as an example, a global distribution of initial productivity in the oceans, formed through composition of data received from the MODIS radiometer onboard the TERRA spacecraft, between May 9 and June 9, 2001 [MODIS, 2002].

Initial productivity is defining in the formation of the planet's carbon cycle. The ocean's carbon cycle is determined by variations in intensity of carbon dioxide absorption, due to photosynthesis of marine vegetation and intensity of carbon dioxide secretion through respiration. The analysis of the global distribution of initial ocean productivity shows that it, and therefore the carbon dioxide budget of the ocean, has a tendency to increase in southern and northern latitudes and in areas of continental shelf where nutrients rise to shallow depths [Vinogradov, 1998; Kondratiev, Krapivin, 2003; Romankevich, Vetrov, 2001; Remote Sensing, 2002; MODIS, 2002].

Fig. 1b shows a global map of chlorophyll concentration distribution, which is an indicator of phytoplankton, based on data from the MODIS radiometer of the TERRA satellite, received in

May 2001. The yellow-green colors on this image correspond to high chlorophyll concentrations (visible in near-polar and equatorial regions, and along coastlines), while the purple and dark blue colors correspond to low phytoplankton concentrations (tropical and subtropical latitudes).

Fig. 2 shows the global distribution of chlorophyll concentration, received from the SeaWiFS (Sea-viewing Wide Field-of-view Sensor) device on the Sea Star satellite, between September 1997 and August 1998 for various ocean areas in orthogonal (a-e) and numeric (f) projections [Bidigare, Trees, 2000].

Thermal infrared and microwave imaging allows study of ocean surface temperature on regional and global scales, which is extremely important in the investigation of many factors affecting, for example, global climate change [Anthropogenic Changes, 1987; Golitsin, 1986; Remote Sensing, 1984; 2000; Climate Change, 2002; Kondratiev, 1992; 2000; Space Methods, 1998; Marchuk, Kondratiev, 1992; Monin, 1992; Bolin, 1996]. Fig. 1c shows, as an example, a global distribution of ocean temperature, received from the MODIS radiometer of the TERRA satellite in May 2001. The red-brown colors identify higher temperatures, while blue and dark blue identify lower temperatures.

Space data is very important for receiving information about processes and phenomena on a regional scale. Therefore, studies of temperature are critical for defining the intensity of heat, humidity, and gas exchange between the ocean and the atmosphere, and the intensity of evaporation, dissolution of carbon dioxide in water, etc [Remote Sensing, 2000; Kondratiev, 2000].

Fig. 3 shows, as examples, distributions of temperature for the sea surface in the western north Atlantic near the east coast of the US. There distributions are built using data from the MODIS radiometer of the TERRA satellite, May 8, 2000 and using data from the AVHRR radiometer (NOAA satellite, 1995). The presented images clearly show the temperature distributions around the gulf-stream ocean current, moving hot water from the tropics into the northern latitudes.

Fig. 4 shows, as examples, images of the Black Sea received in June 2000 using the color scanner SeaWiFS in various spectral ranges (a-c) and a color image synthesized using them (d). The same image shows the distributions of chlorophyll concentration (e), as well as indicators of back scattering by suspended material (f), and indication of absorption by a yellow compound g (*gelbstoff)*. These results were confirmed by comparison with sea truth *in situ* measurements [Burenkov, Kopelevich et al., 2000; 2002; Kopelevich et al., 2002; Bidigare, Trees, 2000].

Information about the height of the ocean surface can be used to determine current velocity and direction distribution, dynamics of cyclonic movements, tide processes, tsunami waves, and other such hydrodynamic phenomena. [Garbuk, Gershenzon, 1997; Ginzburg et al., 2003; Ivanov, 2003; Lazarev et al., 1993; Johnson, Rodvald, 1994; Merrifield, Holloway, 2002]. This is shown in Fig. 5. TOPEX/POSEIDON satellite in 1997 [National, 1998]. In the equatorial portion of the Pacific Ocean, the El Niño phenomenon is clearly visible.

Spectra-zonal imaging allows estimation of the water environment's ecological condition. Figs. 7a,b show, as examples, synthesized fragments of spectra-zonal images received from the KFA-1000 device onboard the satellite "RESOURCE-F1" [Bondur, 1993; 1995]. The image shown in Fig. 7a clearly shows the eutrophication of the coastal zone of the Black Sea in the area around the Dnestr River delta.

The image of the Black Sea Crimea Coast from 1993 (Fig. 7b) clearly shows the pollution of the coastal zone by suspended particles of sand and clay, caused by the Bilbek River outflow [Bondur, 1993; 1995].

One of the most effective aerospace methods for studying the ocean is radar sensing. The main advantage of this method is its all-weather capability and round-the clock operability.

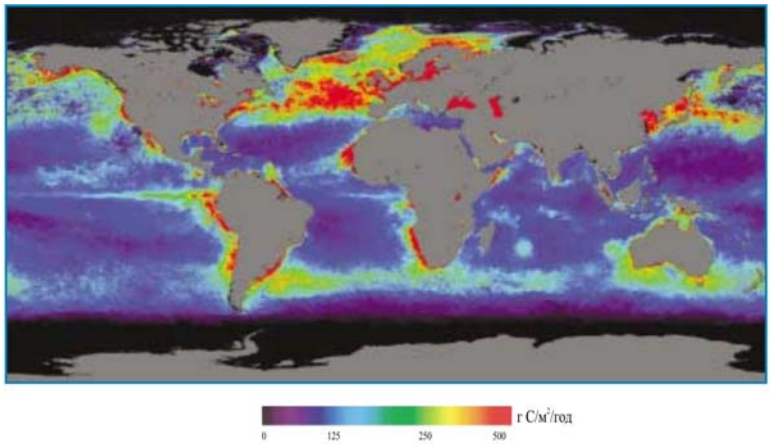

a)

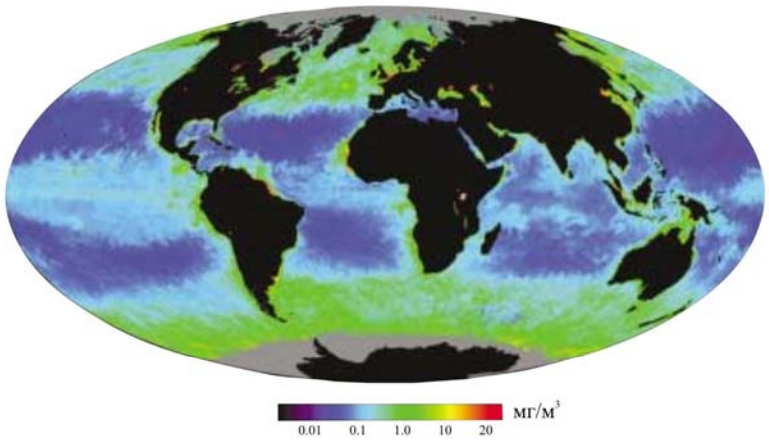

b)

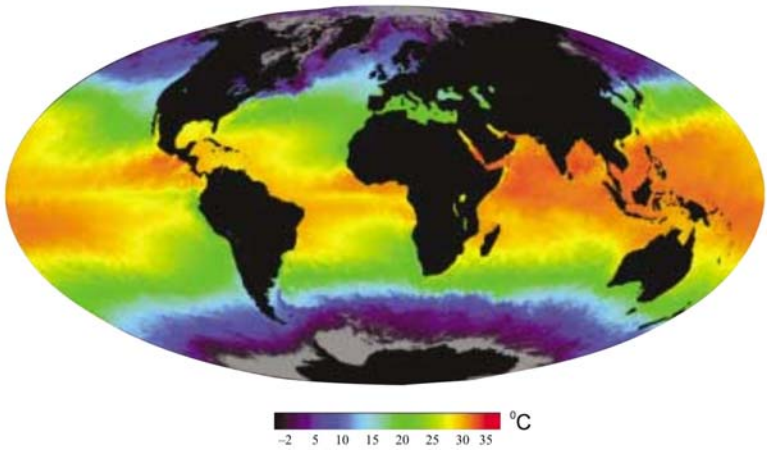

c)

Fig.1. Global distribution constructed from TERRA satellite (MODIS radiometer):
a)primary productivity between May 9 and June 9, 2001 ;
б) chlorophyll concentration in May 2001 ;
в) ocean surface temperature in May 2001 .

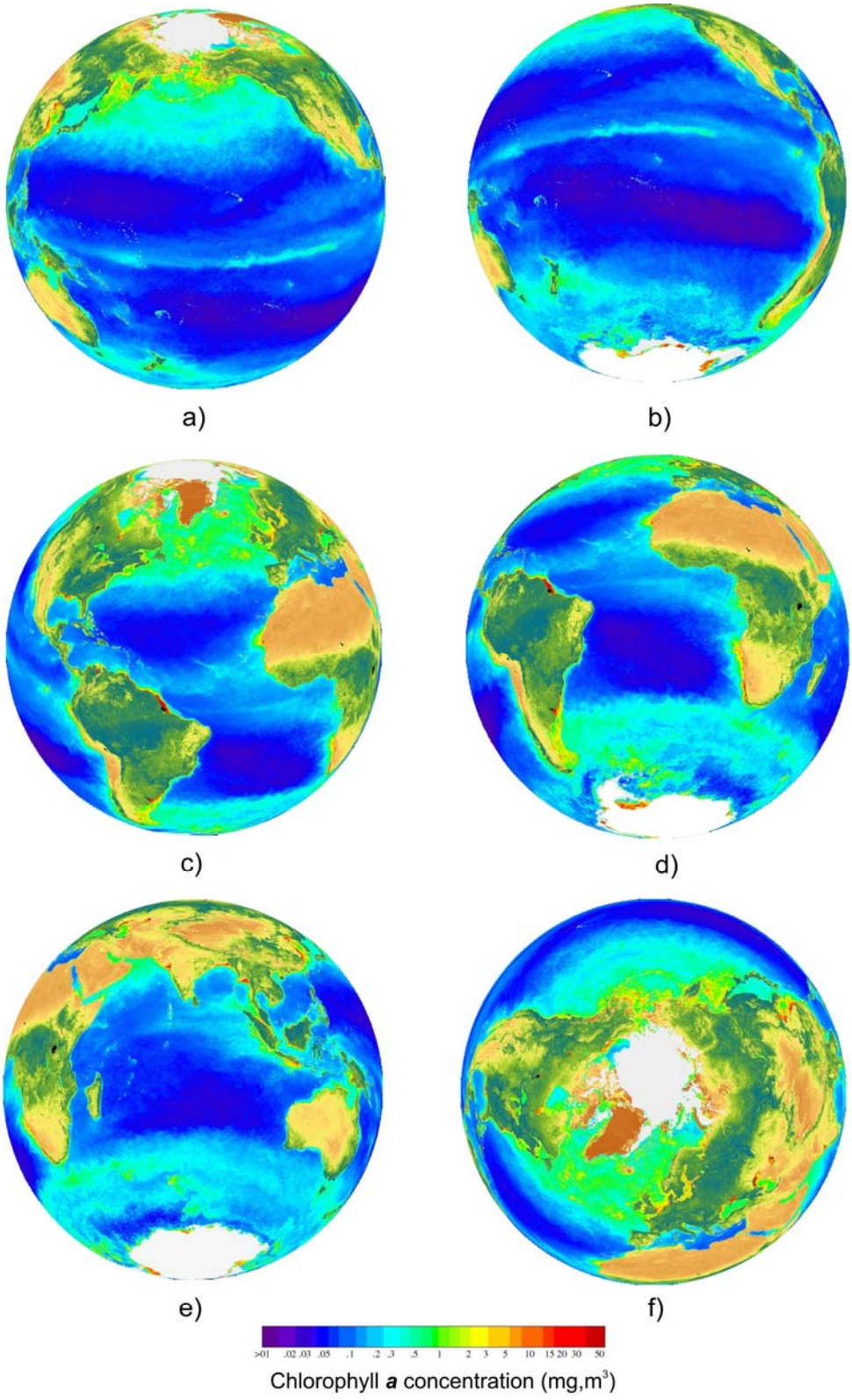

Fig.2.Global distribution of chlorophyll obtained by
SeaStar satellite in September 97 -August 98 with SeaWifs scanner:
a, b -Pacific Ocean ; c, d -Atlantic Ocean ; e - Indian Ocean, f - polar projection

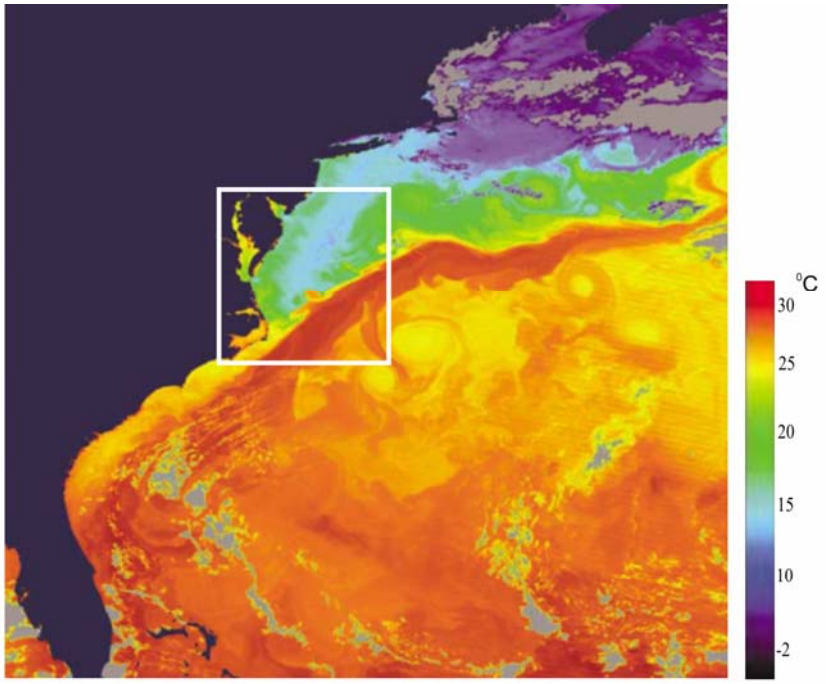

a)

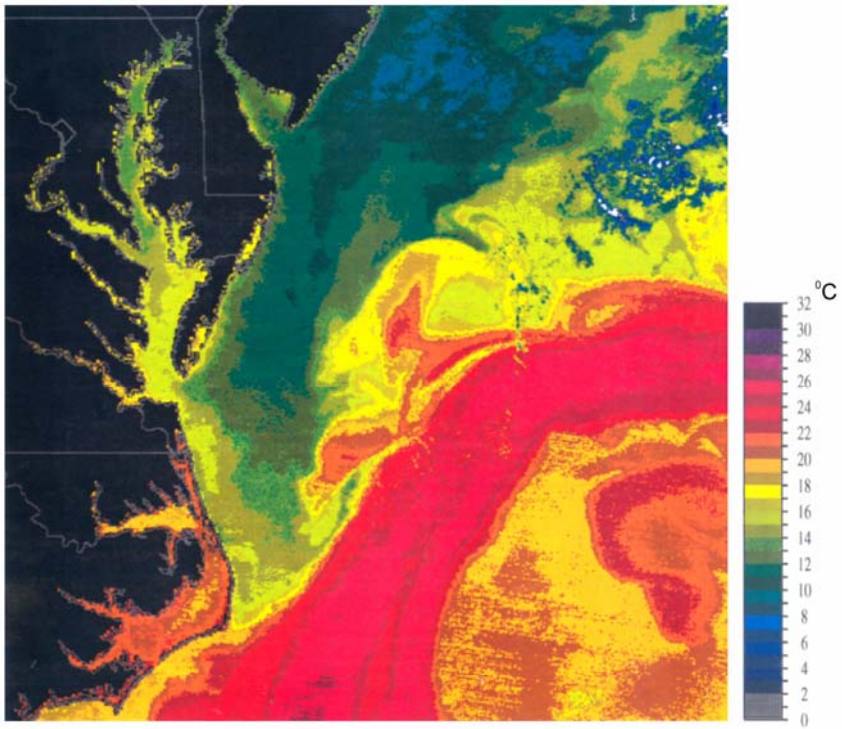

b)

Fig.3. Temperature distribution in West part of North Atlantic (in Gulf Stream current area)
a - from TERRA satellite (MODIS equipment ;May, 8 2000);
b -with NOAA satellite (AVHRR equipment, 1995)

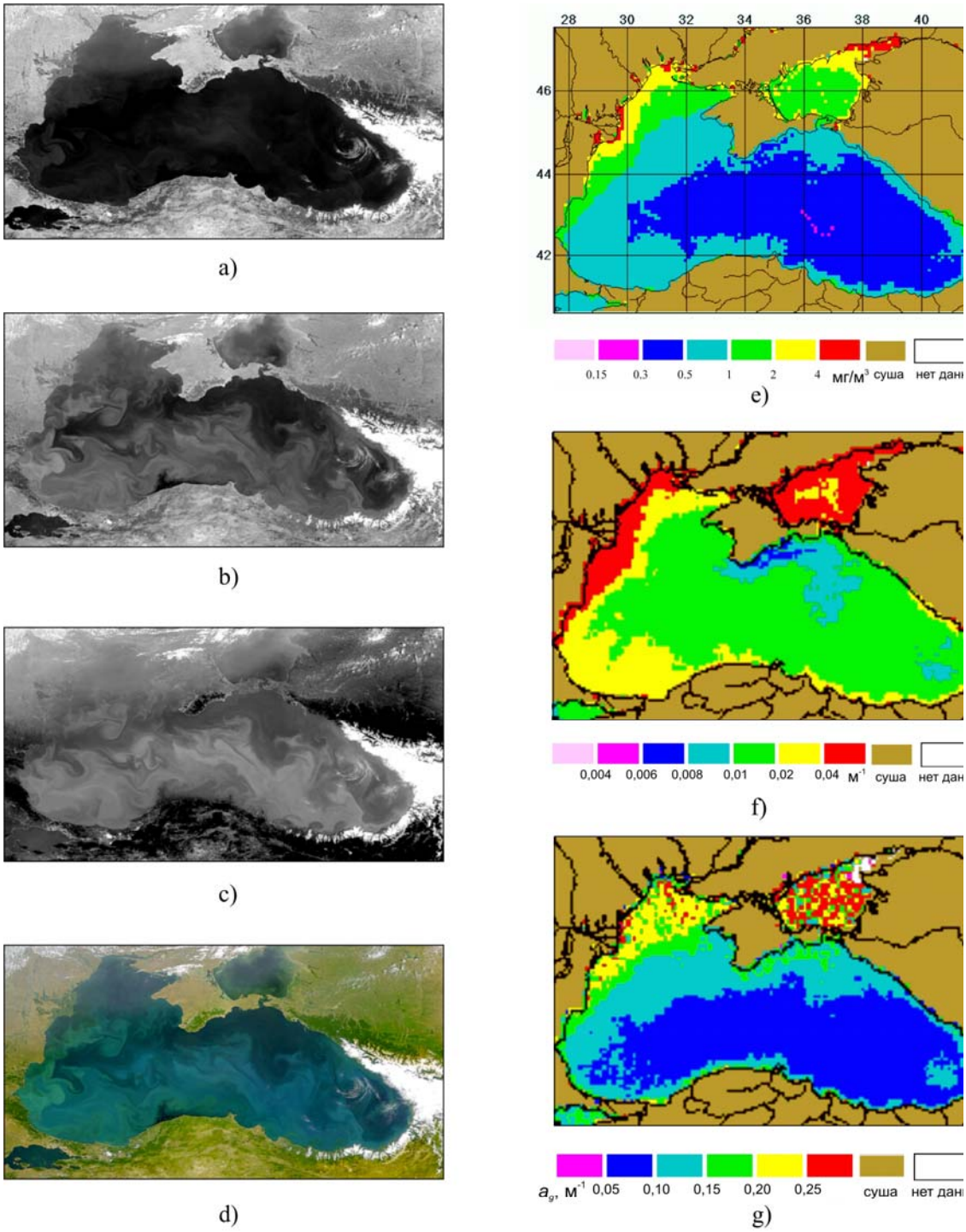

Fig.4. Image of *Black Sea* obtained July, 2000 with SeaWifs in 660-680 nm (a), 545-565 nm (b), 402-422nm (c), as well as synthesized image (d).
Obtained by matching of space and ground truth data: chlorophyll concentration, mg/m^3 (e); backscattering coefficient of suspension, m^{-1}(f); and adsorption coefficient of yellow substance , a_g, m^{-1} (g)

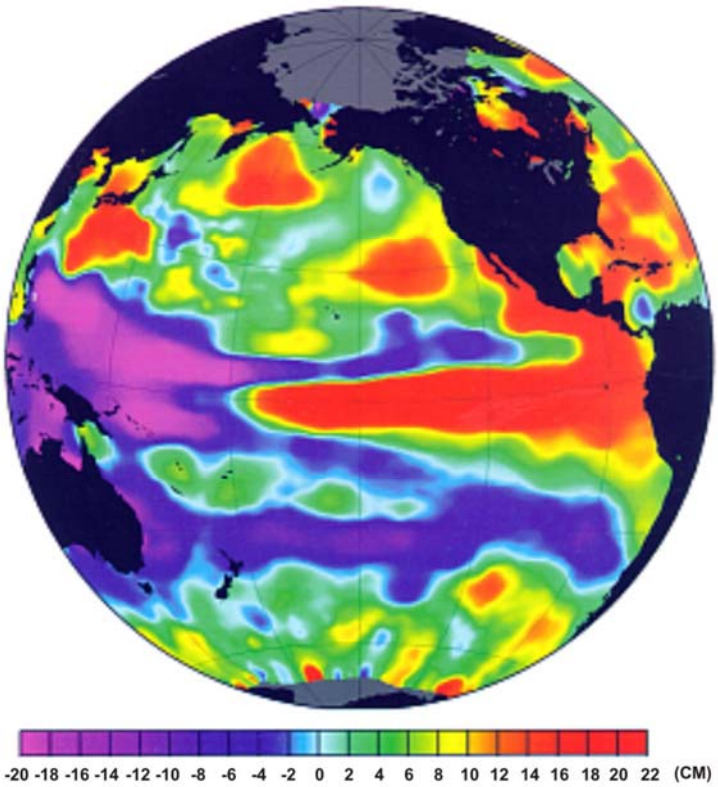

Fig. 5. Global distribution of relative level of Pacific ocean surface obtained by TOPEX/POSEIDON
satellite in 1997 (El Niño effect in equator area)

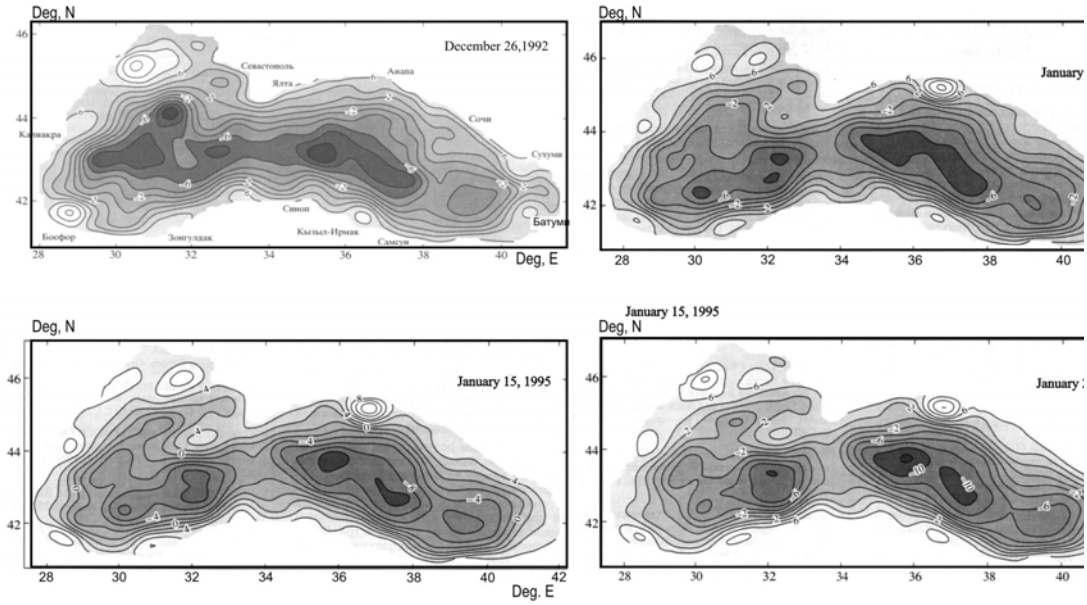

Fig. 6. Dynamics of anticyclones in Black Sea

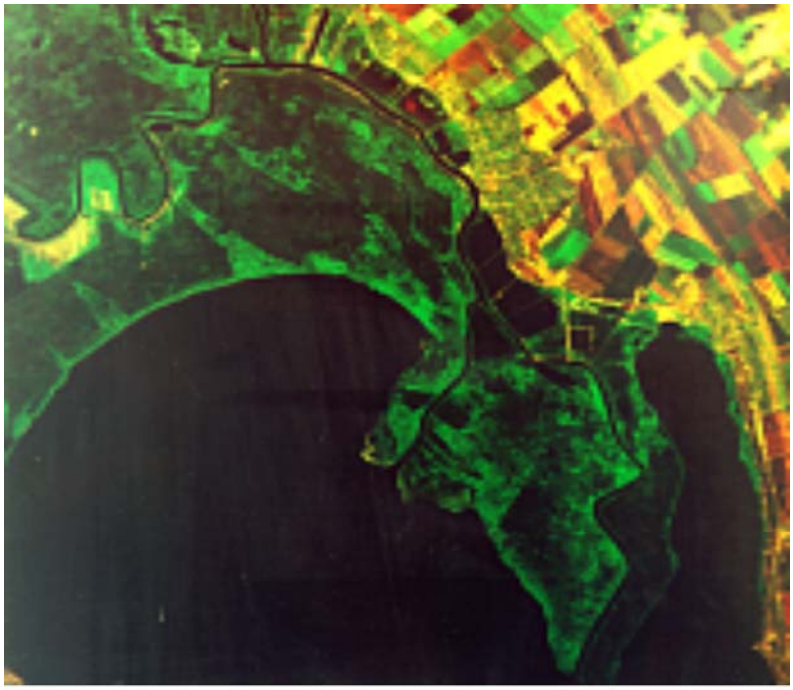

a)

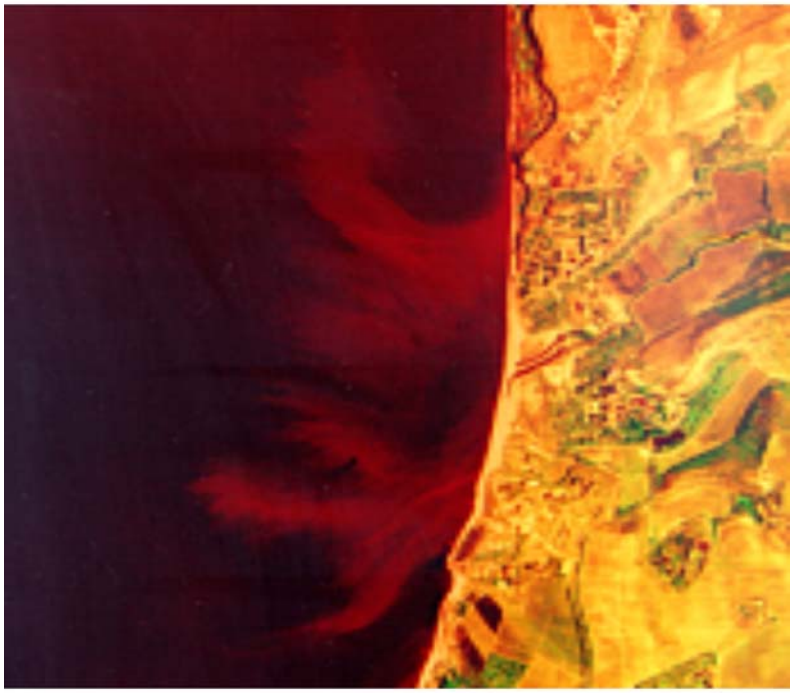

b)

Fig. 7. Delta of Dnestr River (a), pollution of Black Sea shore in the fall
area of Belbek River (b) KFA-1000 image (RESURSE satellite) 1989 (a) and 1993 (b)

Fig. 8 shows examples of radar images of the surface of various bodies of water, acquired from airborne (a,b,c,d) and spaceborne (e) platforms. Figs. 8a,b and c are airborne platform-taken radar images showing surface manifestations of internal waves in the Japanese (a) and Okhotsk (b) seas, and in the area of the Kamchatka Peninsula (c). The images are acquired using a side-looking aerial radar station SLR (TOROS), functioning at wavelength 2 cm with horizontal polarization, providing spatial resolution 15m and coverage strip 15km [Avanesova et al., 1984; Bondur, Voliak, 1984; Bondur, 1995]. The manifestations of internal waves seen on the presented radar images are related with the cold Primorski current flowing around elevated features (Fig. 8a), the interaction of the high-tide wave with the continental incline (Fig. 8b), and the interaction of barotropic high tides with the bottom topography during the complex stratification of water above the continental shelf slope (Fig. 8c).

Fig. 8 d and e contain examples of radar images of the ocean surface in the area of Long Island. The image presented in Fig. 8d was received with horizontal (left) and vertical (right) polarization using SLR (side-looking radar) "Neet", onboard a TU-134 aircraft (wavelength – 4cm, spatial resolution – 15m, coverage width – 15km).

Fig. 8e shows a radar space image of the same area with horizontal polarization taken some years later from the ERS-2 satellite (wavelength – 5.7cm, spatial resolution – 30m, coverage width – 100km).

Both in the airborne and satellite imagery, complicated systems of internal waves with spatial period about 1 km are clearly visible. Especially clear is the stability of their spatial structure. This is due to the interaction of a steady current with the undersea topograpy.

NEW METHODS OF REMOTE SENSING

With the development of aerospace technologies, recent years have seen a substantial expansion of their capabilities in the interest of resolving many scientific and practical issues in oceanology. Amid remote methods developed in recent times, special attention should be given to: the method of remote optical spatial frequency spectroscopy [Bondur, 1986; 1987; 1993; 1995; 2000; 2001; Bondur, 1995]; radar methods [Alperis et al., 1994; Viter et al., 1994; Zidko et al., 1987; Zagorodnikov, 1978; Kudriavtsev et al., 2003; Melentiev, Bobilev, 2001; Mitnik et al., 2003; Mur, Fan, 1973; Radiolocation, 1990; The special issue, 1982; 1983; ATSR-2, 1995; ERS, 1995], including the method of Multifrequency Radio Wave Tomography [Bondur, 1993; 1995; 2001; Bondur, Savin, 2000; Bulatov et al., 2003; Kudriavtsev et al., 2003; Methods, 1996; Shamaev, 1994]; new methods of laser sensing [Bondur, 1993; 2001; Bondur, Zubkov, 2001; Bunkin et al., 1987; Vasilkov et al., 1990; Klishko et al., 1978; Mezeris, 1987; Zubkov, Bunkin, 1995]; methods of noncoherent impulse sensing [Bondur, 1993; 2001; Bondur et al., 1988]; new multispectral, hyperspectral, and other methods [Beliaev et al., 1978; Bondur, 1993; 1995; 2001; Bondur, Savin, 2000; Koptev, 1995; Mishev, 1985; Advanced, 1996; Bondur, 1995; MODIS, 2002; Remote Sensing, 2002]. Using these methods allows real-time identification of polluted regions, estimation of pollutant concentrations, determination of surface wave spectra, meteorological parameters, bottom topography, and other characteristics in various areas of studied bodies of water, as well as study of various processes in the depths and near-surface layers of the ocean [Bondur, 1993; 1995; 2001; Bondur, Grebenuk 2001; Bondur, Savin, 2001;Remote Sensing, 1984; Kondratiev, 2000; Kondratiev et al., 1992; Kondratiev, Krapivin, 2003; Koptev, 1995; Monin, Krasitski, 1985; Oceanology, 1978; Fedorov, Ginzburg, 1988; Atlas et al., 1986; Remote sensing, 2002; Viktorov, 1996].

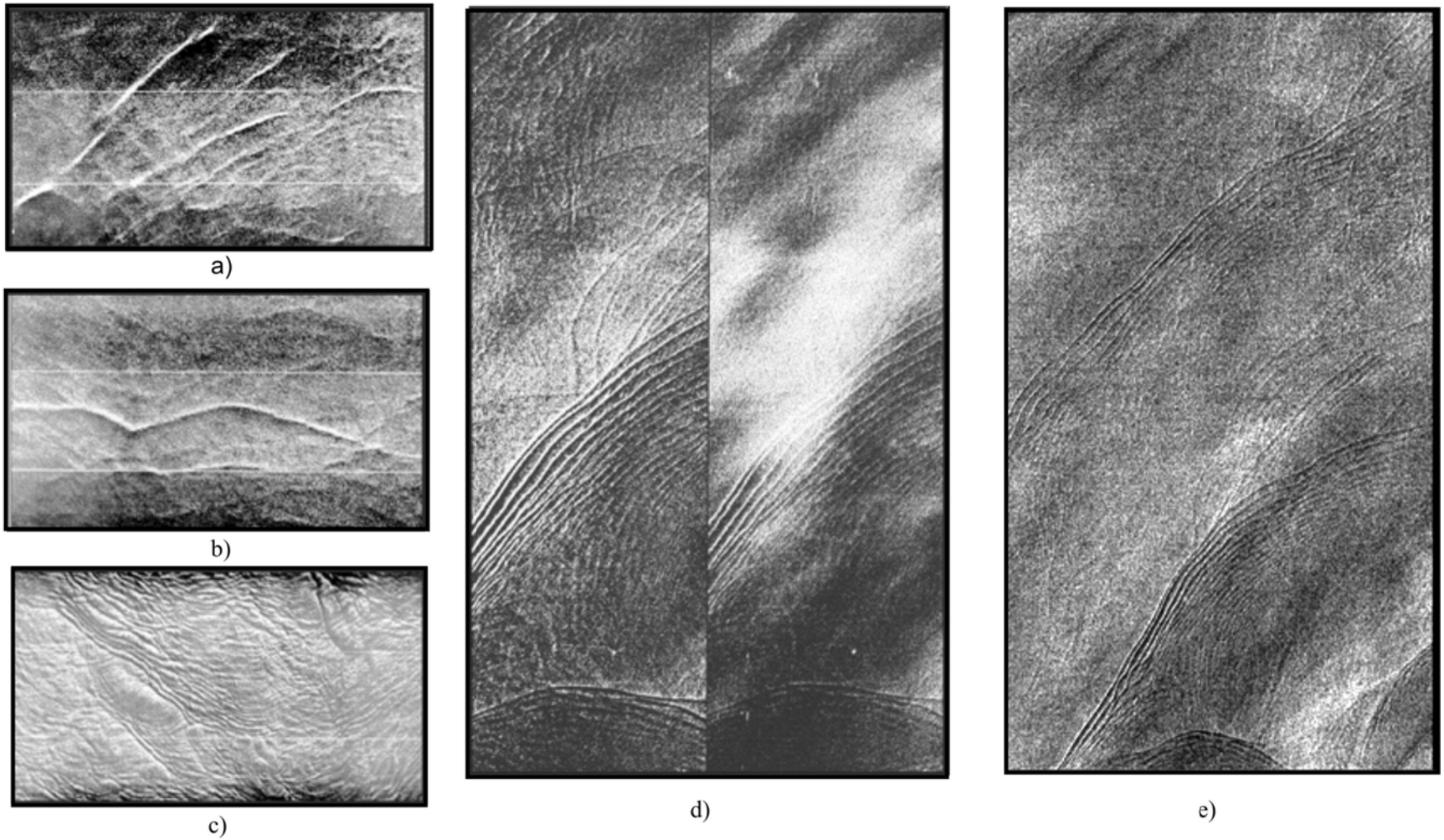

Fig. 8. Examples of aeroimages (a, b, c, d) and satellite image (e) with internal wave manifestations:
a) Japanese sea; b) Sea of Okhotsk; c) water area near Kamchatka; d,e) water area near Long Island

METHOD OF REMOTE SPATIAL FREQUENCY SPECTROMETRY

PHYSICAL BASIS OF THE METHOD

One of the more promising ways of gaining information on the characteristics of surface wave spatial structure and its variation, under the influence of both various processes and phenomena taking place in the ocean and anthropogenic effects, are methods based on the spatial spectral analysis of aerospace images formed in the optical and radio ranges of the electromagnetic spectrum [Bondur, 1986, 1987, 1991, 1993, 1995, 2000, 2001; Bondur, Voliak, 1984; Bondur, Savin, 2001; Zagorodnikov, 1978; Karaev, 2000].

These methods received the most widespread use in the analysis of optical images. In formation of such images, the brightness of radiation registered by the remote equipment in a fixed moment of time at small coverage field angles can visualized as shown in Fig. 9 [Bondur, 1987, 1991, 1993].

$$L(x,y) = L^{(1)} + \left[L^{(2)}(x,y) + L^{(3)}(x,y)\right]\tau_a , \qquad (1)$$

where $L^{(1)}$ - brightness component, caused by scattering in the atmosphere in the direction of the receiver; $L^{(2)}(x,y)$, $L^{(3)}(x,y)$ - brightness component, caused by the reflection from the ocean surface and dispersion in the water depths; τ_a - function of atmospheric transparency.

Expanding (1) in the plane (x,y) into a Taylor series by degree of surface gradient (i. e., incline, slope)

$$\nabla\xi_x(x,y) = \frac{\partial\xi(x,y)}{\partial x}, \nabla\xi_y(x,y) = \frac{\partial\xi(x,y)}{\partial y}$$

we obtain

$$L(x,y) = L^{(1)} + \left[L_0(x,y) + L_1(x,y)\nabla\xi_x(x,y) + L_2(x,y)\nabla\xi_y(x,y) + L_H(x,y)\right]\tau_a , \qquad (2)$$

Where $L_0(x,y)$ - brightness component, not dependent on slopes; $L_1(x,y)\nabla\xi_x(x,y)$ and $L_2(x,y)\nabla\xi_y(x,y)$ - fluctuating components; $L_1(x,y)$ and $L_2(x,y)$ - functions which depend on ambient light; L_H - nonlinear component of brightness.

The nonlinear component of brightness can be neglected under the condition [Bondur, 1991]

$$\sigma_\varphi \frac{\partial}{\partial\bar{n}}\left[L^{(0)}(x,y)\tau_0 + R(\beta)L^{naq}(\chi,\alpha,z_0)\right] << 1, \qquad (3)$$

Where σ_φ - root-mean-square slope; $\bar{n}$ - unit vector normal to the plane at $r(x,y)$; $L^{(0)}(x,y)$ - brightness of ascending radiation reaching the ocean surface from below, e. g., backscattered, scattered light; τ_0 - coefficient of water transmissivity; $R(\beta)$ - Fresnel coefficient of reflection; $L^{naq}(\chi,\alpha,z_0)$ - brightness of radiation from above; χ - angle between the falling rays arriving after reflection at the receiver and the vertical; α - azimuthal angle of the sun, z_0 - zenith angle of the sun.

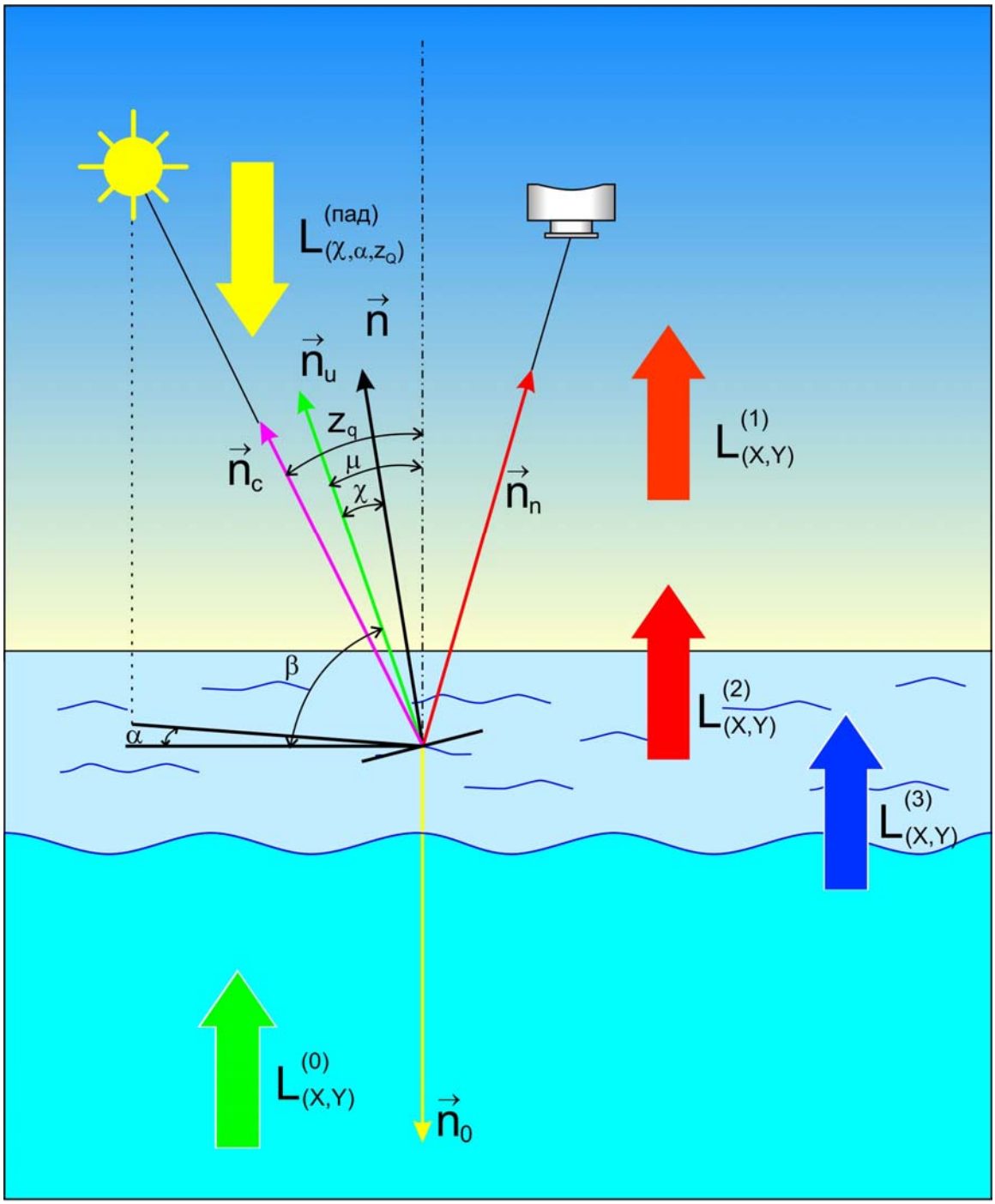

Fig. 9. Diagram of formation of the radiation brightness field for sea surface

The conditions (3) are met only for diffuse illumination and at points distant from the sun's glare. Therefore, in general, the component $L_н$ in (2) cannot be neglected.

If we take a spatial two dimensional Fourier transform of the two dimensional brightness field (2) registered by remote sensors, it is possible to calculate the two dimensional energy spectrum of the original image [Bondur, 1987, 1991; 1993].

$$S(k_x,k_y)=\left|\frac{1}{2\pi}\int_{-\infty}^{\infty}\int L(x,y)\exp\left[-i(xk_x+yk_y)\right]dxdy\right|^2 \qquad (4)$$

Taking into account (2), the energetic spectrum of the image can be represented as

$$S(k_x,k_y)=\left|F\left[L_0\right]\right|^2+\left|F\left[L_л\right]\right|^2+\left|F\left[L_H\right]\right|^2+2(F\left[L_0\right]\cdot F\left[L_л\right]+F\left[L_0\right]\cdot iF\left[L_H\right]+F\left[L_л\right]\cdot F\left[L_H\right]) \qquad (5)$$

where $F[\ldots]$ - Fourier transformation operator, and $L_л\left(x,y\right)=L_1\left(x,y\right)+L_2\left(x,y\right)$ - linear component of brightness.

After elimination of the constant brightness component in (2), for example, through previous processing of the image, expression (5) takes on the form [Bondur, 1991]:

$$S(k_x,k_y)=\left|F\left[L_·\right]\right|^2+\left|F\left[L_H\right]\right|^2+2F\left[L_·\right]\cdot F\left[L_H\right], \qquad (6)$$

Because the component $L_1(x,y), L_2(x,y)$ in (2) depends on the gradients (slopes) of the surface waves at x,y the brightness registered by remote sensing equipment $L(x,y)$ also depends on these components.. Therefore from the image spectra $S(k_x,k_y)$ we can calculate wave slope spectra $\Psi_\varphi(k_x,k_y)$ and/or elevation spectra $\Psi_\xi(k_x,k_y)$. The relationship of these spectra with the image spectra can be written as [Bondur, 1987; 1991; 2000; 2001]

$$\Psi(k_x,k_y)=\hat{W}(k_x,k_y)S(k_x,k_y), \qquad (7)$$

Where $\Psi(k_x,k_y)$ - two dimensional spectrum of slopes and heights; $\hat{W}(k_x,k_y)$ - regenerative operator, depending on the angular distribution of sky brightness, monitoring conditions, and characteristics of remote equipment.

Determining the general form of the operator $\hat{W}(k_x,k_y)$ is a complex problem, but with some assumptions it can be solved [Bondur, 1987, 1991, 1995; 2000, 2001; Bondur, Litovchenko, 1989; Bondur, Murinin, 1991; Bondur et al, 1991; Bondur, Murinin, 1991].

In linear approximation, expression (6) simplifies:

$$S(k_x,k_y)=\left|F\left[L_л\right]\right|^2, \qquad (8)$$

And the relationship between the wave spectrum and the image spectrum takes the form:

$$\Psi(k_x,k_y)=\hat{W}^л(k_x,k_y)S(k_x,k_y), \qquad (9)$$

With $\hat{W}^л$ - the linear regenerative operator.

Bondur and co-workers [Bondur, 1987; 1991; 1993; 2001; Bondur, Murinin, 1991] have proposed a multi-positional method for regeneration of elevation spectra from image spectra in the linear approximation, based on the registration of spatial spectra of many images or many fragments of one image, received under differing lighting or monitoring conditions. Linear methods of regeneration yield good results of images received under diffuse lighting or far away from the sun's glare.

In the general case, during regeneration of elevation spectra from image spectra, it is necessary to take into account nonlinear effects having a substantial role in formation of the image.

In this case, the relationship between wave spectra and image spectra has the form:

$$\Psi(k_x,k_y)=\hat{W}^н S(k_x,k_y) \qquad (10)$$

With $\hat{W}^н$ - the nonlinear regenerative operator.

Additional work [Bondur, 1991; 2001; Bondur, Murinin, 1991] describes and proposes a nonlinear multi-positional method for regeneration of wave spectra from image spectra in linear approximation, taking into account nonlinear effects of optical radiation reflection from the wind driven sea surface.

The applicability of this method has been confirmed experimentally by comparing results of *in situ* wave surface measurements and data received through stereo photogrammetric processing of the images which were taken from a hydrophysical platform (surface platform) [Baranovsky, Bondur et al., 1992; Bondur, 1991; 2001].

THE ESSENCE OF REMOTE SPATIAL FREQUENCY SPECTROMETRY

The essence of Remote Spatial Frequency Spectrometry is shown in Fig. 10. It consists of the following [Bondur, 1986; 1987; 1991; 1993; 1995; 2000; 2001; Bondur, Savin, 2000; Bondur, 1995] sequence of steps:

taking an image of the sea surface using remote sensors installed onboard a spacecraft/satellite, airplane or helicopter, Fig. 10a;

taking the two dimensional spatial spectra of received images or their various subimages, Fig. 10b;

calculating the informative indicators from the spatial spectra for each image or its subimages which characterize the form, topological properties, orientation, moments of inertia, structural properties, energy distributions, etc, Fig. 10c;

statistical analysis of these informative indicators - Fig. 10d;

identification of various phenomena on the sea surface, based on the calculated indicators for the spectra of each image (or its subimages) Fig. 10e;

creation of a map of the studied region based on individual images (stereoscopic reconstruction), Fig. 10f;

determination of significant ocean environment parameters from spectra, spatial geometric and dynamic indicators of the studied phenomena. Fig. 10g.

The method of remote spatial frequency spectrometry can be applied to images formed in various areas of the electromagnetic spectrum (including the radio range).

In cases of necessity, the developed methods are used to reconstruct spectra of inclines or elevations for the ocean surface [Bondur, 1991; 1993; 2001]. Furthermore, calculation of informative indicators for the spatial spectra is conducted, including brightness, geometric, integral, topological and other characteristics describing the form and distribution of energy in two dimensional spatial spectra [Bondur, 1986;1987; 1991; 1995; 2000; 2001; Bondur et al., 1986; Bondur, Starchenkov, 2001]. Using portions of the informative indicators, it is possible to directly determine various parameters of the water environment, described below, as well as highlight areas subject to anthropogenic influences.

For identification on the sea surface of anthropogenic influence zones, preliminary statistical analysis of the received data is conducted [Bondur, 1991; 1995; 2001; Bondur et al., 1986; 1990; 1990; Bondur, Starchenkov, 2001]. Here, “teaching” samples of informative indicators are formed, corresponding to various phenomena on the ocean surface. For each of them, the corresponding statistical characteristics are calculated and threshold levels are determined. Then, search and identification of sea surface areas subject to anthropogenic influences is conducted, using appropriate classification criteria [Bondur, 1991; 1993; 1995; 2001; Bondur et al., 1986; Bondur, Starchenkov, 2001]. Classification can also be done using nonparametric criteria or through cluster analysis methods [Bondur, 1991; 1993; 2000; 2001; Bondur, Savin, 2000; Bondur, Starchenkov, 2001].

The received results allow creation of maps for the studied regions, for which we determine: characteristics of surface waves, distribution of pollutant concentrations, areas of pollution spread and their properties and spatial characteristics.

For realization of the remote spatial frequency spectrometry method, several variants of equipment construction are proposed [Bondur, 1987; 1993; Bondur, Savin, 2001].

Fig. 11 shows, as an example, the complex optical-electronic system for remote spatial frequency spectrometry, designed for installation onboard aircraft and helicopters. In this variant, registration of sea surface images is done by a television camera or optical-electronic system. Their processing, including the spatial spectral analysis, is conducted on an onboard digital computing system, containing a processor for fast Fourier transforms (FFTs). The calculation of informative indicators for these spectra, and their subsequent analysis, is conducted through an onboard computer. In parallel with processing on board, the formed images and their spatial spectra are recorded into onboard magnetic storage for subsequent detailed processing at a land-based computing center [Bondur, 1991; 1993; 1995; 2001; Bondur, 1995]. Fig. 11a shows the outer likeness of onboard means (scanning television camera, and onboard computing equipment). Fig. 11b shows a view of the internal components of the onboard computer, with the motherboard of a special processor capable of carrying out FFTs.

PARAMETERS OF THE MARINE ENVIRONMENT OBTAINED BY IMAGE PROCESSING

Knowing the slope or height spectra, it is possible to obtain many important parameters of the water environment by determining and evaluating their informative indicators. The speed and direction of near-surface wind can also be obtained. The main characteristics defined using remote spatial-frequency spectrometry are:

spectra of slope and height of surface waves, recreated using linear and nonlinear methods;

characteristics of surface waves (number of wave systems, direction of propagation and angular energy distribution for each system, average elevations, lengths, and periods of waves, average length of crests, etc);

changes in the spectral composition of surface wave characteristics, including redistribution of wave energy, attenuation of wave components, and generation of addition spectral harmonics;

speed and direction of near-surface winds, determined by the values of wave numbers, spectral maximums and orientation;

concentrations of surface active substances (surfactants), calculated from the coefficient of dissipation of sea waves;

parameters of internal waves, determined by the characteristics of height and slope dispersion on the sea surface;

characteristics of foam formations (for example, density of occurrence, length of crests, etc..)

topography of the sea bottom and other characteristics.

The spectra of heights or slopes usually have local maxima, caused by various systems of waves and manifestation of various deep phenomena as shown in Figs. 12,14,15 [Bondur, 1986; 1987; 1991; 1993; 1995; 2000; 2001; Bondur, Voliak, 1984; Veter, 1986; Davidan et al., 1985; Monin, Krasitski, 1985; Oceanology, 1978; Rozkov, 1979]. By these maxima, it is possible to determine the number of wave systems and direction of propagation for each system, angular energy distribution, and other characteristics [Bondur, 1987; 1991; 1993; 1995; 2000; 2001; Bondur, Voliak, 1984; Veter, 1986; Davidan et al., 1985; Rozkov, 1979].

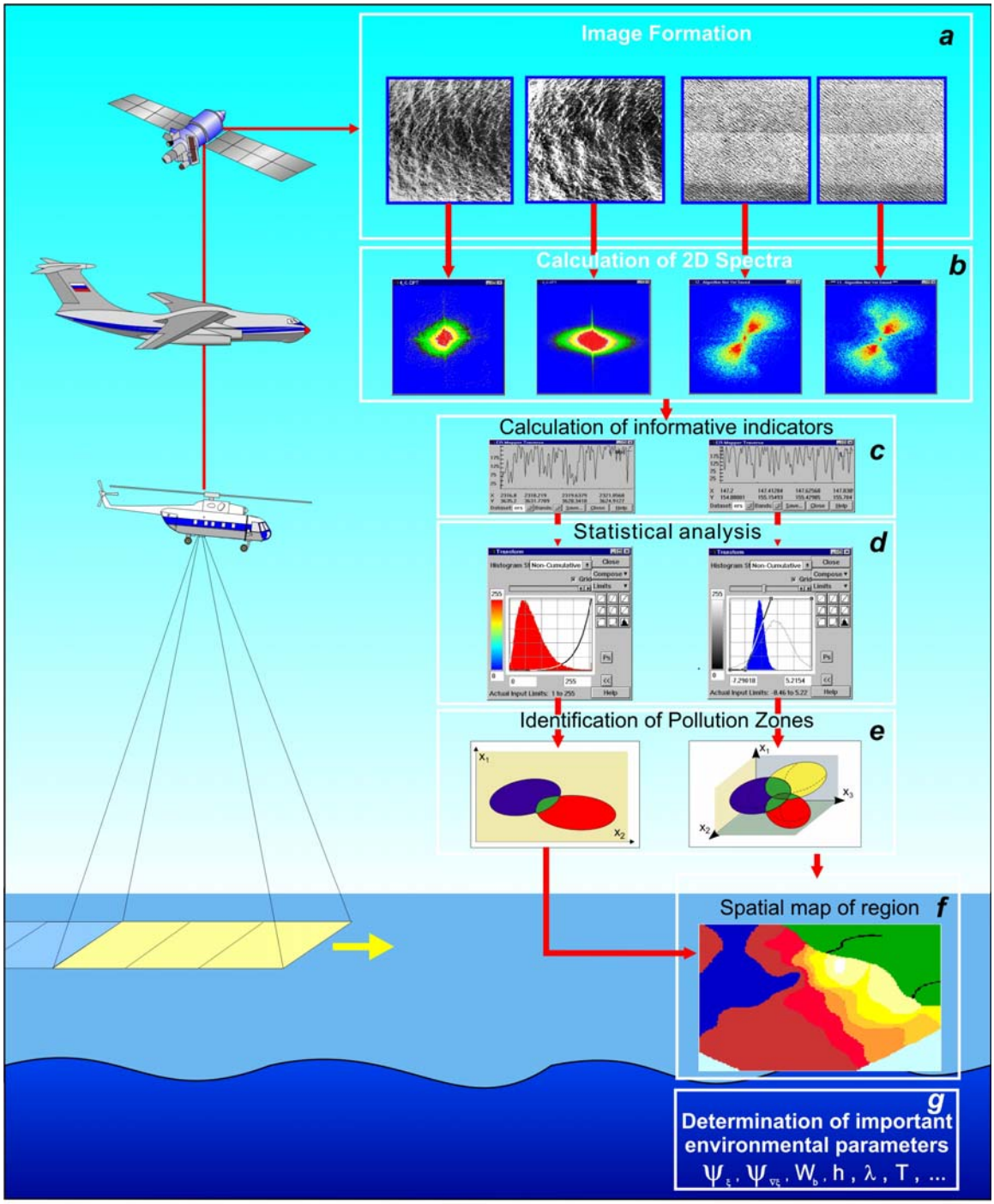

Fig. 10. Illustration of remote optical spatial-frequency spectrometry method

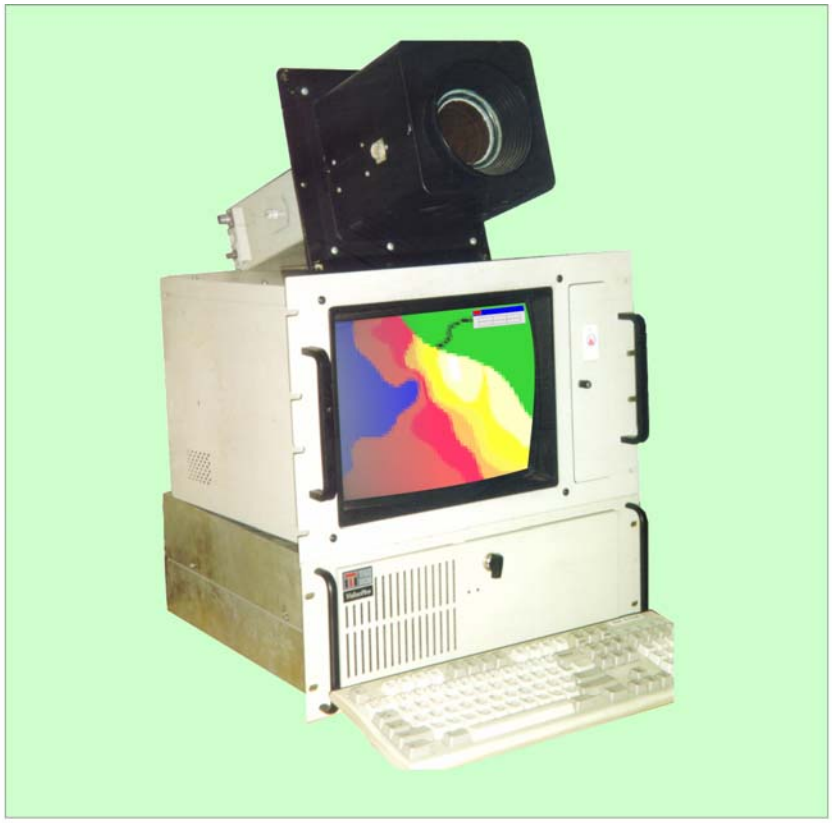

a

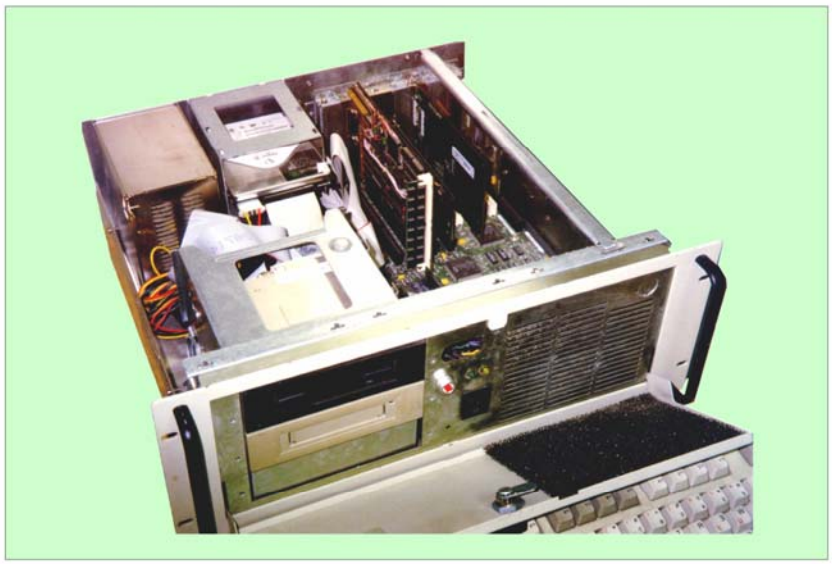

b

Fig. 11. General view of optical-electronic hardware for remote spatial-freguency spectrometry
a - image formation hardware and onboard processor
b - internal elements of onboard processor with dedicated fast Fourier processor

When one system of waves exists on the sea surface, then the direction of its propagation will, as a rule, coincide with the direction of the wind. The methodology for determining the wind speed is related with determining the wave number of the spectral density maximum k_{max} for wind driven waves, received from the image spatial spectra [Bondur, 1987; 1991; 2001]. In accordance with this methodology, the speed of near-surface wind for developed waves is determined by the formula:

$$W_в = \left(0{,}86g / k_{max}\right)^{1/2}, \qquad (11)$$

Where g - gravitational acceleration.

The presence on the sea surface of various anomalies, for example surface active substances (SAS), causes an attenuation of waves in the centimeter range. This results in a decrease in the contrast of slope and height spectra in the area of short waves (see Fig. 13). Based on the contrasts of spectra in areas of SAS, the coefficient of ripple dissipation can be calculated, which in turn is related to the concentration of SAS films. In this way, the wave height and slope spectra allow the determination of SAS concentration values [Bondur, 1987; 1991; 1993; 1995; 2001; Ermakov et al., 1982].

Various phenomena, including those caused by internal waves, turbulence, and anthropogenic influences on the water environment, cause deformation in the spatial structure of surface waving. In particular, they cause the creation of zones with increased and decreased incline dispersion (see Fig. 14, 15). Because the incline dispersion can be found from the incline spectra, these spectra allow the determination of many parameters for internal waves (including their lengths, periods, phase speeds, as well as their spatial geometric characteristics, etc) in regions related with anthropogenic influences.

Two dimensional spatial spectra allow the determination of some characteristics of foam formations, including average and specific density of crests based on the moments of elevation spectra. This is described in detail in the following works: [Bondur, 1991; 1993; 1995; Bondur, Litovchenko, 1989; Bondur, Sharkov, 1982; 1986].

SOME RESULTS OBTAINED BY APPLICATION OF THE METHOD

The use of remote spatial frequency spectrometry is quite effective, for determination of such an important meteorological parameter as the speed of near surface wind $W_в$ [Bondur, 1987; 1993; 1995; 2001].

Fig. 12 shows characteristic images of the sea surface taken at various wind speeds, their two dimensional spatial spectra, and one dimensional cross sections of these spectra with the noted spatial frequency magnitudes. The sea surface images shown on Fig. 12a,d are acquired at sensor height of imaging H_A = 2000 m, and the images of Fig. 12,g – imaging height H_A = 8000 m. Two dimensional spatial spectra, shown on Fig. 12b,e,h have a multi-connected form with several pairs of maxima at dispersed wavelengths. On the images of these spectra, one can see ripples (capillary waves) and wind wave systems.

For the image spectra shown in Fig. 12a the wave number of the wind wave spectral maximum is k_{max} = 0.35 m^{-1} (Fig. 13b,c), and the wind speed, determined by formula (11), is $W_в$ ~ 5 m/s. In measurements taken *in situ* from a ship taking part in the experiment, the wind speed was measured as 5.6 m/s. For image spectra, shown on Fig. 12d, k_{max} = 0.14 m^{-1}, and the wind speed estimate according to (11) was $W_в \cong$ 7.8 m/s. The wind speed received from the ship was = 8 m/s. For the spatial spectra of the image received from 8000m (Fig. 12g), the wave number of the spectral maximum was k_{max} =1.0m^{-1} (Fig. 12h,i). The wind speed according to (11) was $W_в$ = 2.9 m/s; and the ship measurement was $W_в$ = 2.8 m/s.

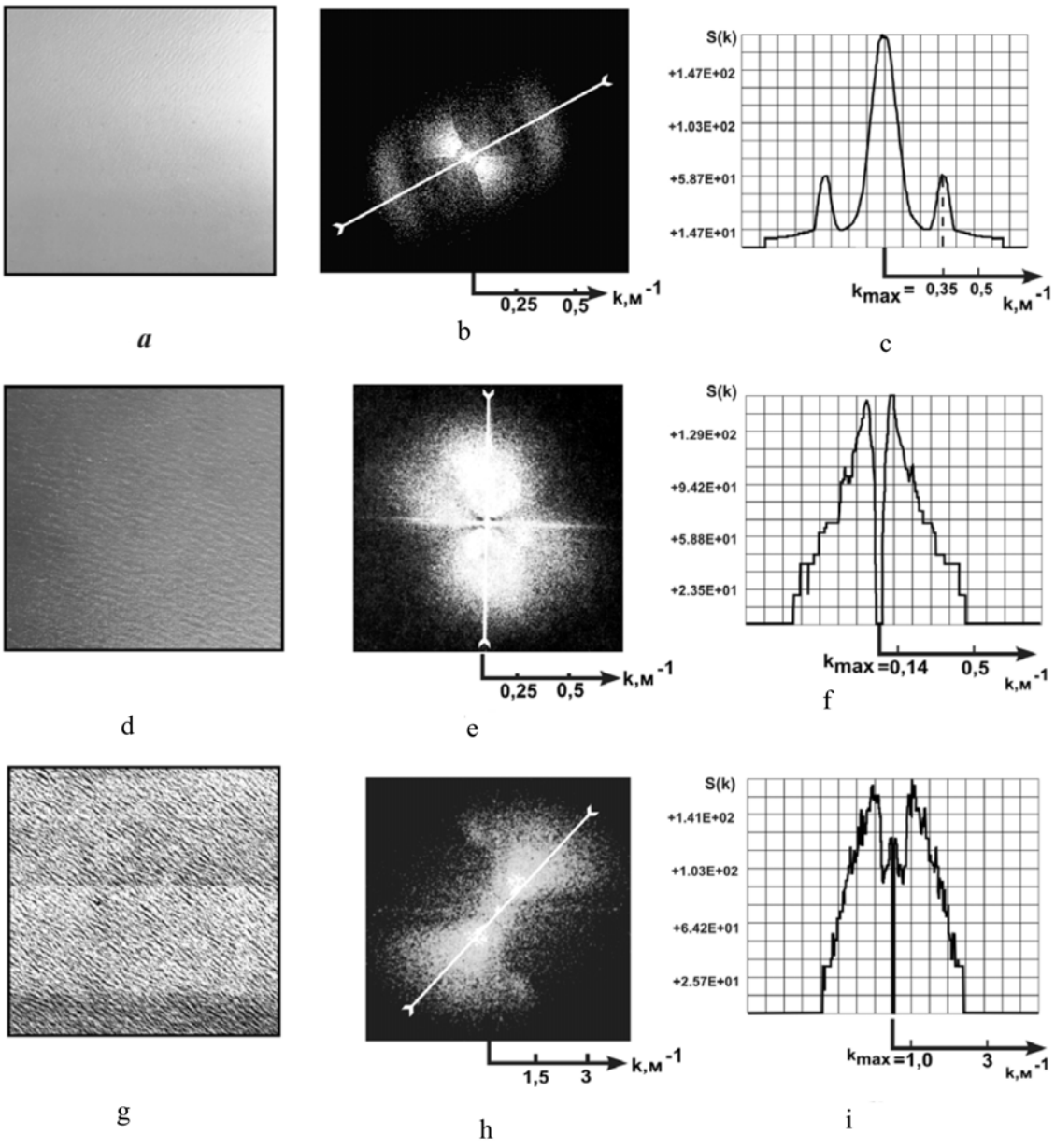

Fig. 12. Sea surface images, obtained from 2000 m= *a,d*; 8000 m=*g*; relevant 2D spatial spectra = *b,e*; one-dimensipnal cross-sections of these spectra in marked directions for different wind speeds = *c,f,i*

The fairly large variation of the wind speed estimates calculated from the spectral maximum wave number for Fig. 12a,b,c from the wind speed measured onboard the ship may be related with the fact, that the studied methodology is based on usage of the Pierson-Moskowitz approximation, which is most applicable for fully developed waves, while the experiment took place where waves were just developing [Bondur, 1991; 2001].

The ability to use 2-d spatial spectra to identify zones with surface active substance (SAS) demonstrated in Fig. 13. This image shows the sea surface with SAS obtained from sensors on platforms above the Black Sea, from a helicopter at 150m. These are (a,b), enlarged fragments of these images (c,d,e), the corresponding two dimensional spatial spectra (f,g,h), their one dimensional cross sections (l,m,n) in the directions shown on (i,j,k). As seen from the these images, the spectra of images with SAS films (Fig. 13g,h,m,n) differ from the spectra for images of clean sea surface (Fig. 13,f,l) in the smoothing of high frequency surface wave components [Bondur, 1993]. Median filtration and color coding of two dimensional spectra (Fig. 13i,j,k) allow better visualization of this difference. Comparing the cross sections of spectra shown on Fig. 13*l* (clean surface) and Fig. 13m,n (SAS film) it is obvious that the slope of the spectra of the SAS image is steeper than the slope of the spectra associated with the clean surface image.

On images received from high altitudes, the slicks caused by surface manifestations of internal waves are seen as long stripes of negative (sometimes positive) contrast. This is seen on Fig. 14a, which shows aerial photographic images taken from a helicopter (altitude H_A = 2000 m) above the Black Sea in an area where internal waves reach the sea surface. Fig. 14b,c show two dimensional spatial spectra for fragments of these images [Bondur, 1993; 1995]. The spatial spectra for fragments of these images have quite a complex configuration, which is caused by the complex form of the slick formations. In fact, the spatial spectra of various image fragments with such formations can be quite dissimilar (see Fig. 14b,c).

The application of remote spatial frequency spectrometry has, for the first time, revealed a phenomena generating local, wideband, and short band ("quasi coherent") spectral harmonics in areas where various deep disturbances (internal waves, turbulence, current fields, etc) influence the perturbed sea surface [Bondur, 1993; 1995; 2000; 2001].

The generation of one or many "quasi coherent" systems of spatial harmonics is shown, for example, in the effects of deep outfalls on sea surface waves.

Fig. 15 shows the appearance of such effects revealed through two dimensional spatial spectra of space images taken onboard the IKONOS-2 satellite, with spatial resolution of about 1 meter, over Mamala Bay off Honolulu, Hawaiian Islands.

The experiments were conducted in September 2002, within the framework of a Russian-American project for monitoring anthropogenic effects on the ecosystems of coastal waters. Fig. 15a shows the initial space image of an area with a deep outfall from Sand Island. Local subimages of size 1x1 km^2 (1024x1024 pixels) were used for spatial spectral processing. Fig. 15c shows a portion of this image with three areas identified below the diffuser of the discharge pipe (marked in orange) in the area of the outfall (anomaly) and far from it (background). Fig. 15d shows a two dimensional spatial spectrum of the background fragment and Fig. 15e shows three analogous spectra of anomalous fragments in the outfall area. As can be seen from the given illustrations, the spectra of the anomalous fragments clearly show additional thin ("quasi coherent") spectral components (central frequency $\nu \sim 0.01075$ m^{-1}, wavelength $\lambda \sim 93$ m). Their generation is related with "quasi coherent" systems of high frequency internal waves,

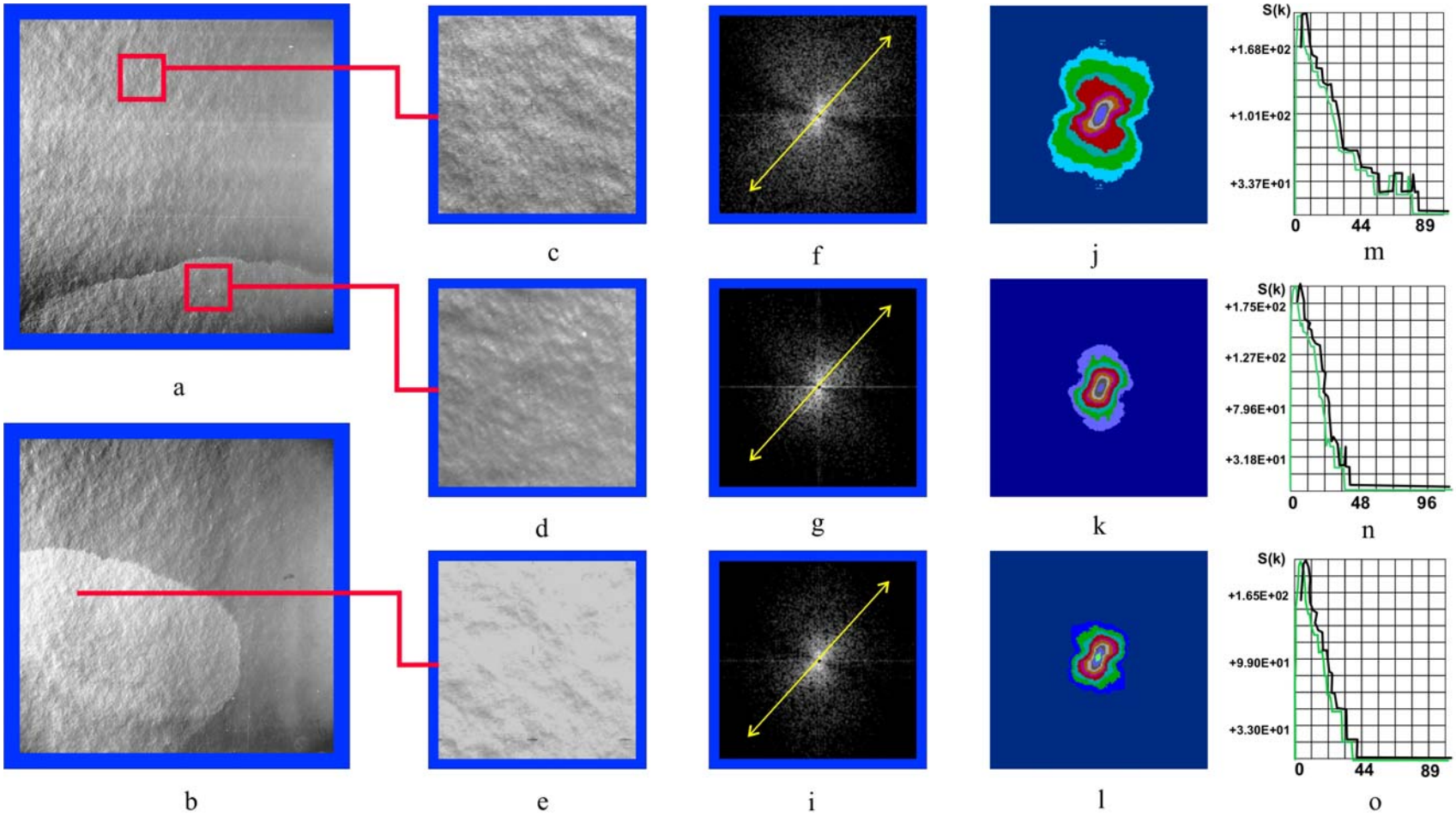

Fig . 13. Images of clean sea surface and with SAS film *(a), (b)*, fragments of images of clean sea surface *(c)* and with SAS *(d,e)*, relevant 2D spatial spectra *(f,g,i)*, 2D spectra after median filtration and color coding *(j,k,l)*, one-dimensional sections of 2D spectra in spectra in selected directions *(m,n,o)*

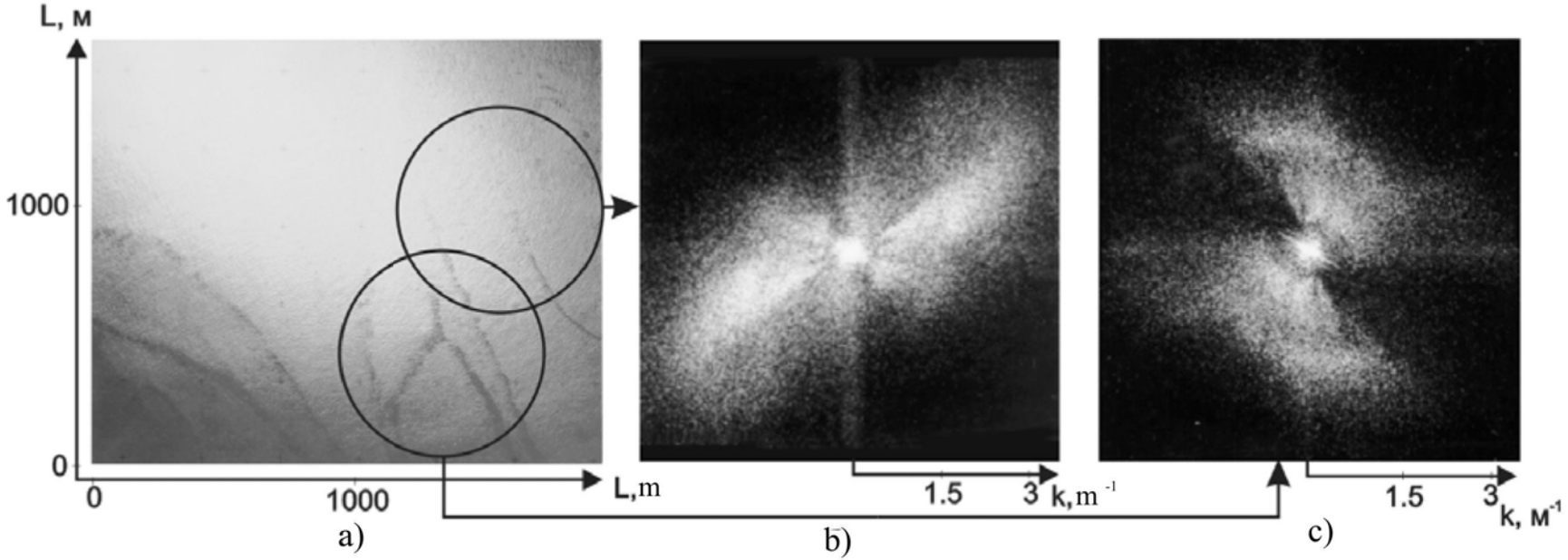

Fig. 14. Image of sleek fields caused by anthropogenic factors (a) and 2D spectra of its fragments (b, c)

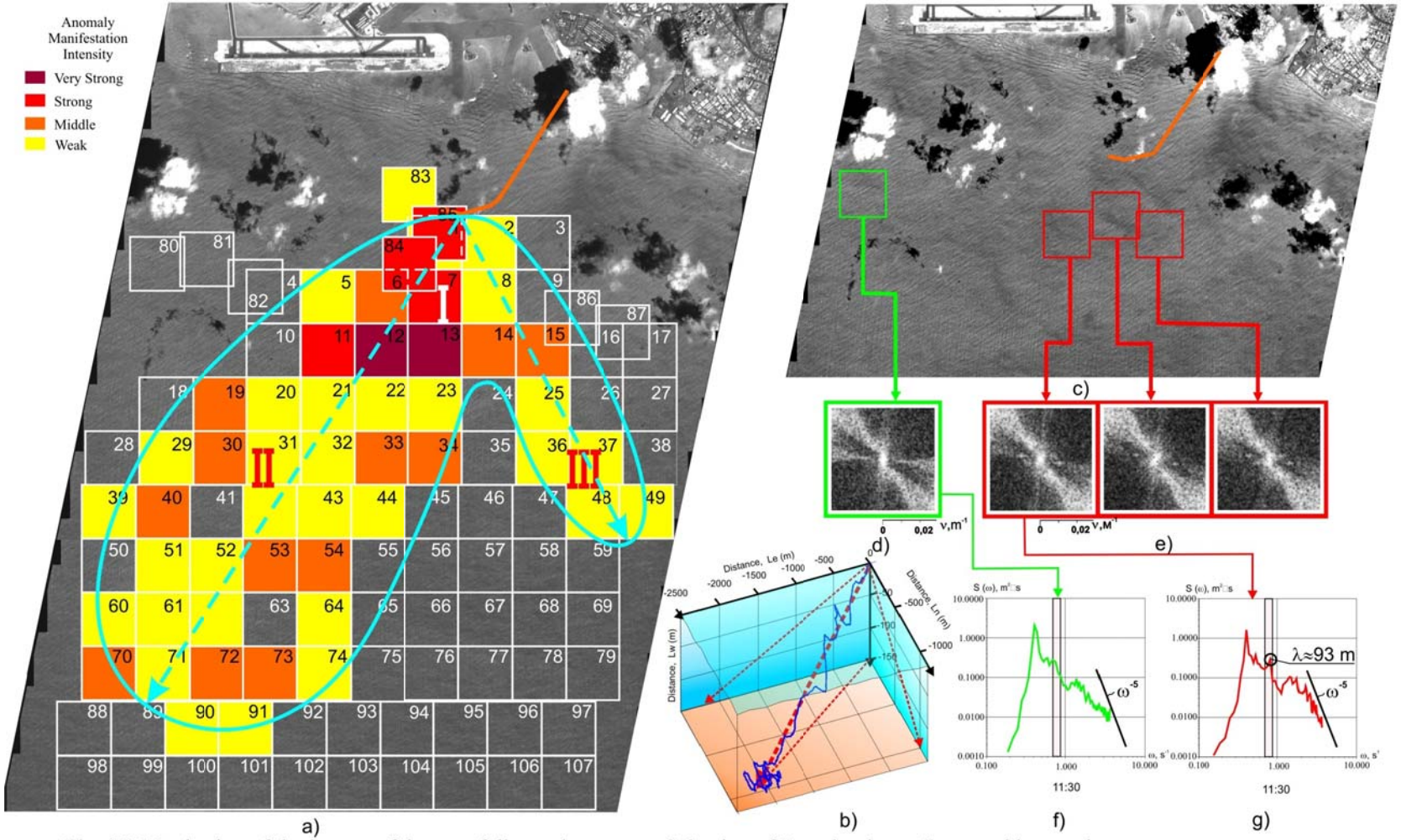

Fig. 15. Monitoring of the impact of deep outfalls on shore areas. Selection of "quasi-coherent" spectral harmonics: a) initial image (IKONOS, ~1 m resolution) with outlined areas for processing and anomaly zones; b) progressive vector diagram of current velocity; c) satellite image fragment; d), e) 2D background spectra (d) and anomaly fragments with manifestation of "quasi-coherent" harmonics (e); one-dimensional frequency spectra from wave sensors in background (f) and outfall (g) areas

caused by streams from the diffuser of the dumping device. The length of these waves is determined by the Brunt-Väisälä frequency $N = [-(g/\rho_0)\, \partial\rho_0 / \partial z]^{1/2}$.

Fig. 15d,e shows one dimensional frequency spectra obtained using wave-graphs at the moment of space imaging (11hours, 20minutes local time) in the outfall area (e) and in the background area, at distance ~ 9 km east of the diffuser (f). As can be seen from these illustrations, the additional spectral component, although not very evident, appears in the one dimensional spatial spectra measured for the outfall zone in the harmonics of the corresponding spatial frequency ν=0.01075 m^{-1} (wavelength $\lambda \sim 93$ m), determined by the dispersion relationship for gravity waves $\nu^2 = 4\pi^2 gk$.

The clear manifestation of such "quasi coherent" spectral components on Fig. 15c exemplifies the advantages of the two dimensional spatial spectral analyses of space images.

Fig. 15a shows the result from identification of a surface anomaly caused by the deep outfall. In this figure, local fragments of the image (size 1x1 km^2) which correspond to two dimensional spectra displaying "quasi coherent" spectral components are colored. The varying intensity of anomaly manifestation is identified using different colors, depending on the energy of additional harmonics. The dark red color corresponds to maximum energy – the presence of a very strong anomaly, the red color – a strong anomaly, orange – a medium anomaly, yellow –a weak anomaly (minimum energy). The entire zone of anomalies zone (highlighted in blue) has the shape of two lobes, the larger of which (length more than 11km and width of about 6km) is stretched in the south west direction (angle about 215°) and the second, smaller lobe (length about 6-7km, width about 2km) is stretched in the south east direction (with angle about 154°).

This form of the surface anomaly is caused by the constructive characteristics of the discharge pipe, which has a sectional diffuser with a specified angle between sections, which, along with the hydrodynamic effect of the current fields on the day of the experiment, caused the formation of the two lobes in the diagram.

Fig. 15b shows a three dimensional view of the progressive vector diagram for the current field. It was derived from data measured by acoustic Doppler current profilers installed near (east of) the diffuser. Fig. 15b clearly displays the direction of the three dimensional current velocity vector, with the dominant transfer moving in the southwest direction (angle about 120°), which is characteristic of the primary seasonal prevailing currents in this region.

This clearly explains the presence of the large lobe, and its direction (~ 215°), found through the spectral harmonics of local fragments from the space image.

At imaging from low elevations, and equipment coverage areas as large as the zone affected by deep hydrodynamic processes or anthropogenic effects, the manifestation of changes in the spatial spectra has a different character.

In these areas, contrasts in spectra develop which are related to the decrement in short wave attenuation [Bondur, 1987; 1991; 1993; 1995; 2000; 2001]. These phenomena are seen throughout the whole regional image and its subimages. For a definitive identification of zones caused by various effects it is necessary to process a series of sea surface images. From this, the spatial geometric and dynamic characteristics of such effects on the sea environment can be determined.

Fig. 16 shows images of clean sea surface (a) in an area of internal wave influence, and their corresponding spatial spectra (c,d), as well as one dimensional spectral cross sections received through processing of a series of similar images (e). A characteristic of the these images is that they are visually indistinguishable; however the spectrum in the area of internal wave influence (b) is more isotropic and substantially smaller, in comparison with the spectrum of undisturbed sea surface (a). This is related with the attenuation of short sea waves caused by internal waves [Bondur, 1987; 1991; 1993; 1995; 2000; 2001; Bondur, Voliak, 1984].

Fig. 16e shows one dimensional cross sections, averaged over 20 realizations and normalized to the full energy $S(k)/I_0$, of a clean sea surface - 1 (wind speed $W_в = 3 \div 4$ m/s) and

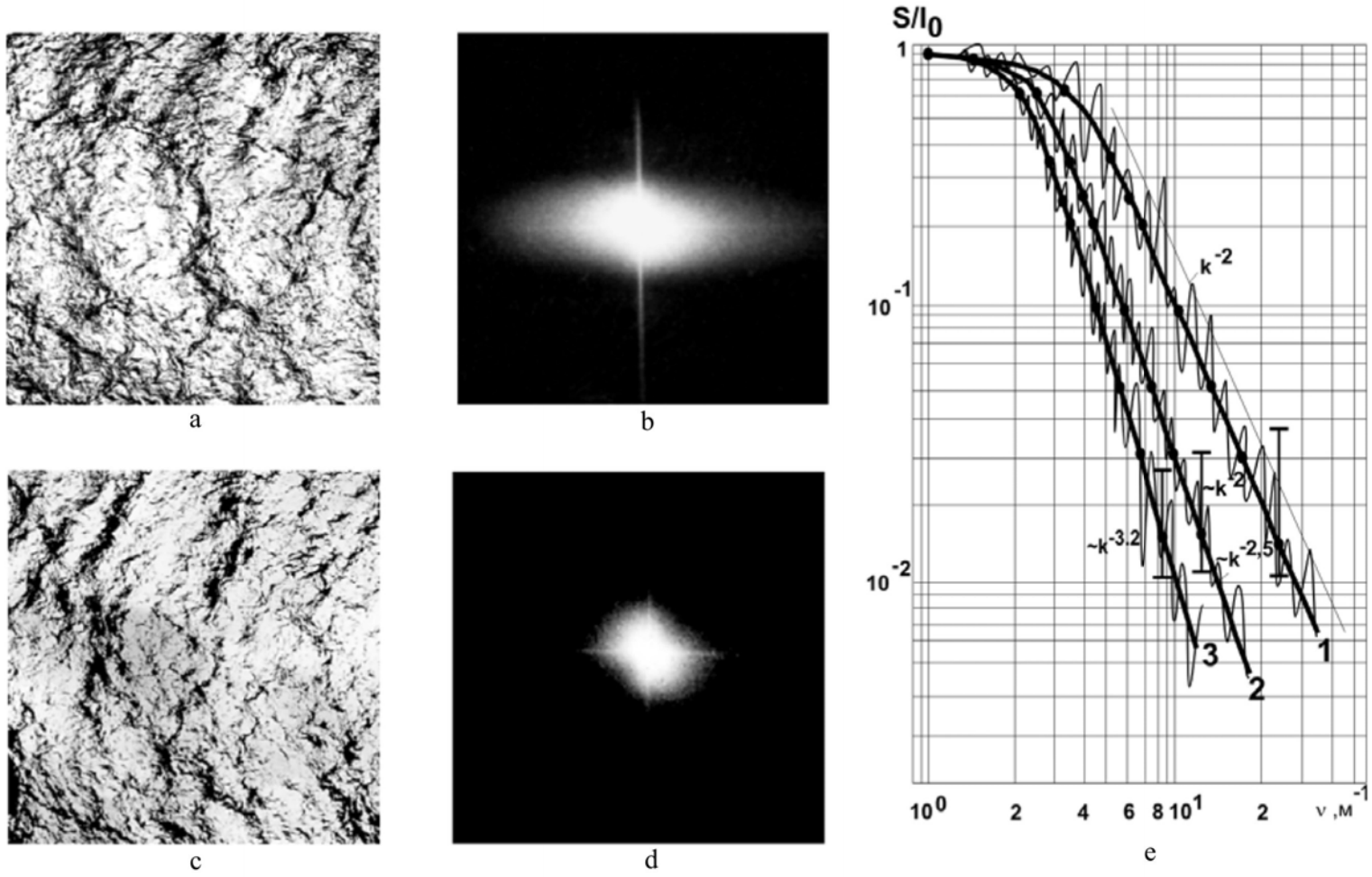

Fig 16. Images of clean sea surface (a) in the area of internal wave influence (b), their 2d (b, d) and one-dimentional (e) spectra

slicks, related to the effects of internal waves, with wind speeds $W_в = 1 \div 1.5$ m/s) - 2 and $W_в = 3 \div 4$ m/s - 3 depending on the spatial frequency ν [Bondur, 1991; 1993; 2000; 2001]. The displayed images reveal an appreciable difference in spectral densities for clean surface and for slicks; the difference in the spectrums increases with increasing spatial frequency and decreasing wind speed, which is the result of stronger small scale wave smoothing.

For approximations of spectral cross sections with the relationship $S \sim \nu^{-p}$, the incline indicators become $p_{ч.п.} \sim 2$ for clean surface, $p_c \sim 2.5$ for slicks with wind speeds $W_в = 3...4$ m/s and $p_c \sim 3.5$ for slicks with $W_в = 1...1.5$ m/s.

For the series of images in the area of internal wave influence and clean sea surface received from low altitudes with $W_в = 1.5 \div 8$ m/s, similar to the ones shown Fig. 16, statistical processing was conducted of spectral contrasts in the areas of slicks and clean surface for spatial frequency $\nu = 25 m^{-1}$.

$$K=-10 \lg [S(\nu)/S_{ч.п.}(\nu)], \quad (12)$$

Where $S(\nu)$ – current value of the spectrum for clean surface and slick; $S_{ч.п.}(\nu)$ – average value for selection of sea surface spectra outside the zone of anthropogenic influence.

Fig. 17 shows histograms of contrast distributions p(K) for one dimensional Wiener spectrum cross sections, for clean surface (a), and slicks, caused by manifestations of internal waves (b) and their combined distribution (c).

Under the histograms (Fig. 17a,b) the maximum K_{max} and minimum K_{min} contrast values from the analyzed selections are shown. For spectra of clean surface, these values were $K_{max} = 5$dB, $K_{min} = -5$ dB, and for slick spectra in areas of internal wave influence - $K_{max} = 20$dB, to $K_{min} = 0$dB.

To the left of the histograms we show parameters of distributions (central moments m_0, m_1, m_2, m_3; coefficients of variation V, asymmetries A, excess E; Pierson parameters), which in series with other characteristics can be used as informative indicators for two dimensional spectra in automated identification of internal wave influence zones, or areas of anthropogenic effects and their meaningful characteristics [Bondur, 1991; 2001]. For processing we used specially developed algorithmic software [Bondur, 1993; 1995; 2000; 2001; Bondur et al., 1986; Bondur, Starchenkov, 2001].

NEW APPROACHES TO USING RADAR METHODS

UNIQUE CHARACTERISTICS OF APPLYING RADAR METHODS TO OCEAN SENSING

Currently, radar methods of ocean sensing have undergone significant development. These methods provide lower spatial resolution and precision in comparison with optical methods, but they are all-weather and allow twenty-four hour monitoring.

The ability to study the ocean using radars installed on aerospace platforms is based on the following effects: [Avanesova et al., 1984; Bass, Fuks, 1972; Bondur, 1993; Bondur, Savin, 2000; Bulatov et al., 2003; Remote Sensing, 1984; 2000; Zidko et al., 1987; Zagorodnikov, 1978; Kalmikov et al., 1968; Kudriavtsev, 2003; Mur, Fan, 1973; Elachi et al., 1977]:

changes in the spectral composition of wind waves manifested as an attenuation or generation of wave components. This is registered by the radar as a change in signal level entering the radar receiver;

dynamic changes on the sea surface leading to Doppler changes in radar signal frequencies during appearance of local currents, caused by the presence of various deep processes and phenomena;

local changes in the dielectric permittivity of sea water, caused by various factors.

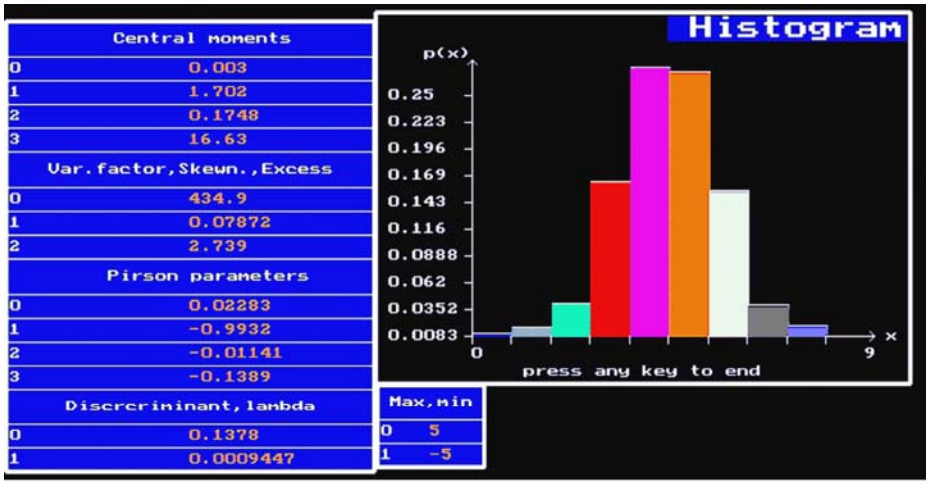

a

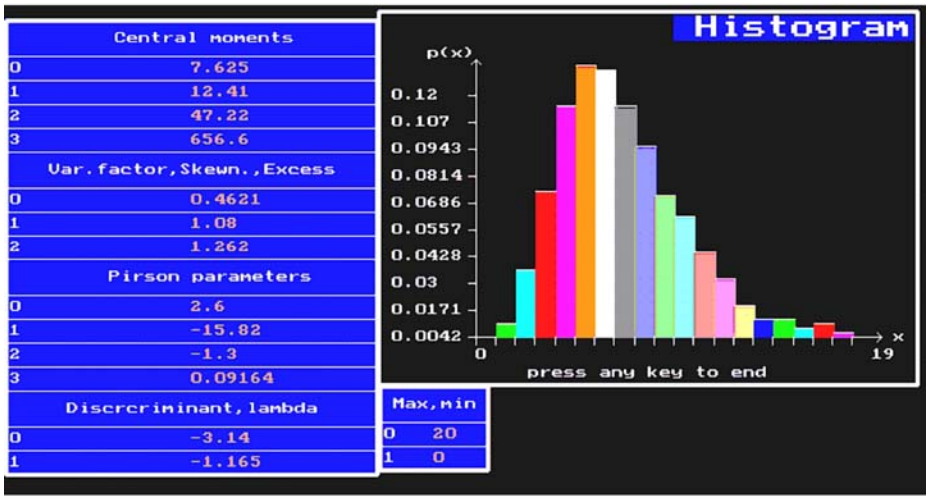

b

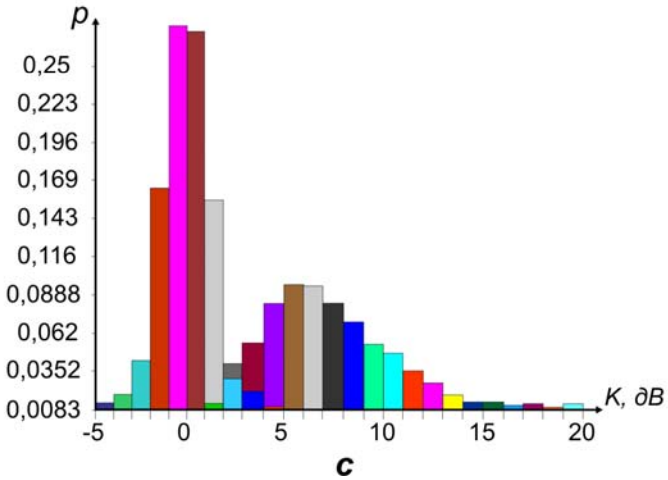

c

Fig. 17. Contrast histograms of one-dimensional sections of Wiener spectra for clean surface (a), slicks (b) and integrated histogram (c)

There are two primary types of radar used during remote sensing of the ocean: side looking radar (SLR) and radar with synthetic aperture (SAR).

The first type of radars are non-coherent systems that allow registration of a two dimensional image of the sea surface in a coordinate plane using the viewing distance and azimuth. The primary disadvantage of side looking radar is low spatial resolution.

We know of many types of radars that at various times were used for ocean study. As examples, let us note the results received from aerospace side looking radars "Neet" and "Toros" (USSR, Russia) [Avanesova et al., 1984; Bondur, Voliak, 1984; Bulatov et al., 2003], the “Chaika” space systems [Bondur, 1993; 1995; Bondur, Savin, 1992; 2000; Savin, 1993; 2000], "Kosmos-1500" [Bondur, 1993; 1995; Zidko et al., 1987; Kondratiev et al., 1992, Koptev, 1995; Lazarev et al., 1993] (USSR) and others, which have shown the ability to register spectral components of waving or zones of internal wave interaction with the sea surface, the ability to determine the speed of near-surface wind and other characteristics, as well as usefulness in ice control [Remote Sensing, 1984; 2000; Zidko et al., 1987].

For remote sensing of the ocean environment, it is most effective to use radars with synthetic aperture, using coherent accumulation of signals. For increasing the spatial resolution of radar images, signal phase data is used [Alperis et al., 1994; Zidko et al., 1987; Radiolocation, 1990]. The physical principal of synthesis is based on the procedure of concurrent filtration with correction of phase, so that all signals coming from the surface element during the time of synthesis Δt are co phased. This allows us to increase the spatial resolution on the sea surface to $d_A/2$, where d_A – real aperture of the antenna, independent of distance [Radiolocation, 1990; Zidko et al., 1987; The special issue, 1982; 1983]. Also, SARs can be used for estimating the current speeds on the sea surface due to the Doppler effect [Bondur, 1993; Bulatov et al., 2003; Zidko et al., 1987; Bondur, Savin, 2000; Satellites, 2001; Shamaev, 1994].

Radars based on the principle of synthetic aperture are a powerful means for receiving information about ocean conditions. Results are well known from the aerospace SAR system "Volna" [Bondur, Savin, 2000; Methods, 1996; Savin, 2000; Shamaev, 1994], "Ekor" [Vladimirov et al., 1991] (Russia), space-based SAR "Akor", which was installed on the spacecraft "Almaz" (USSR, Russia) [Alperis et al., 1994; Viter et al., 1994; Kondratiev et al., 1992; Lazarev et al., 1993], SAR “Sir A,B”, installed on the satellite "Seasat" (USA) [Lazarev et al., 1993; The special issue, 1982; 1983], SAR of the "RADARSAT" satellites (Canada), "ERS-1" and "ERS-2" (Europe) [Melentiev, Bobilev, 2000; Mitnik, 2003; ATSR, 1995; ERS, 1995; Johnson, Rodvald, 1994], «Space Shuttle» («Endeavour») (USA) [Satellites, 2001] JERS (Japan) [Garbuk, Gershenzon, 1997; Satellites, 2002] and others.

The data received from these SARs allowed estimation of the sea wave spectrum, parameters of internal waves in coastal areas, current speeds, bottom topography and other characteristics of the ocean over a wide area of surveillance, as well as ecological and ice monitoring.

FORMATION OF RADAR SEA SURFACE IMAGES

As is well known, the radar signal is formed by the concurrent effect of reflecting sea surface elements $z\ (x,y)$ taking into account the “weight” function of the irradiated area [Avanesova, Voliak, 1984; Bass, Fuks, 1972; Bulatov et al., 2003; Zidko et al., 1987; Zagorodnikov, 1978; Kalmikov, 2003; Mur, Fan, 1973]:

$$U_{вых}(xy) = \int_{-\infty}^{\infty}\int_{-\infty}^{\infty} z_м(xy)W(\xi - x, \eta - y)d\xi d\eta = z \otimes \hat{W}, \qquad (13)$$

Where (ξ, η)- two dimensional spatial impulse characteristics of the radar,

$\otimes$- symbol for convolution.

In accordance with the well known theory of radio wave scattering, the sea surface is divided into elemental scatters (facets) [Bass, Fuks, 1972]. If the angular size of these facets extends at least through the width of one interfering beam of the antenna directivity diagram (ADD), then the conditions of irradiation are equivalent to uniform irradiation, and the average value of the specific effective scattering surface $\overline{\sigma_0}$ does not depend on the sighting angle (or the sideslip angle Θ). The intensity of the reflected signal arriving at the input of the receiver $P_{вх}$, in this first zone is equal to [Zubkovich, 1968]:

$$P_{вх} = \frac{P_{пер} \cdot G_д^2 \cdot \lambda^2}{(4\pi)^3} \cdot \frac{f^4(\Theta)}{R_H^3} \alpha \cdot \frac{c\tau_u}{2} \cdot \sigma_0, \qquad (14)$$

Where R_H – slant range from the radar to the center of the irradiated area; $P_{пер}$- radiative intensity of the radar; G_0 - antenna coefficient of amplification (antenna gain); λ- radar wavelength; $f^2(\Theta)$ - characteristics of the ADD; α- width of ADD in azimuthally direction; c - characteristic of light; τ_u- duration of radiated impulse.

In the second zone, when the angular size of the facet takes up only a part of the ADD interferential beam, the intensity falls rapidly and becomes proportional to $P_{вх} \sim R_H^{-7}$ [Avanesova, Voliak, 1984; Bass, Fuks, 1972; Bulatov et al., 2003; Elachi, Brown, 1977].

The borders of transition between these two zones corresponds to the declination angle, equal to

$$\Theta_{гр} \approx \frac{\lambda}{5h_M}, \qquad (15)$$

where h_M - height of the wave.

When the height of the wave is small, the transition borders appear already at sideslip angles ~10-12°. As wave intensity increases, this border moves away towards smaller values ~0.5°-1° (h_M~0.5-1 m). In this case the specific effective scattering surface (SESR) of the sea surface at $\Theta > 50°$ can be expressed as [Zubkovich, 1968; Bass, Fuks, 1972]:

$$\sigma_0(\Theta > 50°) = \frac{\left|\Gamma_0(\varepsilon_{МП})\right|^2}{2\sigma_\Theta^2} \cdot \exp\left(-\frac{tg^2\beta}{2\sigma_\Theta^2}\right), \qquad (16)$$

where $\beta = 90° - \Theta$- angle, measured from nadir;

$\Gamma_0(\varepsilon_{МП})$- Fresnel complex coefficient of reflectivity (at Θ=90°);

$\varepsilon_{МП}$- relative complex dielectric permittivity of the sea surface;

σ_Θ^2- dispersion of sea wave slopes.

Where Θ < 50°- radar dispersion by the gently sloping structure of the sea surface can be expressed as [Kalmikov et al., 1968]

$$\sigma_0(\Theta < 50°) = 4\pi\left(\frac{2\pi}{\lambda}\right)^4 \cos\beta \left|\Gamma_\kappa(\varepsilon_{МП}, \beta)\right|^2 \Psi_h(\kappa), \qquad (17)$$

where $\Gamma_\kappa(\varepsilon_{МП}, \beta)$- complex coefficient of reflection, different from Fresnel's;

$\Psi_h(k)$ - high quality portion of the spatial spectra of wind wave heights, not dependent on wind speeds $\vec{W}_в$ and determining the backscattering of the UHF signal from point $k = \frac{4\pi}{\lambda} sin\,\beta$.

As was already noted, one of the effects related with the manifestations of internal waves or anthropogenic effects on the sea environment is deformation of fine-structured components of sea waves, and the often appearing effect of "smoothing" or generation of additional spectral components [Arumov, Bondur et al., 1981; Bondur, 1991; 1993; 1995; 2000; 2001; Bondur, Voliak, 1984; Bondur, Grebenuk, 2001; Ermakov et al., 1982; Monin, Krasitski, 1985].

Clearly, the appearance of changes in density of the height spatial spectrum $\Delta\Psi_h$ due to the effect of sea surface "smoothing" or generation of additional spectral components will lead to the

appearance of relative contrasts $\Delta\Psi_h/\Psi_h$ and, therefore, to contrasts in the SESS $\frac{\Delta\sigma_0}{\sigma_0}$, that will be detected by the radar.

For analysis of the influence of changes in the dielectric permittivity of the sea environment during calculation of the signal fields reflected from a statistically uneven surface, we can use the Kirchoff approximation [Bass, Fuks, 1972; Bulatov et al., 2003; Kalmikov et al., 1968; Kudriavtsev, 2003; Elachi, Brown, 1977].

In this case, the complex amplitude of the signal (voltage) exiting from the receiving antenna is written as [Bass, Fuks, 1972; Methods, 1996; Shamaev, 1994; Elachi, Brown, 1977]

$$\dot{U} = \frac{jk_0 Q\dot{F}_0 \cos\beta_0}{2\pi R_0^2} \iint_S G^2(\alpha_a, \beta_a) exp\left[-2jk_0(R_1 - h\cos\beta)\right] dxdy, \qquad (18)$$

where $k_0 = \frac{2\pi}{\lambda}$ - wave number of the radiated electromagnetic wave;

$$Q = \sqrt{\frac{P_{изл} G_0 A_{эфф} R_{нагр}}{2\pi}};$$

$$F_0 = 1 - \frac{2\cos\beta_0}{\sqrt{\varepsilon}},$$

$A_{эфф}$ - effective area of the antenna; $R_{нагр}$ - active resistance of the receiving antenna; $\dot{\varepsilon}$ - complex relative dielectric permittivity of the environment; R_0 - distance to surface (without unevenness); h - height of unevenness; R_1 - distance to surface (with unevenness); β_0 - beam declination angle (β_0=90^0-θ); $G(\alpha_a, \beta_a)$ - coefficient, taking into account the seafloor form.

Changes in the complex dielectric permittivity of water $\Delta\varepsilon$, for example, under the influence of deep hydrophysical processes or anthropogenic influences, will lead to a change in signal amplitude entering the receiving antenna ΔU (caused by the change F_0), i.e. to a relative contrast $\left(\frac{\Delta U}{U}\right)_{загр.}$ in areas of such effects.

The mapping on radar images of centimeter waves, and also the energy carrying components of waves, is explained by the "two-scale model", which takes into account the resonance (Bragg) mechanism of ripple dispersion on the waves, as well as modulation due to large scale waves [Bass, Fuks, 1972; Zagorodnikov, 1978]. This problem with the "two-scaled model" is solved using the method of small disturbances, determining the resonance scattering mechanism and Kirchoff method, describing high smooth disturbances, the height of which is large in comparison to the radio wave lengths. The averaged value of the SESS, the specific effective scattering surface, depending on the local sideslip angle, in this case is determined by the expression [Bass, Fuks, 1972; Bulatov et al., 2003; Zidko et al., 1987; Zagorodnikov, 1978]:

$$\sigma^0(\theta) = \iint \sigma_P^O(\theta) P(\nabla\xi_x, \nabla\xi_y) d\nabla\xi_x d\nabla\xi_y, \qquad (19)$$

where $P(\nabla\xi_x, \nabla\xi_y)$ - density of wave incline distribution; $\sigma_P^O(\theta)$ - SESS, specific effective scattering surface determined from (11).

Note, that the mentioned theory for radar signal formation describes quite well the back scattering of radio waves at sideslip angles $\Theta \geq$ 10…20°. For sideslip angles less than 5°…10°, shadowing of waves significantly affects the SESS. Therefore, for lesser sideslip angles (usually characteristic of airplane-based radar), it is necessary to take into account other mechanisms for formation of radar images.

A series of works, an overview of which was published in Bulatov et al., 2003, were dedicated to nonresonant mechanisms of radio wave scattering by the sea surface. This has allowed the authors to propose a modification of the "two scale model" by adding another scale, and taking

into account the contribution of steep breaking waves, the sizes of which (length ~ 1 m, height 10…20 cm) occupy a middle position between Bragg (centimeter) waves and longer (decimeter) gravity waves. Such a model allows us to consider the unique characteristics of radar signal formation at glancing ocean surface sensing angles.

PHYSICAL BASIS AND ESSENCE OF MULTIFREQUENCY RADIO WAVE TOMOGRAPHY

Based on the discussed principles of formation for radar signals from the sea surface, a series of methods for radar sensing are developed. Among them we should note the method of "Multifrequency Radio Wave Tomography" (Fig. 14, 15) [Bondur, Savin, 2000; Methods, 1996; Shamaev, 1994]. Taking into account the well known simplifications of the above mentioned theoretical assumptions, it can be determined that reflected radar signals are proportional to amplitudes of wave components, satisfying the conditions of resonance (Bragg) scattering [Bass, Fuks, 1972; Zubkovich, 1968; Kalmikov et al., 1968; Mur, Fan, 1973; Elachi, Brown, 1977]

$$k = 2\,\mathrm{k_o}\,\cos\theta, \qquad (20)$$

where k - wave vector of the surface wave; $\mathrm{k_o}$ - wave vector of the radiated electromagnetic wave; θ - sideslip angle.

The model of resonance refraction (19) can be accepted for sideslip angles θ of no less than 5^0. This is confirmed by numerical experiments based on Kirchoff's method, which solve the problem of diffraction from an uneven surface [Avanesova, Voliak, 1984; Bass, Fuks, 1972; Bulatov et al., 2003; Kudriavtsev, 2003; Methods, 1996; Shamaev, 1994].

The radar registers the energy of the reflected signal, which is determined by the specific effective scattering surface (SESS).

$$\sigma_{p}^{o}(\theta) = 16\pi k^4 \left|F(\varepsilon,\theta)\right|^2 S\left(\bar{k}_p\right), \qquad (20)$$

where $\bar{k}_p$ - wave number of the resonance scattering wave; $F(\varepsilon,\theta)$ - function, depending on the dielectric permittivity and sensing angle; $S\left(\bar{k}_p\right)$ - value of the wave spectrum at resonance wavelength.

In analyzing the spectral composition of wind waves, we should deduce from the dual effect of deep hydrodynamic processes a deviation of the radar signal from Bragg condition results and from the condition connecting the average ocean wave length $\bar{\Lambda}_{мв}$ for energy-carrying waves with $W_в$ wind force through the presence of small "ripples".

As is well known, the signal spectrum of ocean and sea waves is quite broad (from millimeter waves to waves with lengths in tens and hundred of meters) [Veter, 1986; Davidan et al., 1985; Monin, Krasitski, 1985; Rozkov, 1979]). Therefore, in the surface waves spectra there always exist Bragg components to which different types of radars respond [Bass, Fuks, 1972; Zagorodnikov, 1978; Zubkovich, 1968; Kalmikov et al., 1968; Mur, Fan, 1973]. Therefore, as was already noted earlier, any changes in the spectral composition of the wave components will be registered by a radar observing the sea surface, initially in the form of changes in received (reflected) signal amplitude.

In fact, in an area where internal waves exit or pollutants appear on the surface, there can be a decrease in the SESS, specific effective scattering surface (negative contrast), in the case of sea waving state greater than 0, or an increase in the SESS (positive contrast), in the case of 0 intensity (calm weather). This is also an effect caused by the case where there are entrained bubbles or particulates in pollutants [Avanesova, Voliak, 1984; Bondur, 1991; Bondur, Voliak, 1984; Bulatov et al., 2003, Methods, 1996].

In the second case, influence on the sea surface causes changes in the period of long-wavelength energy carrying spectral components due to decreased effectiveness of energy transfer from ripples to long waves $\Lambda_{мв}$ [Bondur, 1993; 2000; Bondur, Voliak, 1984; Methods, 1996; Bondur, 1995].

The relationship of $\Lambda_{мв}$ and $W_в$ (wind speed) is achieved through the coefficient $q_в$, which for developed waves has a value of about $q_в \approx 1.92$, so $W_в \approx q_в \sqrt{\Lambda_{мв}}$ [Veter, 1986; Monin, Krasitski, 1985; Oceanology, 1978].

In exceptions related to the appearance of deep disturbances or pollution of the sea environment, the relationship coefficient $q_в$ changes. In constant wind speed this causes a change in average wave length $\overline{\Lambda}_{мв}$. Therefore, the radar must respond both to changes in the SESS and to local changes in average wave period $\overline{T}_в$ in the area of pollution. So it is efficient to have radar that works in two or more ranges of waves – centimeter, for identifying of changes in capillary waves, and meter (decimeter), in identifying the average length of energy carrying gravity waves.

In principle, it is possible to work in only one wavelength in the centimeter range, because long waves modulate the capillary waves; this is manifested in radar images as a periodic wave structure, and corresponding changes in wave periods in areas of deep processes or pollutant influence. However, in the interest of receiving the most information about the spectral composition of radar signals connected using the Bragg relationship with the sea wave spectrum, it is efficient to have on board the airborne platform during conduction of flight experiments radar working on two or more discrete wavelengths (λ_1 and λ_2...) [Bondur, 1993; 1995; 2001; Bondur, Savin, 2000; Methods, 1996; Shamaev, 1994].

After receiving the spatial spectrum *S(k)* of the radar signal from the sea surface (Fig. 18), we work from the effect of resonance refraction under which the length of the surface wave and the length of the radar wave are "tightly" related.

Therefore, if we choose radar wavelengths separate enough (wave numbers k_1, k_2 k_3 in Fig. 18), then we can in the first approximation estimate the frequency dependence of the sea wave spatial spectrum.

For defining the characteristics of curve *S(k)* under a limited number of radar carrying wavelengths, we use the dependence of wave numbers on the cosine of the sideslip angle (Θ). Under correctly defined experimental methodology, we can get, due to differences in sighting angle of the sea surface, additional components of the spectrum in the area of wave number changes Δk_i by about ~10-15% deviation from wave number k_i [Bondur, Savin, 2000; Methods, 1996; Shamaev, 1994; Bondur, 1995].

The actual influence of change in sea wave spectral composition by influence of deep disturbances or pollution is manifested in the appearance of increment $\Delta S_i(k)$ (Fig. 18).

Radar evaluation of the presence of currents on the sea surface can be conducted in two ways: spectral and Doppler. In the spectral method, based on the complete dispersion ratio

$$\omega = \left(gk\right)^{\frac{1}{2}} + U_T k \ , \qquad (22)$$

where U_T - current velocity, we must first find the frequency spectrum $S(\omega)$ (or instantaneous spectrum) and spatial spectrum *S(k)* (or the spectrum averaged across frames). After which, for the energy-carrying peak we find ω_{max} and k_{max} and calculate current speed U_T.

In the case of the Doppler method, we can immediately determine the Doppler shift of reflected signal frequency

$$F_D = \frac{2U_T}{\lambda} cos\,\Theta \, . \qquad (23)$$

If the current is perpendicular to the flight, then the radar beam is directed along or against the current. However, there exist complicating factors, first of all, those related with the final width of the beam $\alpha_{аз}$ (azimuthal antenna directivity diagram) and speed of carrier movement $V_н$, which caused the appearance of Doppler widening in the frequency spectrum

$$\Delta F_D = \left(\frac{2V_T}{\lambda}\right) \cdot \alpha_{аз} \, . \qquad (24)$$

The signal spectrum $S(\omega)$ from the radar, installed on a moving carrier, during observation of sea surface is formed through convolution of reflected signals $S_1(\omega)$ at the stationary antenna, and signal from radar movement $S_2(\omega)$ over still ("frozen") surface.

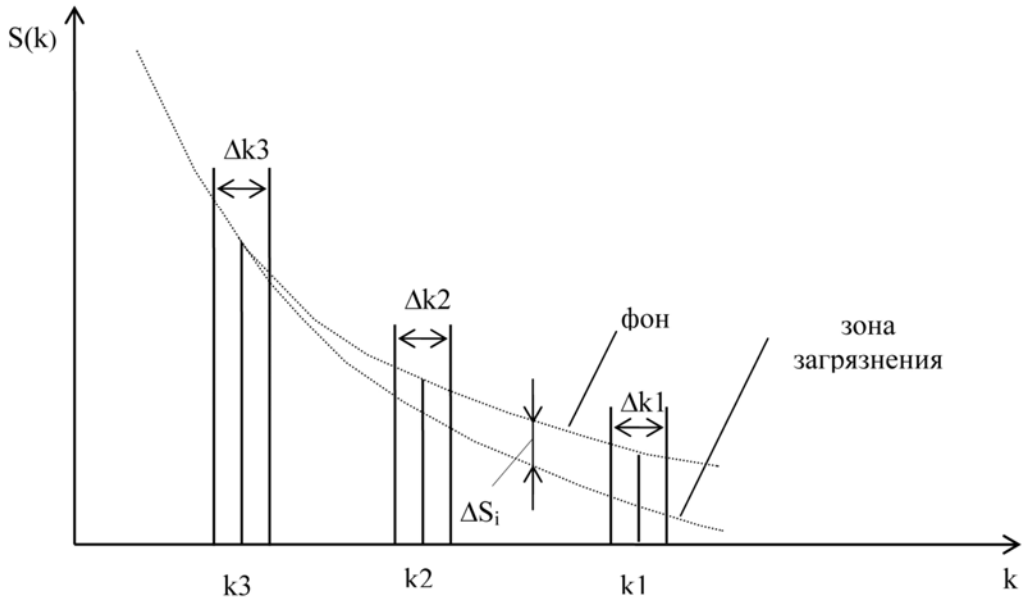

Fig. 18. Evaluation of sea surface spatial spectra with multi-frequency radio wave-graphy

In the case of the appearance of a current (and corresponding spectrum $S_3(\omega)$)), the signal spectrum $S(\omega)$ will be formed as a result of double convolution:

$$S(\omega)=S_1(\omega)*S_2(\omega)*S_3(\omega), \quad (25)$$

where * - convolution symbol.

The "convolution" operation includes cross-multiplication of areas and summation of dispersion. Therefore, in order to separate the components of the spectrum it is necessary to use other methods for radar surveillance. One such other method is the introduction of an additional beam $Л_2$, directed relative to the primary beam at some azimuthal angle $\varphi_{разв}$ (Fig. 19) [Bondur, Savin, 2000; Zidko et al., 1987; Bondur, 1995].

In addition, in order to identify the Doppler signal shift, it is necessary for the radar conducting surveillance to be coherent.

Clearly, in case of the existence of current there must be a widening of the signal spectrum, in comparison to the case where there is no current on the sea surface. In order to find this widening of the spectrum, it is necessary to either conduct imaging of the surface at two different times (one beam imaging), when there is current and when there is no current, or to conduct imaging of the surface simultaneously at two different points, one where there is current and one where there is none (two beam imaging).

Therefore, for measuring currents we must build the methodology of the airplane's flight in such a way that the primary beams of the radar ($Л_1$ at λ_1 and $Л_2$ at λ_2) are directed "with" or "against" the flow of polluting materials (Fig. 19).

In the case of a two beam system, we must conduct comparison of the Doppler shift in beams $Л_1$ and $Л_2$, and in the case of a one beam system, we can use a system of Doppler filters, calibrated to various Doppler frequencies in the reflected signal spectrum.

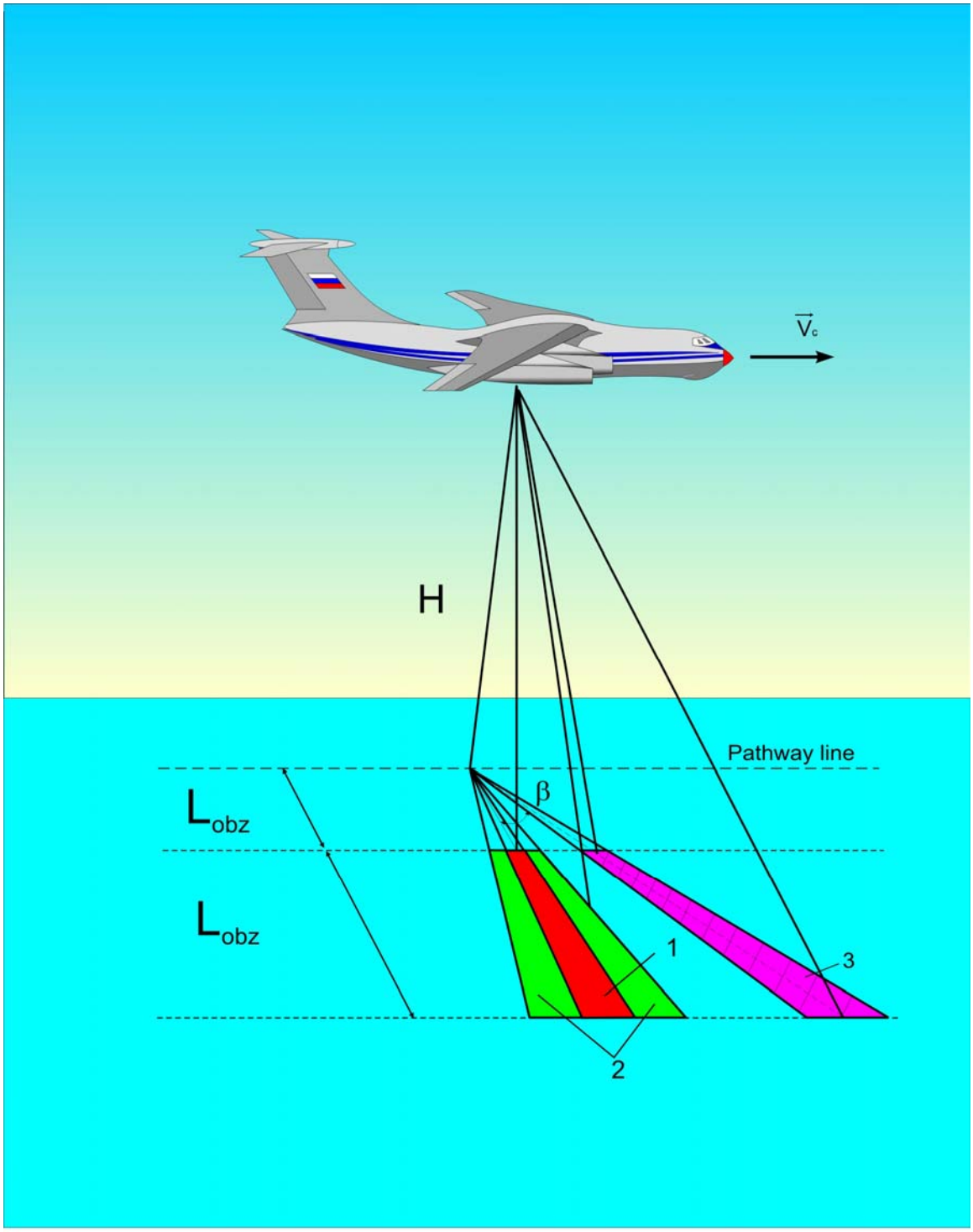

Fig. 19. Diagram of sea surface sensing using the method of multi-frequency radio wave tomography

The unique characteristics noted above show, that for the reconstruction of several harmonics of the spectrum we must use radars with multiple wavelengths λ_1, λ_2, different sideslip angles (Θ_1,Θ_2) and multiple beams (for example, two), distributed along the azimuth. Such a method has been named Multifrequency multiple beam Radio Wave Tomography [Bondur, 1991; 1993; 1995; 2001; Bondur, Savin, 2000; Methods, 1996; Shamaev, 1994; Bondur, 1995].

The essence of this method is illustrated on Fig. 20 [Bondur, 1991; 1993; 1995; 2001; Bondur, 1995]. It consists of the following:

formation of radar images on multiple, (assume, for example three), wavelengths (λ_1, λ_2, λ_3) under various viewing angles and under different azimuths using multiple, (three), beams (Fig. 20a);

reconstruction of the sea surface spectral characteristics (Fig. 20b);

calculation of informative indicators for initial radar images or their spectra, and statistical analysis of these indicators (Fig. 20c);

identification of regions of interest (Fig. 20d);

development of a map of the studied region with highlighted areas (Fig. 20e**)**;

determination of significant parameters of the water environment (Fig. 20f).

Practical realization of the method of Multifrequency Radio Wave Tomography is a powerful instrument for remote monitoring of the ocean.

EXAMPLES OF THE USE OF RADAR METHODS FOR OCEAN SURFACE SENSING

The effectiveness of radar methods for remote indication of various processes and phenomena in oceans and seas has been confirmed through many experiments [Arumov, Bondur et al., 1981; Bondur, 1993; 1995; 2001; Bondur et al., 1999; Bondur, Voliak, 1984; Bondur, Savin, 2000; Bulatov, 2003; Viter et al., 1994; Zidko et al., 1987; Zagorodnikov, 1978; Methods, 1994; Shamaev, 1994].

Fig. 21a shows a radar image, received from the Russian spacecraft “Almaz-1” in an area with various anomalies. These anomalies are identified on individual fragments (Fig. 21b,c,d,e). They are caused by slicks of various origins, including pollution and deep outfalls. The results of processing this image using specially developed algorithms and software [Bondur, 1993; 1995; Bondur, Starchenkov, 2001] are shown on Fig. 21f and fragments (Fig. 21g,h,i,k).

After processing, the clarity of the anomalies increased substantially (contrasts in signal amplitudes have increased from 2 to 10 times in comparison with the initial image). In all cases, anomalies appear as decreased amplitude of the radar signal from the (SESS specific effective scattering surface), caused by suppression of both gravitational and capillary wave components.

Fig. 22 shows, as an example, radar images (a,b,c), their two dimensional spatial spectra (d,e,f) and their azimuthal cross sections (g,h,i) in areas of internal wave manifestation (b,c). Two dimensional spectra in areas of internal waves are more elongated (Fig. 22e,f) in comparison with the more isotropic spectra of clean sea surface (Fig. 22d), which attests to the possibility of their automatic identification based on various informative indicators.

For automated identification of anomalies caused by various phenomena, for example pollution of the water environment, based on radar images, the first step is defining the system of identification, the essence of which is the creation of two separate classes, “background” and “anomaly”. In each class a selection of informative indicator values is conducted, their statistical characteristics are calculated, and corresponding thresholds for dividing these classes are determined. Then the selection under study is analyzed. Based on the values of informative indicators in this selection, the areas are assigned to one of the above mentioned classes using various criteria (Neiman-Pierson, Fisher, likelihood ratio, etc). Some results of such processing are presented in the works [Bondur, 1993; 2001; Bondur et al., 1999; Bondur, 1995].

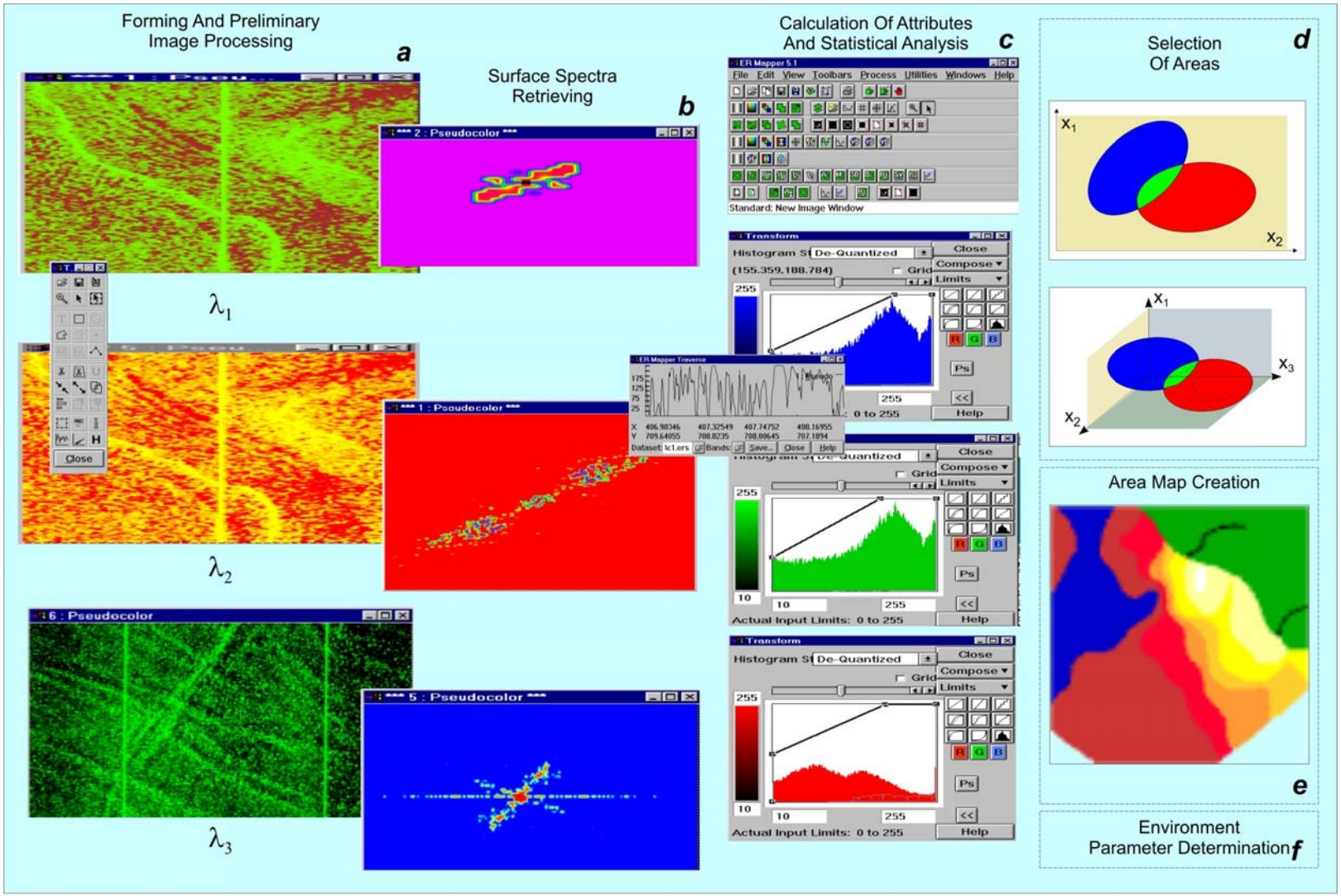

Fig. 20. Illustration of the main principles of the multi frequency radio wave recording

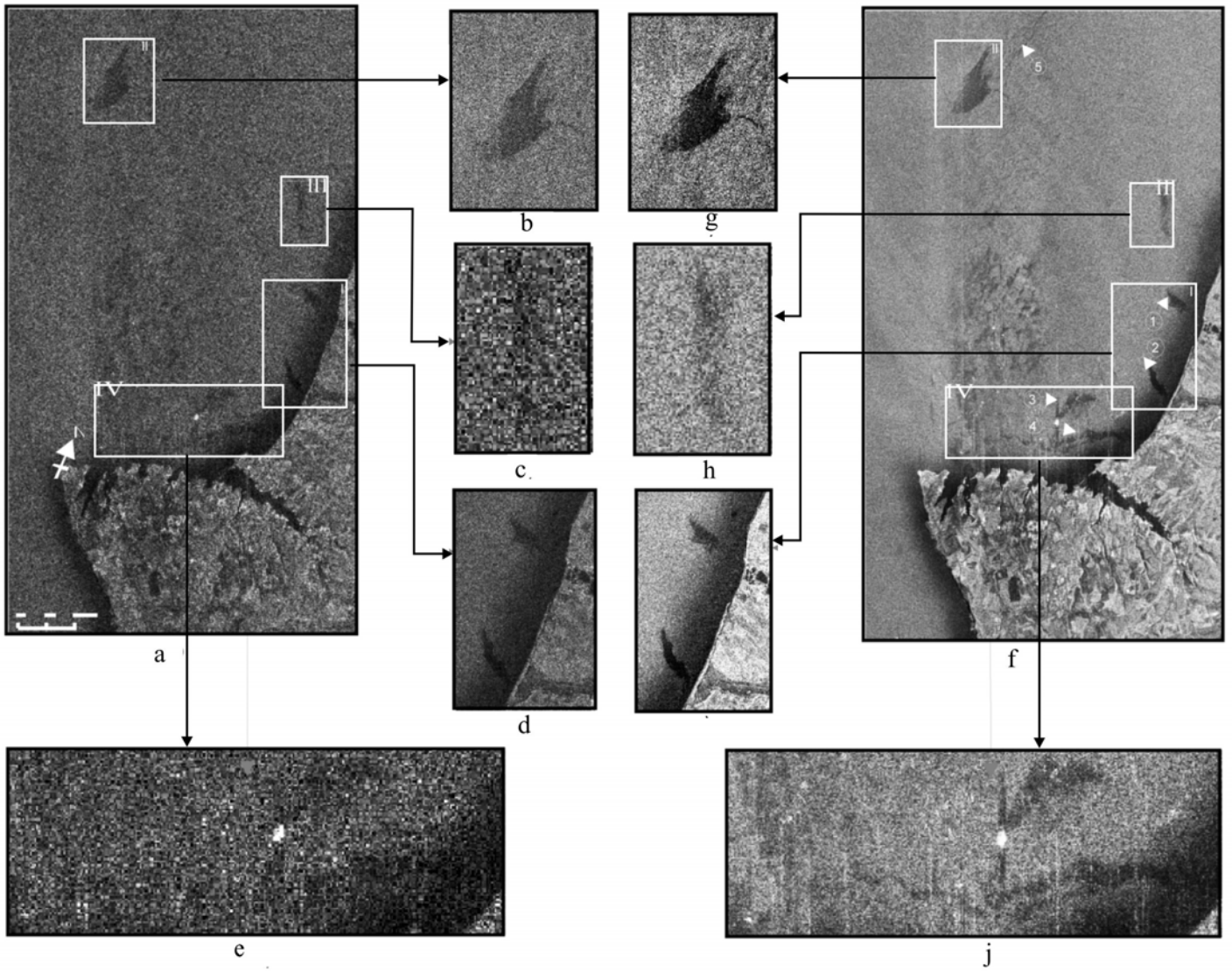

Fig. 21. Processing of space radar images of the Black Sea coastal area: a - initial image;
b, c, d, e - magnified fragments of the initial image; e - processed image;
g, h, i, j - magnified fragments of processed image

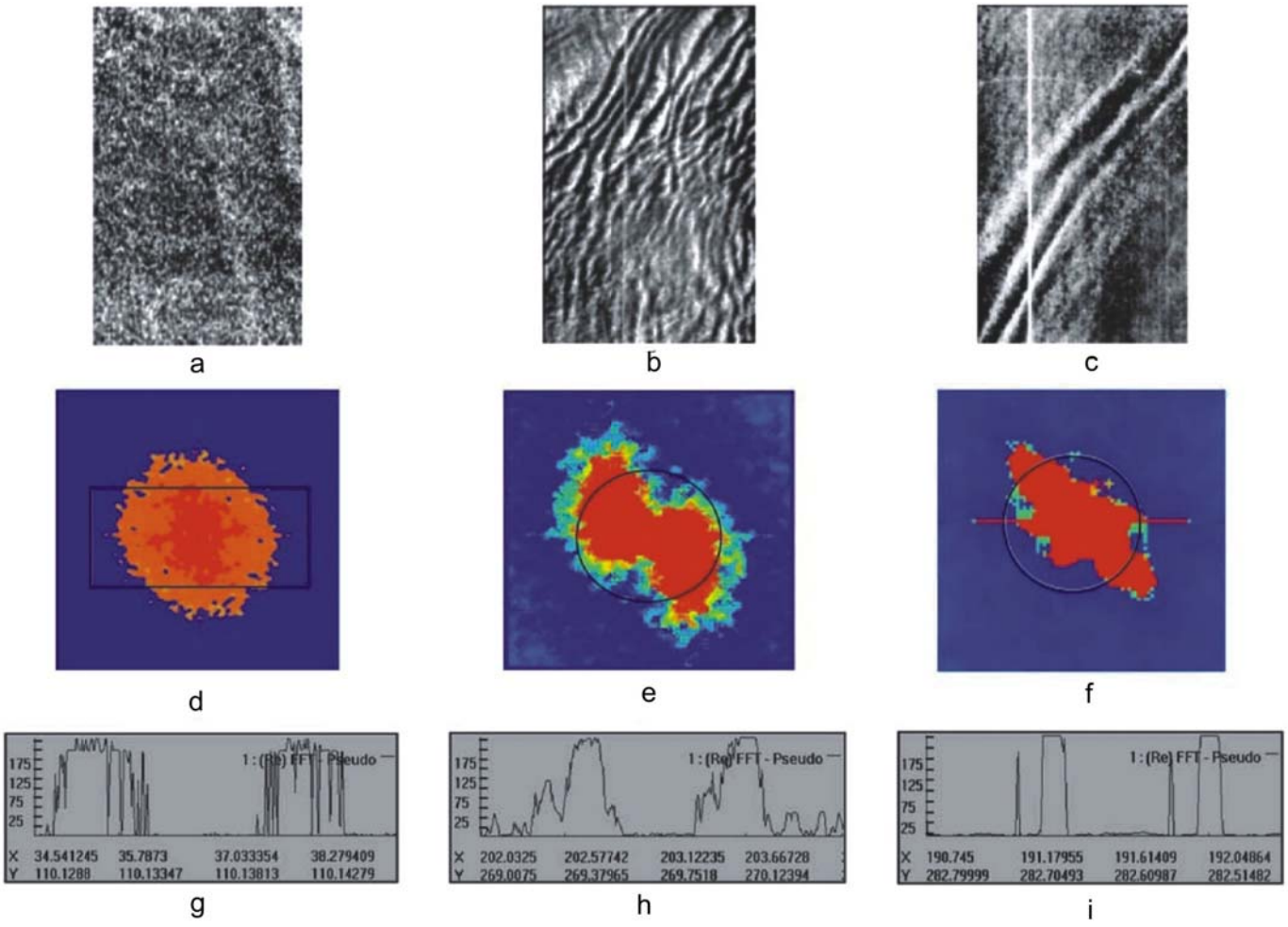

Fig. 22. Results of spatial spectral processing of sea surface radar image fragments:
a) clear sea surface; b), c) manifestation of internal waves; d), e), f) 2D spatial spectra;
g), h), i) cross sections in choosen directions

Fig. 23, 24 demonstrate with examples the capabilities of the developed methods. They show results received from satellites «JERS-1» and «RADARSAT» for coastal regions near the island of Oahu (Hawaii). Sections of these images were processed with the purpose of identifying pollution caused by river outfalls and deep dumps.

Fig. 23 shows the results of processing a radar image received by the satellite «JERS-1» (spatial resolution ~ 25 m, wavelength 23.5 cm, horizontal polarization).

Other than the procedures shown on Fig. 23 (formation of the two classes of selections, statistical analysis, two dimensional representation, classification), we also conducted initial processing. This processing consisted of smoothing and normalizing of the radar signal histogram, as well as filtering with a 3x3 pixel averaging filter for suppression of speckle-noise in the initial image.

For identification of pollution zones, we used a classification algorithm based on various types of inter-class distances from the teaching selection defined by the optimal informative indicators.

As a result of the conducted processing, three anomalous regions have been identified, labeled with numbers on the lower left fragment of Fig. 23. Anomalies 1 and 2 are caused by river outfalls in the western portion of the island of Oahu, and anomaly 3 is caused by the Waianae Outfall.

Fig. 24 shows the results of analogous processing of three radar images, receiving from onboard «RADARSAT» (spatial resolution 8-9m, wavelength 5.6cm, horizontal polarization). The images are received on September 4,6, and 11 for the waters of Mamala Bay, during an international project on monitoring anthropogenic influence on coastal waters, caused by a deep outfall from Sand Island (depth of outfall 70m, distance from shore 2.5km). Fig. 24a shows initial synthesized geo-referenced radar images, Fig. 24b – processed images with highlighting of magnified sections in areas of background and anomaly, caused by a deep outfall. The analysis of radar images, received on various days of the experiments under different hydro meteorological conditions, testifies to the different manifestations (size, contrast, form, orientation, distribution, etc) of the surface anomaly related with the slick, caused by the exit of the deep outfall's disturbance onto the surface.

The presented results testify to the effectiveness of the application of radar methods towards monitoring anthropogenic influence on the sea environment.

SPECTROMETRIC, MULTISPECTRAL AND HYPERSPECTRAL METHODS

For study of many processes and phenomena taking place in the depths, upper layer, and surface of oceans and seas it is very effective to apply spectrometric methods. These methods allow the identification of radiation spectra in the visible and infrared ranges of the electromagnetic spectrum, and characteristics of the sea environment such as spectral coefficients of reflection and absorption, coefficients of spectral brightness, concentration of suspended particles, etc. [Beliaev et al., 1978; Bondur, 1991; 1993; 1995; Kondratiev et al., 1992; Lazarev et al., 1993; Mishev, 1985; Moiseenko, 1994; Savinikh, Solomatin, 1995; Bondur, 1995; Johnson, Rodvald, 1994]. In conducting such studies, small-sized high speed spectrometers were used [Beliaev et al., 1978; Lazarev et al., 1993; Mishev, 1985; Moiseenko, 1994], as well as microprocessor video spectrometric systems, intended for formation, visualization, and registration of ocean target spectra along with simultaneous photography from onboard aircraft and piloted spacecraft [Kondratiev et al., 1992; Lazarev et al., 1993; Mishev, 1985].

For study of spectral as well as spatial characteristics of the sea environment, multispectral equipment can be used [Bondur, 1993; Garbuk, Gershenzon, 1997; Remote Sensing, 1984; Kienko, 1994; Kondratiev et al., 1992; Koptev, 1995; Lazarev et al., 1993; Moiseenko, 1994; Bondur, 1995;

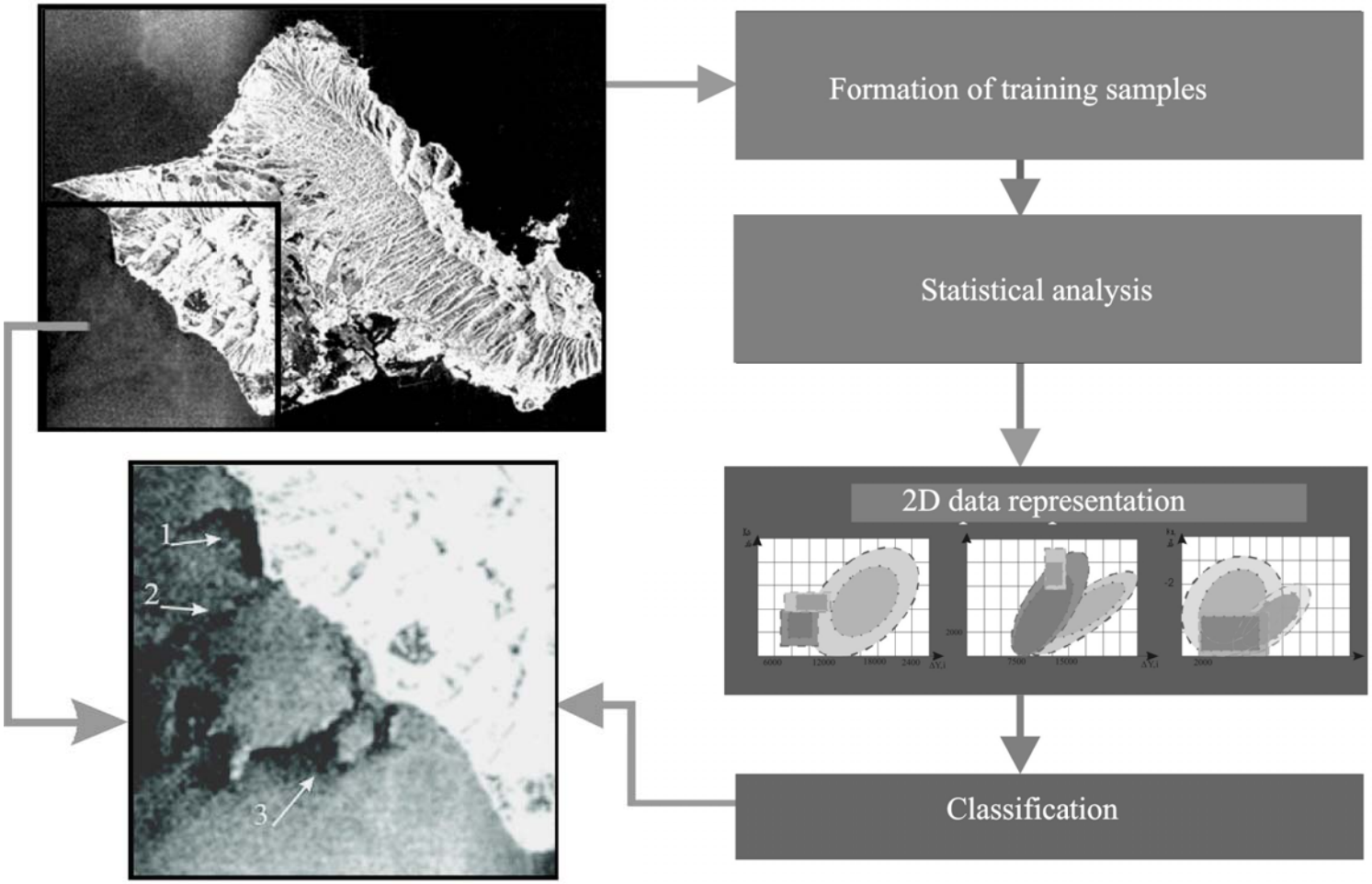

Fig. 23. Detection of anomalies caused by Oahu Island Outfall (Hawaii) from JERS satellite radar image

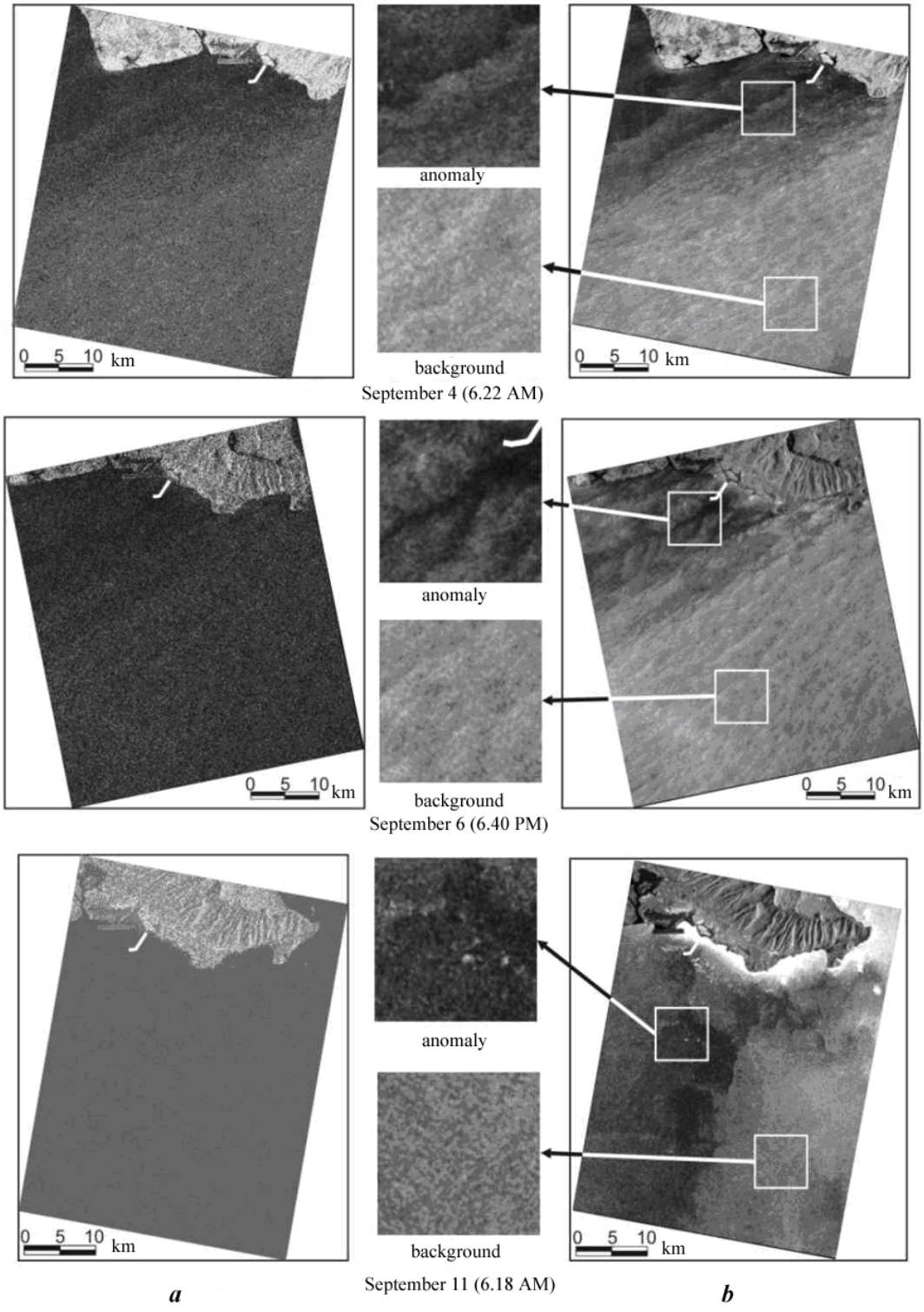

Fig. 24. Results of processing radar images taken by RADARSAT during monitoring of antropogenic influence on *Mamala Bay* (Honolulu, Hawaii) in September 2003:
***a* - synthesis of geometrically corrected and georeferenced images; *b* - processed images**

Johnson, Rodvald, 1994; Viktorov, 1996; MODIS, 2002], as well as so called hyperspectrometers, which allow for high speed formation of images, and simultaneous recording of information from a large number of adjacent spectral channels for each image channel [Bondur, 1993; 1995; 2001; Advanced, 1996; Bondur, 1995; Remote Sensing, 2002].

Some results of applying multispectral equipment towards global studies of the ocean are shown on Fig. 1 and 2 of this work.

Currently such studies can be conducted for example from onboard satellites AQUA and TERRAEO-1, etc.

The effectiveness of multispectral methods for regional studies is demonstrated on Fig. 25, which shows a series of images received in 1993 from Russian sensors (resolution ~ 12 m) (camera MK-4, spacecraft «RESOURCE-F») in various spectral regions of the visible range for an area of the Black Sea near the Crimean Peninsula. Based on this data, we can build maps of the studied region, consisting of a color-coded composition of images registered in various spectral ranges, allowing the identification of areas with differing spectral characteristics, caused by varying degrees of pollution. On these images it is clear that each different spectral range highlights unique characteristics of the sea surface and upper layer, and these are related to the influence of anthropogenic factors in coastal waters. The image presented in Fig. 25f, the result of joint processing, clearly shows the influence of Sevastopol's primary sewage outfall on the coastal waters.

Fig. 26 shows some results received from spaceborne multispectral equipment with high spatial resolution (about 4m) onboard the "Ikonos-2" satellite for coastal waters around Oahu Island, Hawaii.

The images, and the results of their processing shown on Fig. 26a, were received on July 28, 2000 in the area around the Honouliuli outfall. The images presented on Fig. 26b were received on September 2, 2002 in the area of Sand Island.

The sequence of steps for the processing method consisted of the following:

preliminary processing by convolution with a 3 x 3 pixel mask, increasing contrast for separate spectral channels, synthesis of pseudo-color images, light balancing based on spectral components;

thematic processing, consisting of the calculation of informative indicators, their statistical analysis, and nonparametric classification.

Fig. 26a shows initial fragments of channel images, as well as some intermediate and final results of multispectral image processing. Fig. 26b shows initial images and the final result of their processing. In both cases, the deep outfalls almost do not appear on the initial images. However, after processing, they are clearly visible. In both cases, the anomalies related with deep outfalls are caused by an increase in cloudiness of the near-surface ocean layers, which leads to an increase in light scattering, appearing most strongly in the blue and green spectral channels.

The more powerful outfall, from Mamala Bay in Sand Island (maximum capacity about 65 million gallons per 24 hours) discharge depth 70m, distance from shore approximately 2.5 miles) appears as a fairly large anomaly, having two clearly visible lobes, having southwest and southeast orientations. The length of the bigger lobe reaches about 9km, and the width about 3.8km. The smaller lobe has a length of about 2.5km and a width of about 2km. The form of this anomaly, associated with a deep outfall, is caused by the physical and geometric dimensions of the discharge device (diffuser length, and bends) as well as the specifics of the current fields on the day of the experiment. The currents, as well as profiles of temperature and salinity, were measured using stationary buoy stations and ships taking part in the experiment. These *in situ* results facilitated the analysis of space data.

One of the potential hyperspectral devices for monitoring coastal waters is the airborne AAHIS system, which provides imaging with speeds of 55 frames per second, width of coverage strip - 200m,

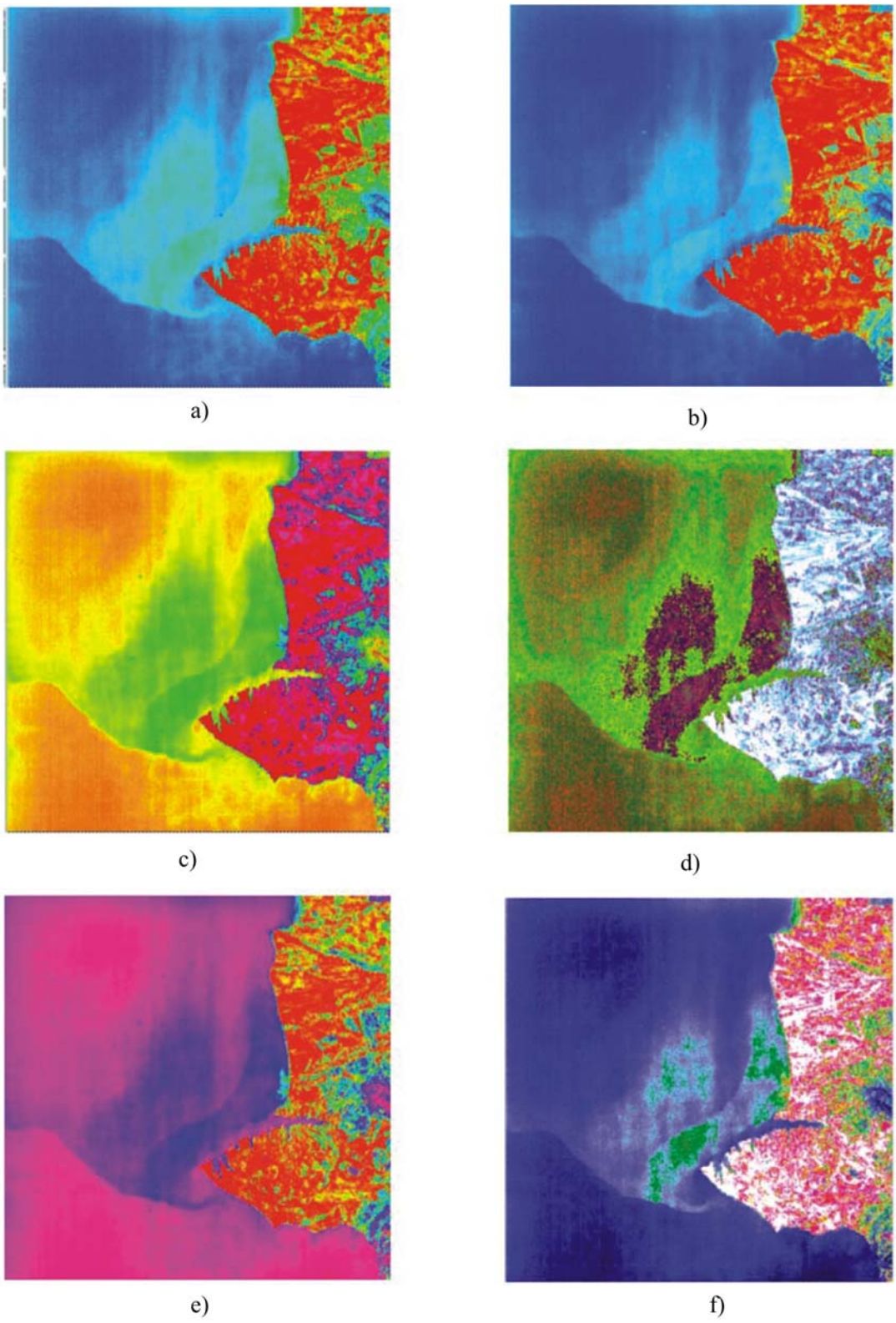

Fig. 25. Results of image processing for the Black Sea area near Sevastopol

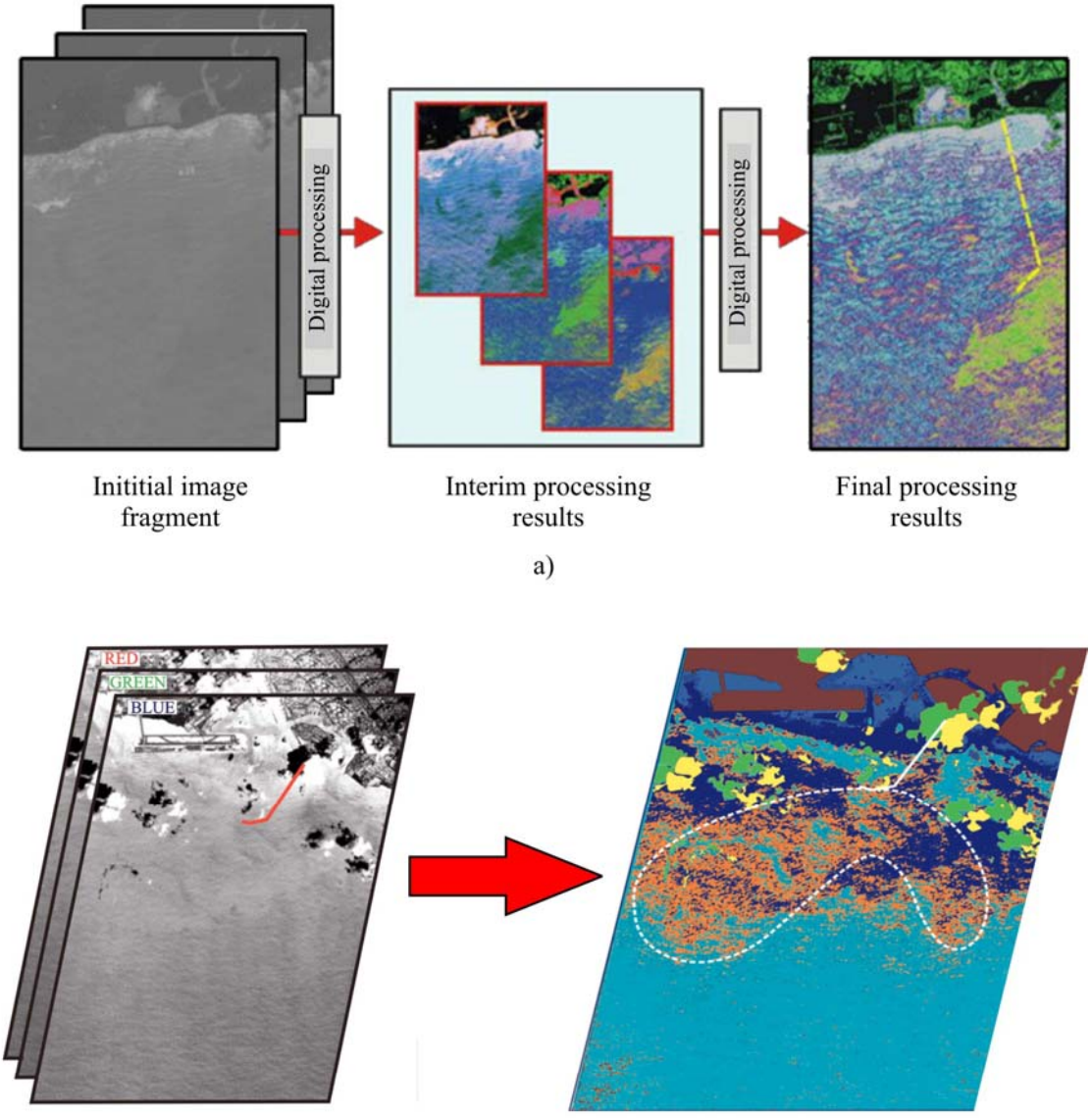

Fig 26. Detection of anthropogenic influence areas caused by Oahu Island outfall using multi-spectral space images: a) image processing for Honoululu outfall (July 28, 2000); b) image processing for Sand Island outfall (September 2, 2002)

and a spatial resolution of 1m from an elevation of 1000m. Every pixel of the image is divided into 288 spectral channels, in the range of 432-832 nm, with spectral resolution 5.5nm [Advanced, 1996].

The developed Russian hyperspectral device "Electron" provides a coverage strip of 300m and spatial resolution of about 0.8m from a 1km elevation. It provides spectral resolution of 5nm in the spectral range of 430-760nm [Bondur, Savin, 2001].

Currently, the problems preventing wide use of hyperspectral aerospace methods are a lack of effective methods for processing and interpretation, as well as the difficulty of accurately verifying data received in this way. However, at present these problems are the subject of intense activity and in the near-term we should expect promising results from the use of these highly capable sensors.

LIDAR METHODS

Lidar methods provide sensing of the ocean deep at depths of several tens of meters. Using them, we can measure the variations of such characteristics of the water environment as cloudiness, temperature, salinity, concentrations of primary biogenic elements, heavy metals, oil products, dissolved organic compounds, etc. These methods are based on various effects of laser radiation's interaction with the water environment [Bondur, 1993; Bondur, Zubkov, 2001; Bunkin et al., 1987; Klishko, Fadeev, 1978; Mezeris, 1987; Oceanology, 1978; Bondur, 1995; Keeler, Ulich, 1997; Keeler, 2003].

For measuring the physico-chemical parameters of the environment, we can use the laser-spark method, the method of laser correlation spectroscopy, and other methods.

The content of dissolved organic compounds can be measured by way of analyzing combinational refraction and fluorescence spectra, induced by laser radiation.

Using surface imaging lidars to evaluate the statistics of glint from a wind driven ocean surface, we can determine many characteristics of wind waves and their changes under the influence of various anthropogenic factors [Bondur, 1995].

Today, a new effective method for laser sensing has been developed, based on analyzing the local gradient extrema (LGE) in the backscattered return signal, related with the use of modified approximation of the lidar equation, taking into account the effects of multiple scattering in the small-angle approximation [Bondur, 1993; 1995; 2001; Bondur, Zubkov, 2001].

The method allows the determination of polluted zone size in three dimensions, its internal structure and dynamics, and study of the effects of natural hydrodynamic processes (tides, currents, and others) on these characteristics.

Fig. 27 shows examples demonstrating the capabilities of lidar sensing methods. These are the horizontal distributions of phytoplankton chlorophyll "a" (a), and fluorescence parameter (b) in the Black Sea's surface layer, obtained using fluorescence lidar.

Fig. 28 shows examples of applying the developed LGE method towards dynamic identification of zones containing anthropogenic influences, caused by pollution of near-surface ocean layers. Fig. 28a shows vertical distributions of local gradient extrema for clean water along a path of about 3km length, and Fig. 28b,d show these distributions for polluted zones. The maximum pollution appears as an increase in water cloudiness (brighter colors on Fig. 28b,d), and the localization of the pollution zone is found in the area of the thermocline layer (17c,d). From Fig. 28b,c,d we can see, that polluting compounds can seep through the thermocline layer (c) [Bondur, 1993; 1995; 2001; Bondur, Zubkov, 2001].

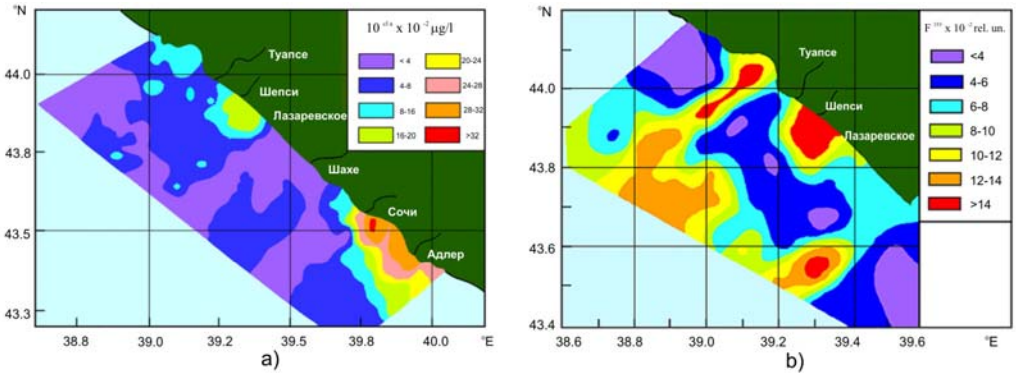

Fig. 27. Distribution of chlorophyll a phytoplankton concentration (a), and fluorescent parameter (b) in the subsurface layer of the Black Sea obtained with lidar method

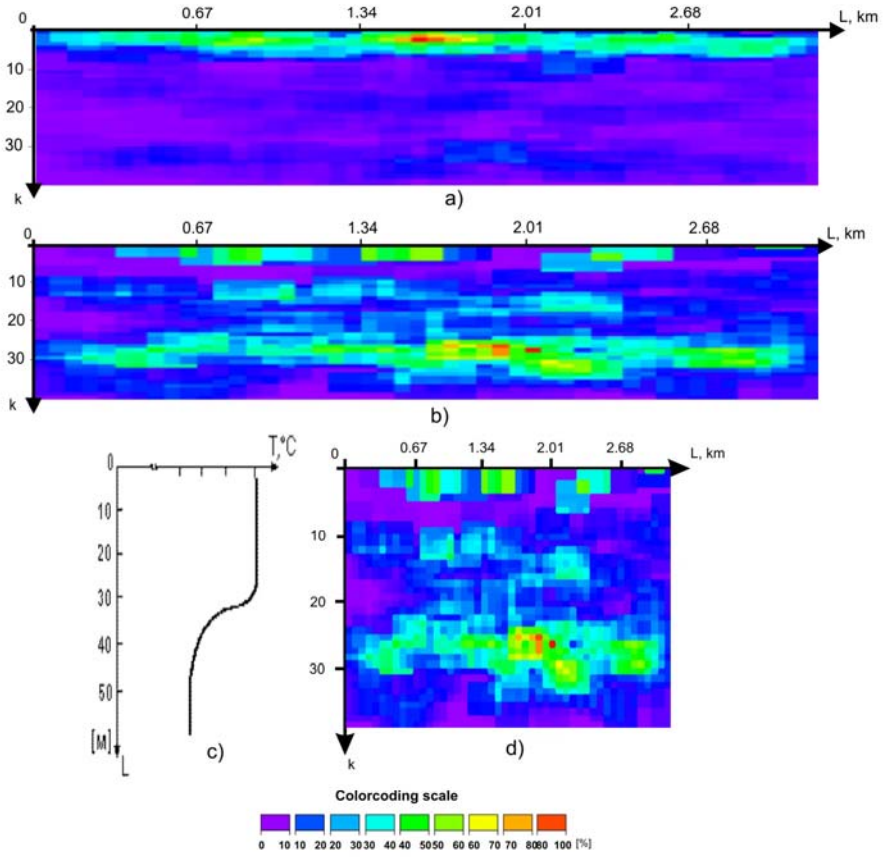

Fig. 28. Distribution of local extrema of the gradient in a vertical cross-section of the sea environment: a) clean sea water; b) contaminated water.
Comparison of laser sensing results (d) with contact measurements of the temperature profile (c)

NONCOHERENT PULSE ILLUMINATION AND SENSING OF THE SEA SURFACE

One of the more effective methods for remote sensing of oceans and seas is a method based on registering the brightness field reflected from the perturbed surface at its illumination with an impulse source. Such a method allows a substantial widening of the areas (time, weather) of application for remote systems, by providing the capability of 24 hour availability during various meteorological conditions.

The brightness field registered during impulse illumination of the sea surface by a source of small angular dimensions differs substantially from the brightness field of natural illumination. This is related to the fact that because of the small angular dimensions of the source, the primary contribution to the return radiation comes from glints, which originate at points of specular reflection and meet the following conditions.

$$\vec{n}_n' = 2(\vec{n}_n, \vec{n}) - \vec{n}_n \in \omega_L, \tag{26}$$

Where $\vec{n}_n$ - unit vector in the direction towards the receiver; $\vec{n}$ - unit vector of normal and surface; ω_L - cone, in which the source is seen from a point on the surface.

The brightness field of the disturbed sea surface can be written as:

$$L(x,y) = L_1[\varphi(x,y)] \cdot \delta[\bar{n}_n'(x,y), n(x,y)], \tag{27}$$

where $L_1[\varphi(x,y)]$ - brightness of the elongated glint patch visible at angle φ.

$$\delta(\bar{n}_n', n) = \begin{cases} 1, if\ \bar{n}_n' \in \varpi_L \\ 0, if\ \bar{n}' \in \varpi_L \end{cases} \tag{28}$$

The images, formed during illumination of the sea surface by an impulse source of small angular dimensions, can be used for evaluation of the function describing the distribution of sea wave slope and height spectra.

Such results provide critical input for determining the speed of near-surface winds, identification of pollution zones, evaluation of internal wave parameters, and current characteristics, for example.

Fig. 29 shows images of the sea surface obtained during experiments conducted from a sea-based hydrophysical platform in the area of Katsiveli Village, Crimea, during illumination by a noncoherent impulse source (xenon flash lamps with arc discharge, pulse energy 68 Joules, impulse duration about 3ms [Bondur, Borisov, 1988; Bondur, 1993]. The image, shown of Fig. 29a, was the result of stacking 32 pulses, and the images on Fig. 29b,c,d,e – are from only 1 pulse. The near-surface wind speed was $W_в$=6m/s.

local maxima visible on Fig. 29e at an angle of 30° from the horizontal correspond to surface waves with length λ ~ 5 cm.

Fig. 29f shows one dimensional cross sections of the two dimensional spatial spectrum on Fig. 29e, in the directions of ~ 15^o and ~ 30^o relative to the horizontal. On the one dimensional cross section of the spectrum obtained at the angle of ~ 15^o, we see a spectral maximum at wave number $k_0 \cong 120$ rad/m, as well as another maximum corresponding to the second harmonic at wave number $k_1 = 2\ k_0 = 240$ rad/m. Fig. 29f also shows results of approximations for various areas of the one dimensional spectra using the power function $\Psi(k) \sim k^{-p}$. The values of the power indicators for this approximation have values from -1 to 3, depending on the interval chosen.

These results demonstrate the effectiveness of this method for remote study of surface waves.

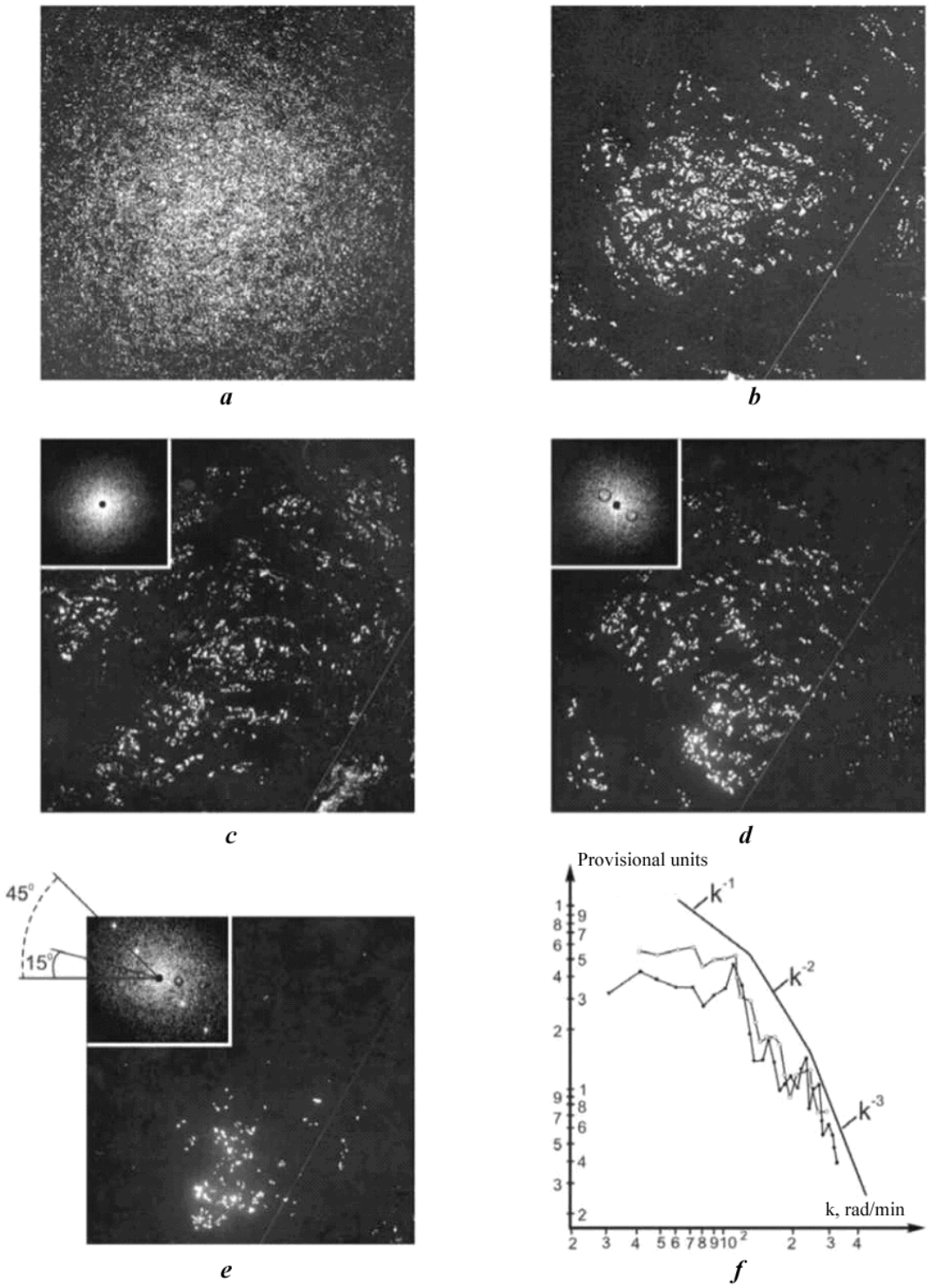

Fig. 29. Images of sea surface during impulse illumination with a non-coherent source: *a* - with 32 pulse accumulation; *b,c,d,e* - using a single pulse. 2D spatial spectra of relevant images (*c,d,e*). One-dimentional cross-section of 2D spectra (*e*) in specified directions (*f*).

Fig. 29,c,d,e also show two dimensional spatial spectra of the corresponding images, formed during impulse lighting. The prominent spectral maxima, visible on Fig. 29e at angle 45° are caused by a special mask, used for calibration of the results of coherent optical processing. The

METHODS FOR REMOTE IDENTIFICATION OF SEA BOTTOM TOPOGRAPHY

The study of seafloor topography, especially in coastal areas, has an important practical value. Today, measurement of bottom topography is usually done using sonar installed on ships; this allows mapping the bottom topography for limited regions. Topographic mapping over wide areas using traditional methods is very expensive and time consuming.

In the following section, methods for remote bottom topography of coastal zones are shown which are based on the detailed study of variations in surface wave characteristics. These variations reflect the hydrodynamics associated with bottom current flow over and around the various bottom topographical features [Bondur, 1993; 1995; 2001; Bondur, Grebenuk, 2000]. These methods are based on:

the use of dispersion relationships between frequency and length of surface waves during changes in sea depth;

refraction effects of surface gravitational waves in coastal areas;

on transformation effects of surface waves in a field of nonuniform currents, flowing through the uneven bottom topography.

In addition, bottom topography can be conducted through analysis of photodensitometric analysis of aerospace images.

Let us provide some examples of this technology which was used for the purpose of measuring bottom topography in coastal sea areas using optical and radar images.

Processing of radar images of the sea surface with manifestations of the seafloor topography allows collection of data on the spatial sizes and contrasts of regions where the surface wave structure is influenced by bottom topographic features.

Fig. 30 shows examples of processed radar images with surface manifestations of sea floor topography, obtained from the SAR onboard the "Almaz-1" spacecraft in the area of the Karskie Vorota Strait [Bondur, 1995; 2001; Bondur, Grebenuk, 2000].

On the image shown in Fig. 30a we see a complex surface picture, shown in the form of hydrological fronts caused by currents, and systems of internal waves having mostly sub-latitudinal orientation closer to Vaygach Island. On the radar image shown in Fig. 30b, we see trains of internal waves, a series of linear elements stretching from the Sakhalin Peninsula towards the southeast, and a series of linear anomalies in the northeast section of the image.

Existing bathymetric maps (scale 1 to 250,000) are shown on Fig. 30c,d.

Bathymetric maps revised based on radar images, with identified lineaments (dashed lines) are shown of Fig. 30e,f.

Fig. 31 and 32 contain the results of a remote study of bottom topography in the waters of Florida Bay, under the work of the Russian-American Commission on economic and technological cooperation [Bondur, 1995; 2001; Bondur, 1995]. For this, we used data received for the area around Caloosa Key, in the Florida Gulf (Fig. 31). For refining the bottom topography, we used maps (Figs. 31a,b), a bathymetric map, as well as optical images received from Russian space equipment (Cameras KFA-4000 – Fig. 30d and KVR-1000 – Fig. 31e) and from aircraft (Fig. 31c, from the American side).

Fig. 32a shows a map (scale 1 to 50,000) with initial bathymetry (dashed lines) and results of revision based on space images (solid line) [Bondur, 2001; Bondur, Grebenuk, 2000].

For validation of remote bottom topography identification methods and assessment of their effectiveness, results received from space images were compared with results of measurements by sonar, lidar, and measuring rod.

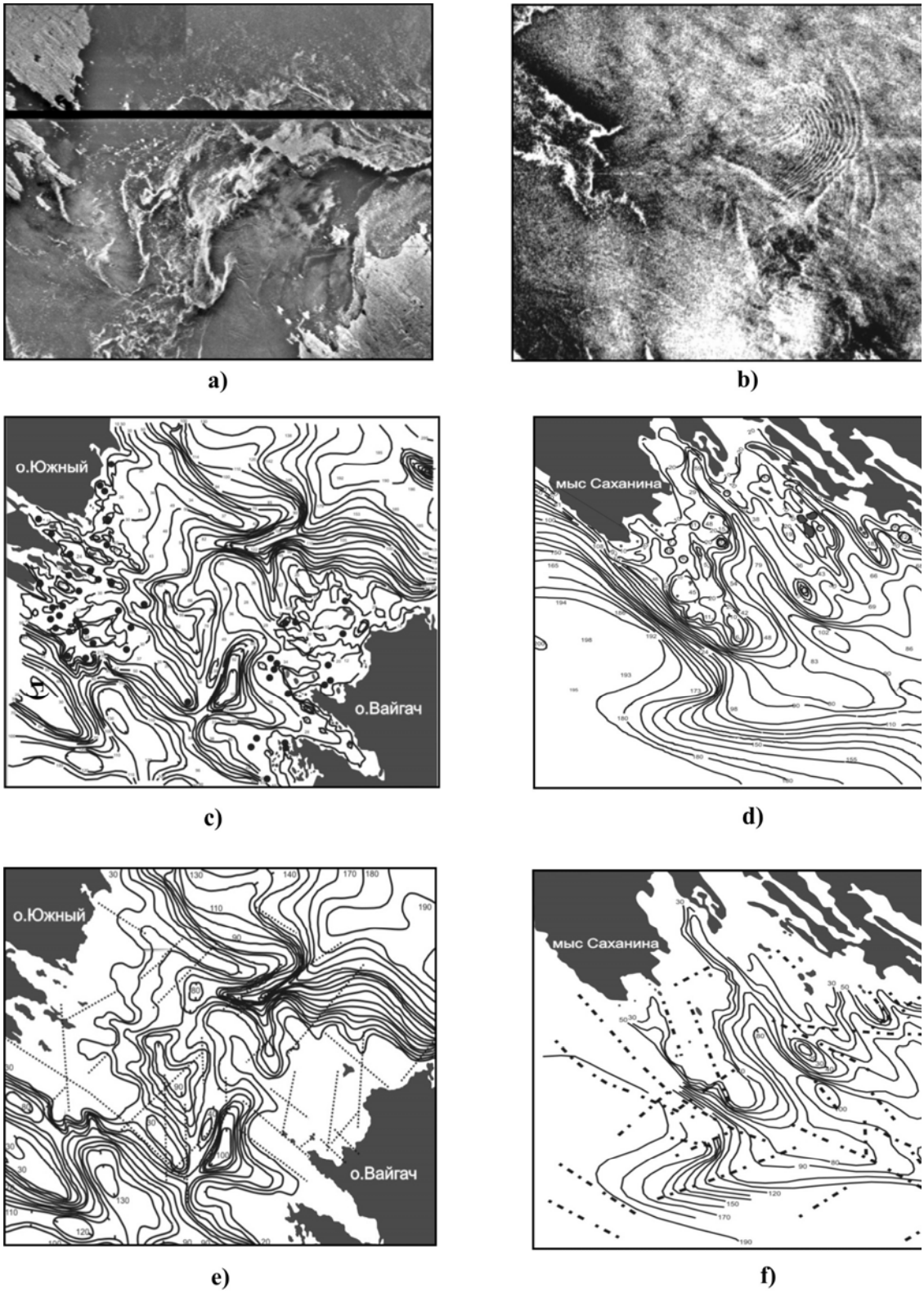

Fig. 30. Remote bottom topography in Kara Strait area with manifestations of bottom topography: a, b - existing bathymetryc maps; c, d - space radar maps; e, f - revised bathymetric maps. Solid lines - isobaths with 10 m step; dashed line - lineaments

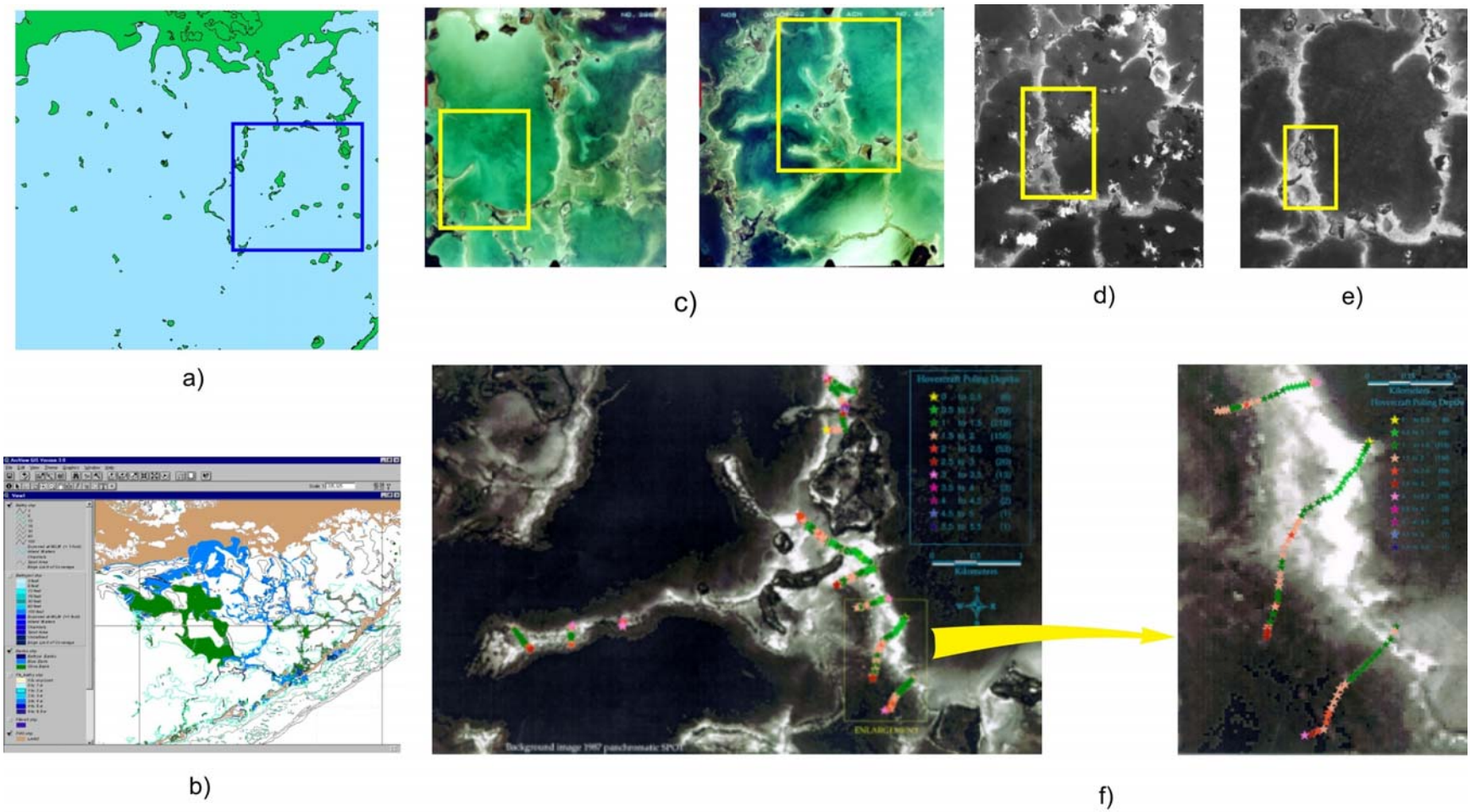

Fig. 31. Remote bottom topography of Florida Bay: a, b - maps of the area; c - aerial photography; d - image acquired by KFA-1000 hardware; e - image acquired by KVR-1000 hardware; f - image from SPOT satellite and enlarge fragment with marked pathways and results for sonar depth measurements

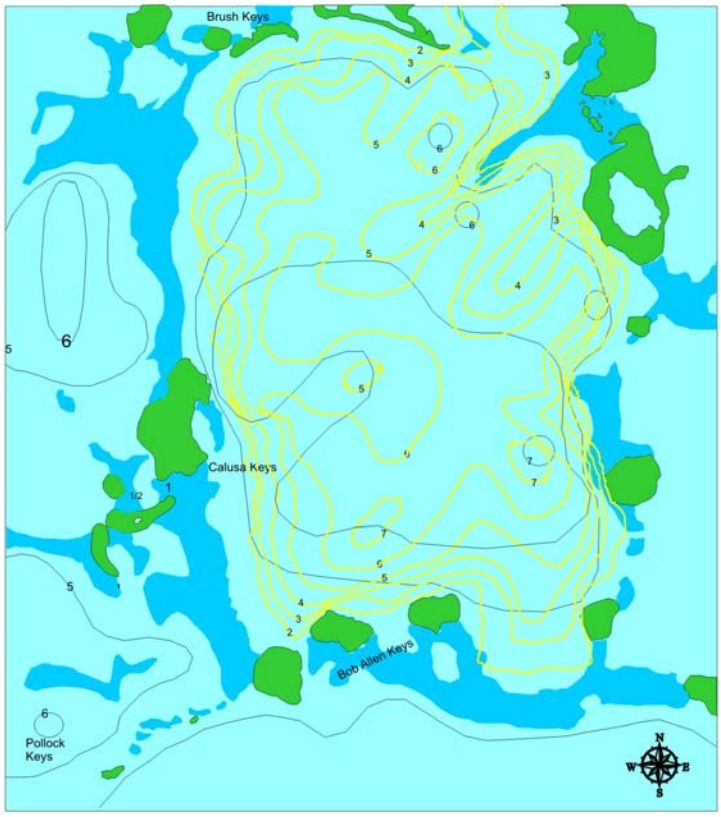

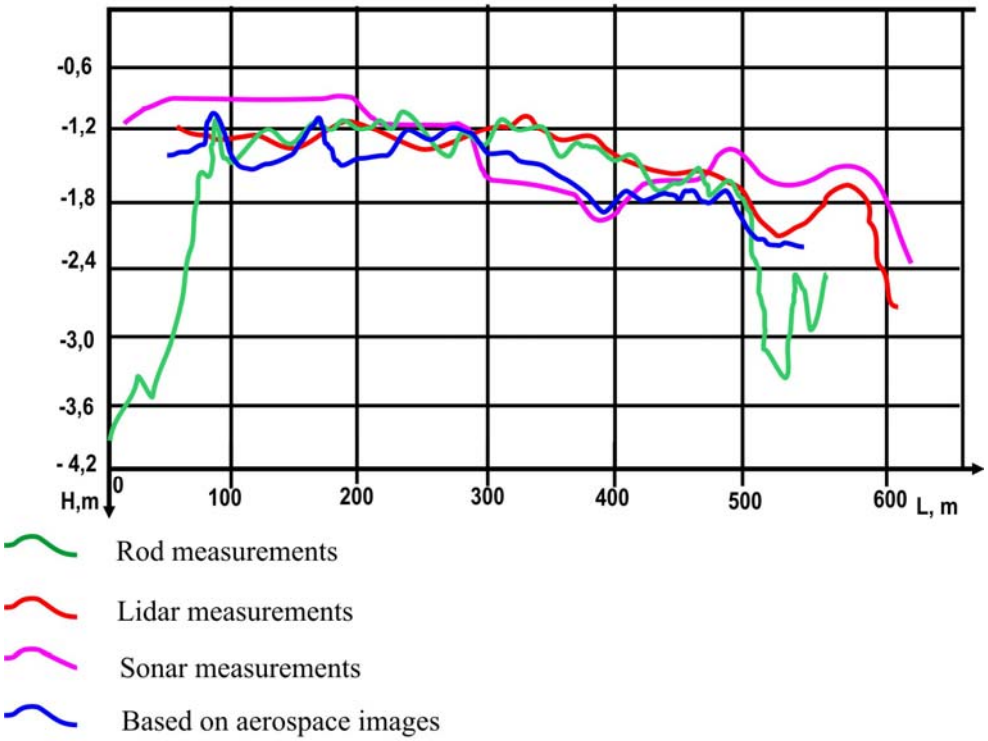

Fig. 32. Specifying Florida Bay bathymetry using optical images (a). Comparison of results obtained using different methods (b)

Routes of measurement (600m) using helicopter-based lidar system SHOALS, sonar (installed on a boat), and a measuring rod, are shown on part of an image for the SPOT satellite (Fig. 31f).

Depth profiles, received using various methods, are shown on Fig. 32b.

Analysis of error in depth measurements (relative to contact measurements) have shown that for the remote method, based on the use of aerospace images, the mean root-mean-square error was 0.14m, and for the lidar method such error was 0.16m.

The results of comparing bathymetric data acquired by various alternative methods have confirmed the accuracy of these aerospace methods.

APPLICATION OF MODELING METHODS

In recent years, modeling methods for various ocean processes have seen substantial development. At the same time, numerous experiments have been carried out and the results have been compared with the prediction of these various models. Substantial results were received, for example, from modeling the climatic characteristics of the global ocean and its regions, as well as current dynamics and water circulation in various seas [Ibraev, Sarkisian, 2001; Dianski et al., 2002; Marchuk et al., 1984; Sarkisian, 2003; Sarkisian, Zunderman, 1995; DYNAMO, 1997; Ezer, Mellor, 1994; Levitus, 1994; Paiva et al., 1999; Smith et al., 2000].

For modeling, we use a whole system of nonlinear, nonstationary equations describing the thermohydrodynamics of the ocean on the spherical earth, developed by Academician G.I. Marchuk and his students [Dianski et al., 2002; Marchuk et al., 1984; Sarkisian, 2003]. The effectiveness of the developed models increases strongly with the usage of aerospace data.

There is continuing interest in modeling fields of electromagnetic signals from the surface of the ocean which are registered by space platforms.. Such methods provide systematic accumulation of data about various processes and phenomena taking place in the ocean, across a wide range of monitoring conditions, and allow us to conduct synthesis of sea surface images in various spectral ranges (using the phase spectrum method) in case of limited *a priori* data or its total absence.

The methodology of such modeling, and the results obtained, are described in detail in the following works: [Bondur, 1991; 1995; 2000; 2001; Bondur, Savin, 1995; 2000; Bondur, et. Al, 2003].

Recently, more attention has been paid to developing modeling methods allowing the evaluation of anthropogenic influence on sea ecosystems. [Beliaev, Konduforova, 1990; Bondur, 1993; 1995; 2001; Bondur, Grebenuk, 2001; Vinogradov, 1998; Vladimirov et al., 1991; Oceanology, 1977; Bondur, 1995]. In solving this problem, the modeling of a specific ecology is based primarily on a system approach, in which the relationships between phenomena have primary meaning and the phenomena themselves secondary meaning [Beliaev, Konduforova, 1990; Bondur, 1991; 1993; 1995; Bondur, 1995]. Ecological systems of sea water environments, like all ecological systems, pertain to the class of “complex” systems [Beliaev, Konduforova, 1990; Bondur, 1993; Bondur, Grebenuk, 2001].

During their modeling we must note, that when the changes taking place in the environment are slow, then we can limit their description to unchanging statistical representations. Forecasting the consequences of relatively fast-moving processes cannot utilize statistical representations, and a shift to a dynamic representation with involvement of evolutionary models is required. In this case, the characteristics of the environment can be studied either by separate components or parameters, or by conceptual models of the ecosystem [Beliaev, Konduforova, 1990; Bondur, 1993; 1995; Bondur, 1995].

Mathematical models of any complex system, which can be used for modeling the ecosystems of sea environments, are separated into three primary types – empirical, theoretical, and semi-empirical [Beliaev, Konduforova, 1990; Bondur, 1993; Bondur, 1995].

Empirical models – these are a set of mathematical expressions approximating experimental data on system state parameters and influencing factors. For such models, there is no need for any conceptual understanding of the development or internal relationships in the system.

Theoretical models – theoretical models of a system are built based on the synthesis of common conceptions about individual components of their processes and phenomena, based on fundamental laws describing the interactions of mass and energy. Such models for ecosystems are built on the basis of common *a priori* assumptions about the structure and relationships between the components and their elements.

In additional to theoretical and empirical approaches, ecosystems can also be modeled using semi-empirical models [Beliaev, Konduforova, 1990; Bondur, 1993; Bondur, Grebenuk, 2001].

The transfer of mass and energy takes place continually through any ecological system. During this time, elements of the system take part in some processes repeatedly, creating closed cycles. As a result, for modeling of ecosystems, the creation of straightforward linear mathematical models (representing every aspect of the studied system) is extremely difficult. It requires the use of large-scale models with huge amounts of mathematical relationships and variables. Because of the massive size of these models, analytical study becomes unacceptable, and problems of identifying informational parameters and adequacy testing become very difficult [Bondur, 1991; 2000; Bondur, Savin, 1995]. Therefore, during development of models for ecosystems, especially ecosystems of coastal waters, it is effective to use a system of partial models, reflecting particular aspects of the studied process [Bondur, 1991; 1993; 2000].

The goal of modeling in our case is the creation of universal, space-time models for sea water ecosystems under conditions of anthropogenic pressure. For creating such models, it is necessary to identify groups of parameters characterizing their condition, structure, relationships and processes taking place in the studied ecosystem. The set of these parameters can be separated into the following main groups:

initial, which includes parameters affecting the input of the system and limitations imposed during the modeling process;

ouput, reflecting real characteristics of the studied phenomena;

condition parameters, determining the internal structure of the ecosystem and the dynamics of its function;

controlling parameters, causing direct affect on the studied process;

perturbing parameters, varying randomly with time, and influencing the system in such a way as to disturb the functional relationship between input and output.

A simplified block diagram of the sea water ecosystem model is shown on Fig. 33 [Bondur, 1993; 1995; 2001].

To the group of initial conditions, (initial state) we can assign partial models, describing the conditions of the primary components of the ecosystem and processes taking place inside it. Foremost, to them we can assign:

climatic model of the region;

a model of the source of anthropogenic influence, describing the conditions of discharge, distance from shore, seafloor and main natural currents; variations in size and frequency of discharges, and other characteristics;

hydrothermodynamic model;

hydrodynamic models of anthropogenic influence on the water environment;

models of contaminant diffusion;

experimental data, received during field tests, generally using aerospace methods;

Limitations, imposed in the process of modeling, are ecological standards determining a system of norms, rules, and requirements necessary for carrying out activities in certain areas.

Within the list of limiting parameters, we can include the system of environmental conservation activities, determined to provide the most effective regime for ecosystem existence. Based on their designation, they can be separated into [Bondur, 1993; Vladimirov et al., 1991]:

social, taking into account work with environmental protection Agencies, preparation of educational programs with ecological focus, preparation of specialists in the areas of ecology and rational use of nature, various work with the public, and others;

legislative, providing legislative acts dealing with the natural environment -use in the coastal area, limitations on harvesting of seafood, regulation of tanker traffic, stimulation of environmental protection activity, creation of protected sea areas, etc;

technical solutions, to which we can assign creation of decontaminating devices, and development of new technologies for decontamination, regulation of outfalls, regeneration of coastal vegetation, etc.

The parameters of the ecosystem condition under anthropogenic influence can be models of the ecosystem's main components, including the hydrobiological block (characteristics of biota), hydrochemical block (contents of nitrates, phosphates, suspended and dissolved organic compounds), a biogenic component block (characteristics of water mass, seafloor soil, near-water air layer), and pollutant field calculation block. These models are derived as a result of calculating the parameters of partial models entering the input of the system [Bondur, 1993; 1995; 2000; 2001; Bondur, Grebenuk, 2001; Bondur, Savin, 1995; 2000; Zurbas, 1977; Marchuk et al., 1984; Ozmidov, 1986; Sarkisian, 2003; Sarkisian, Zunderman, 1995] (see Fig. 25). The conversion mechanism is realized using a model taking into account the effects of conditions. Based on the analysis of the composition of living and nonliving components in the studied ecosystem, amounts and types of pollutants, their variability in time and space, as well as ecological norms accepted for the region, an ecological risk model was derived.

The output parameters of the model include the results of calculations, describing space-time variations of biotic ecosystem components and pollutants (chemical compounds, suspensions, and biological pollution), numerical estimations of ecological risk, as well as optical and acoustical fields, characteristics of biological process, etc. (see Fig. 33). These parameters can be represented in the form of thematic layers of a geoinformation system (GIS).

Using the proposed systems approach towards modeling coastal water ecosystems makes possible targeted accumulation of experimental and theoretical data on significant parameters of the regional model, as well as scientifically based optimization of software and technical tools for analyzing information, received from monitoring of various phenomena related with anthropogenic effects on coastal waters.

For evaluation of various anthropogenic influences on oceans and seas, we have developed mathematical models for the transfer of pollutants in the water environment and on the surface. The developed models allow forecasting of pollutant propagation under the influence of various factors (wind, current, diffusion, etc.) over fairly long periods of time. These models also allow us to assess the location and concentration of polluting substances, to analyze possible scenarios for development of these processes under variation of hydrometeorological conditions, to evaluate the consequences of pollution influence on the ecological condition of the environment, and to develop recommendations for their elimination.

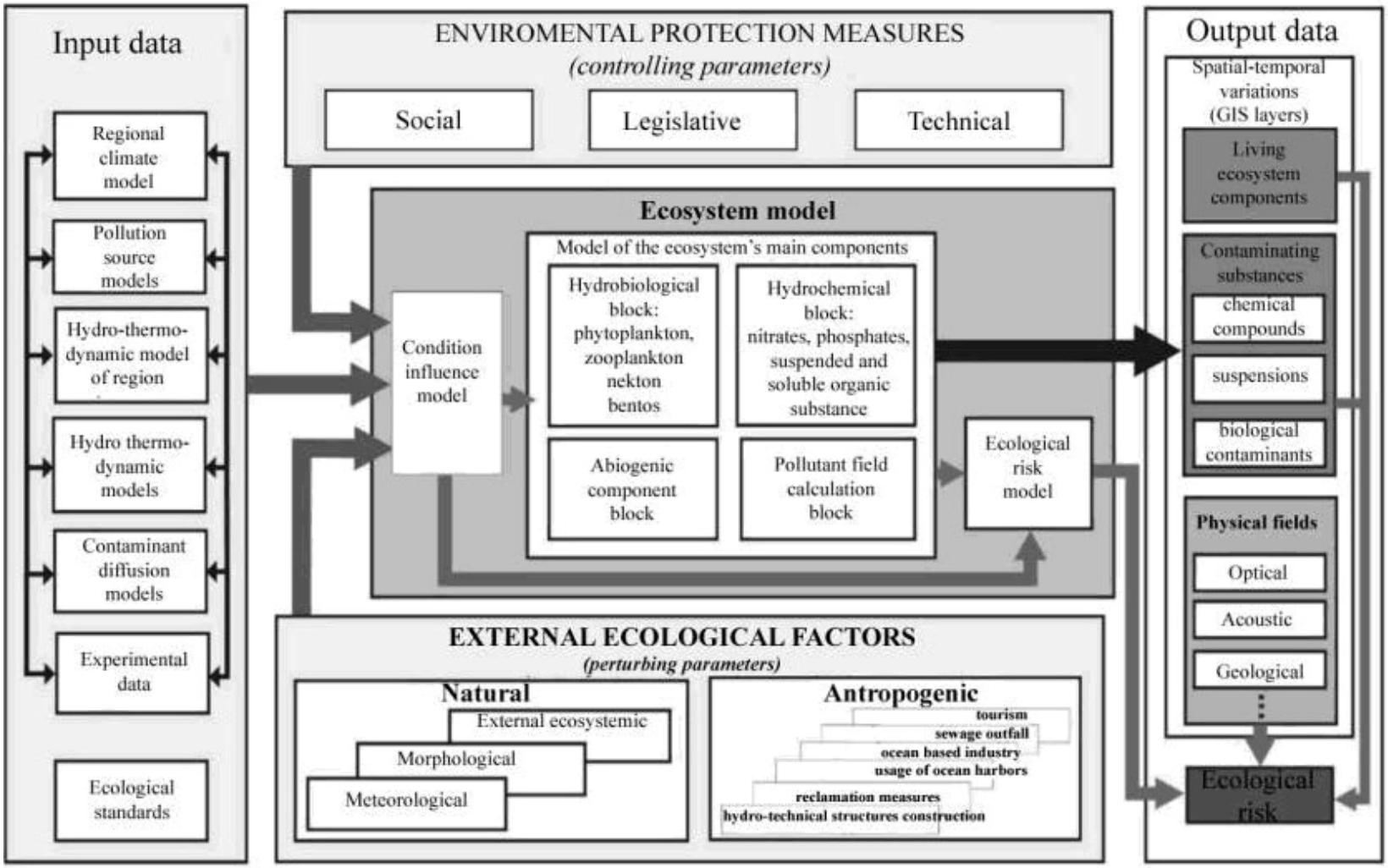

Fig 33. Block diagram for anthropogenic influence on marine ecosystems

ORGANIZATION OF SEA AND OCEAN MONITORING

To organize sea and ocean monitoring, we can propose a complex system, the structure of which is shown on Fig. 34 [Bondur, 1993; 1995; Bondur, Savin, 2000]. The system, as defined, includes various sources of information (aerospace assets, surface ships, buoy stations, submersible monitors, and underwater hydroacoustical systems), regional information-analytical centers for reception and analysis of data (RIAC), and the informational-analytical center of the system (IAC). For communication of information within the system, narrowband and wideband space and surface communication channels will be used.

To gather information, we propose using space and aerial means, as well as sensors installed on ships and autonomous buoy stations. Hydroacoustical systems are another attractive means.

Fig. 34 shows, as an example of aerospace means, radar sensors, including equipment for Multifrequency Radio Wave Topography, optical-electronic means, equipment for remote spatial frequency spectrometry as well as hyperspectral, infrared, and UHF radiometric thermal imaging tools installed on various spacecraft, airplanes and helicopters. On aircraft and helicopters as well as on ships, it is effective to install radars for registration of a wide spectrum of water environment parameters.

The proposed scheme of this complex system has been approbated during conduction of monitoring in various water environment near the territory of Russia (water environments of the Black, Baltic, and Barents seas, zones of the pacific ocean coastline of Russia) as well as during realization of international Russian-American projects for monitoring of Florida bay, and the waters around the Hawaiian and South Californian coastlines [Bondur, 1993; 1995; 1995; 2000; 2001; Bondur, Voliak, 1984; Bondur, Grebenuk, 2001; Bondur, Savin, 2000; Bondur, 1995].

CONCLUSION

In this work, we have described the unique characteristics of aerospace methods, technologies and systems, as well as the main directions of their application in modern oceanology. We have analyzed the physical premises for registering various types of informative parameters for the water environment, which makes possible study and monitoring of a wide spectrum of processes and phenomena in the oceans and seas. These processes manifest themselves as variations in fields of reflected, scattered, and radiated electromagnetic waves, detected and recorded by aerospace sensors in various spectral ranges.

We have described in detail the physical bases and implementation of new ocean sensing methods, first of all methods such as remote spatial frequency spectrometry and Multifrequency Radio Wave Tomography. In addition, we have discussed various multispectral, lidar, thermal, altimetry methods and a method using noncoherent impulse sensing. These methods are extremely effective for studying the fine structure of surface waves, and their change under the influence of various deep

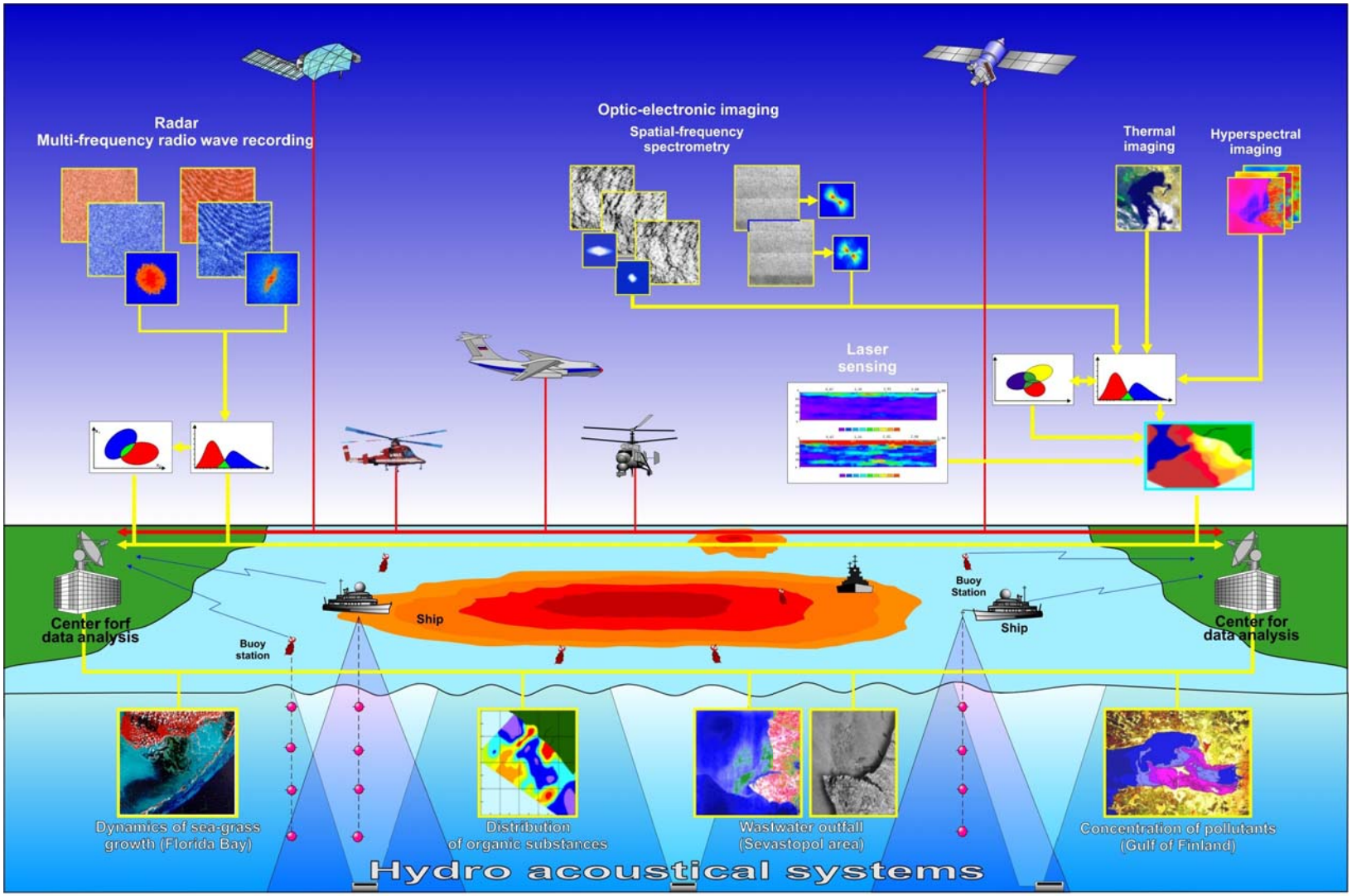

Fig. 34. Complex system for sea and ocean monitoring

processes. This capability can then be used to study the physical processes of the ocean depths through their manifestation in the surface/near surface layer.

Examples are given describing the use of remote spatial frequency spectrometry for reconstruction of surface waving spectra, determination of the character of wave processes, identification of areas subject to the influence of internal waves and various anthropogenic factors, remote identification of near-surface wind speed, and revised mapping of bottom topography.

Results have been presented which describe the discovery of such new effects as the generation of quasi-coherent spectral harmonics in areas of interaction with surface waves with high frequency internal waves caused by deep outfalls, as well as smoothing of high frequency surface waving components due to attenuation in areas containing internal waves and various pollutions.

Statistically defined parameter values have been received for power approximations of spatial spectra $S \sim R^{-P}$ for surface waves, as well as for slick fields, caused by the influence of internal waves at various wind speeds (W_b=1,5…8 m/s), taking on values from 2 to 3.5. Statistical characteristics have also been received for spectral contrasts between the normal ambient surface and internal waves, the maximum values of which reach 20 dB.

Based on the analysis of the unique characteristics of radar signal formation from perturbed ocean surface, we have developed principles of multifrequency, multibeam sensing, on various wavelengths (more than 2), in multiple directions (2 - 3) and under different angles, allowing the reconstruction of surface wave spectra as well as identification of the presence of surface currents using spectral and Doppler methods.

Using the developed methods and technologies of space information analysis, we have conducted processing of space radar images for identification of various pollutions in coastal waters of the Black Sea near the city of Sevastopol, and the in the waters surrounding Oahu Island (Hawaii).

We have demonstrated the effectiveness of multispectral, thermal, and altimetry methods for analysis of global and regional distributions of color characteristics, primary productivity, chlorophyll concentrations, surface temperature, and ocean levels, based on data from the space sensors SeaWiFS, MODIS, NOA's (AVHRR), and TOPEX/POSEIDON. Examples have been shown describing the application of proposed methods and technologies for processing multispectral images towards identifying areas of propagation for various pollutions, as well as anthropogenic effects related with deep outfalls, based on space data received in the waters of the Black Sea and Hawaiian islands.

We have described the application of active optical methods, based on the use of lidar and equipment for noncoherent impulse sensing, towards assessment of chlorophyll distributions, fluorescence parameters, and monitoring of zones with elevated turbidity (caused by pollution of deep ocean water layers), using the developed method of local back scattering gradient extrema. Also, studies of statistical characteristics of perturbed ocean surface can be carried out.

We have introduced methods for coastal bottom topography, based on the use of radar and optical images, and shown examples of their application to mapping the bottom topography. By measuring and imaging surface effects the water environment around the Karski Vorota straight and Florida Bay were mapped. The accuracy of the methods was confirmed by comparing its data with contact, lidar, and sonar measurements.

We have described approaches towards modeling various hydrodynamic processes in the ocean and fields of electromagnetic radiation at input into aerospace equipment, as well as towards complex modeling of anthropogenic effects on ecosystems of water environments. These approaches are based on the use of remote sensing data.

We have proposed a complex system for monitoring the waters of oceans and seas, based on the use of various aerospace means, ship-based equipment, buoy stations, and hydroacoustical systems, as well as modern methods of communication, and software methods for processing and

interpretation of data, which have been applied towards the monitoring of waters in Russian seas, the Florida Gulf, the Hawaiian islands, and the South California coastline.

Our analysis shows that the current level of development of aerospace remote sensing methods taking into account the perspectives for their development, introduces broad new capabilities for conduction of large-scale studies and monitoring for solving many problems, particularly in view of newer developments and additional improvements becoming available. These include issues related to the study of global ocean environments, the study of current fields and circulatory movements of various scales, the study of interactions between the ocean and atmosphere and their effects on the earth's climate, the study of geological structure and natural resources in oceans and seas, estimation of their biological productivity and their contribution into the planet's carbon dioxide cycle, as well as identification and analysis of the consequences of anthropogenic effects on water environments.

The unquestionable advantages of aerospace methods, and their rapid development in the last decades towards substantially increased quantity and trustworthiness of significant registered water environment parameters, as well as increased dynamics and detail, and the development of methods for processing and interpretation of the received data, all testify to the fact their contribution to solving the problems of modern Oceanology in the near future will be very significant.

REFERENCES

Avanesova G.G., Voliak K.I., Shugan I.V. Measurement of wave characteristics using side-looking radar. Theory and experiments. Research on hydrophysics // Proceedings of Physical Institute, USSR Academy of Sciences, Vol.156, M.: Nauka, 1984, pp. 94-123.

Ibulatov N.A. Ecological remnants of the cold war in the seas of the Russian arctic M.: GEOS, 2000, 307 p.

Alpers V., Bruning K., Vilde A., Etkin V.S. et al., Imaging of sea surface waving using synthetic aperture radar (comparative analysis of data from "Almaz-1" and ERS-1). // Research of Earth from Space. 1994, №6, pp. 83-95.

Anthropogenic changes in climate. *Eds*. Budiko M.I. and Israel Yu.A., L.: Gidrometeoizdat, 1987, 406 p.

Aruzmov G.P., Bondur V.G. et al., Spatial spectral analysis of radar and photographic images of the sea surface in the presence of oil pollution. Reprint materials, Institute of Space Research USSR Academy of Sciences, Abstract 616, 1981, 19 p.

Baranovski V.D., Bondur V.G., Kulakov V.V., Malinnikov V.A., Murinin A.B. Calibration of remote measurements of two dimensional spatial spectra of waving using optical images //Research of Earth from Space, 1992, № 2, pp. 59-67.

Basovich A.Ya., Bahnov V.V., Talanov V.I. Transformation of wind waving spectra by short wave trains of internal waving // Izvestia USSR Academy of Sciences Series of Physics of atmosphere and ocean, 1987, Vol. 23, №7, pp. 694-706.

Bass F.T., Fuks M.M. Dispersion of waves on statistically uneven surface. M.: Nauka, 1972, 436 p.

Belchanski G.I., Alpitski I.V. Comparative analysis of algorithms for evaluating the parameters of sea ice using on satellite data from "Ocean-01" based on models of linear mixtures and neutron networks // Research of Earth from Space, 2000, № 4, pp. 40-54.

Beliaev V.I., Kisimovski L.I., Pluta V.E., Stepanin E.A. Small-dimensional high speed spectrometer MCC-211. Applied Spectroscopy. 1978, Vol.29, №6, pp. 1070-1073.

Beliaev V.I., Konduforova N.V. Mathematical modeling of coastal ecological systems. Kiev, Naukova Dumka, 1990, 242 p.

Bondur V.G. Methods of modeling radiation fields at input into aerospace remote sensing systems // Research of Earth from Space, 2000, №5, pp. 16-27.

Bondur V.G. Models of radiation fields for remote sensing systems. Lectures. Moscow State University of Geodesy and Cartography. Moscow. 1991, 389 p.

Bondur V.G. Modeling of two dimensional random brightness fields at input into aerospace equipment using the phase spectrum method // Research of Earth from Space, 2000, № 5, pp. 28-44.

Bondur V.G. Monitoring of the environment. Lectures. Moscow State University of Geodesy and Cartography, Moscow, 1993, 426 p.

Bondur V.G. Operative remote evaluation of the conditions of the ocean-atmosphere boundary from the spatial spectra of images // In: "Optical-meteorological research of the earth's atmosphere". Novosibirsk, Nauka, 1987, pp. 17-30.

Bondur V.G. Operative remote spatial-frequency spectrometry of the ocean surface. Proceeding of 6th National School-Seminar on Data Processing, Frunze, 1986.

Bondur V.G. Principles for development of a space-based earth monitoring system for ecological and natural resource aims // Bulletin of Universities. Series: Geodesy and Aerophotoimaging, 1995, № 1-2, pp. 14-38.

Bondur V.G. Problems in aerospace monitoring of the ocean. In: Research in the area of Oceanology, atmospheric physics, geography, ecology, water problems and geocryology. M.: GEOS, 2001, pp. 87-94.

Bondur V.G., Arzenenko N.I., Linnik V.N., Titova I.L. Modeling of multispectral aerospace images of dynamic brightness fields // Research of Earth from Space, 2003, № 2, pp. 3-17.

Bondur V.G., Borisov B.D. et al., Brightness field of the sea surface during artificial impulse illumination // Transfer of images in the earth's atmosphere. Tomsk Branch of Siberian Division, USSR Academy of Sciences, Tomsk, 1988, pp. 42-45.

Bondur V.G., Vlasenko V.A., Krilov V.M. Coding of images in sub-perceptual space // Issues of Radioelectronics, 1990, Vol. 13, pp. 17-28.

Bondur V.G., Vlasenko V.A., Krilov V.M. Initial processing of images in sub-perceptual space // Issues of Radioelectronics, 1990, Vol. 12, pp. 43-54.

Bondur V.G., Voliak K.I. Optical spatial spectral analysis of sea surface images. Research in Hydrophysics //Physical Institute, USSR Academy of Sciences. M.: Nauka, 1984, pp. 63-78.

Bondur V.G., Grebenuk Yu.V. Aerospace methods of bottom topography in coastal zones of oceans and seas. // Research of Earth from Space, 2000, №6, pp. 59-73.

Bondur V.G., Grebenuk Yu.V. Remote indication of anthropogenic effects on the sea environment, caused by deep outfalls: modeling and experiments // Research of Earth from Space, 2001, № 6, pp. 49-67.

Bondur V.G., Zubkov E.V. Lidar methods for remote sensing of the oceans upper layer // "Optics of atmosphere and ocean", 14, №2, 2001, pp. 142-143.

Bondur V.G., Kulakov V.V., Lobzenkova N.P. Algorithms for classifications of image spatial spectra in optical-digital processing systems // Proceedings of the 6th all union seminar school on optical processing of information. Frunze, 1986, pp.148-152.

Bondur V.G., Kuleshov Yu. P., Savin A.I. System for optical-digital processing of aerospace images with high informative content // Proceeding of VIII National symposium on laser sounding of the atmosphere. Tomsk, 1995, pp. 87-89.

Bondur V.G., Litovchenko D.Ts. Relationships between images of the ocean-atmosphere boundary and spatial characteristics of the foaming activity field. Proceedings of Xth National Symposium on distribution of laser emission in the atmosphere // Tomsk, 1989, 5 p.

Bondur V.G., Litovchenko D.Ts., Starchenkov P.A. Results of research into anthropogenic pollution of coastal waters based on radar space images // Bulletin of Universities. Geodesy and Aero imaging. 1999, № 3, pp. 85-96.

Bondur V.G., Murinin A.B. Recreation of surface waving spectra from image spectra, taking into account nonlinear modulation of the brightness field // Optics of Atmosphere. 1991, Vol.4, № 4, pp. 387-393.

Bondur V.G., Savin A.I. Concepts for creation of an environmental monitoring system for ecological and natural resource aims // Research of Earth from Space. 1992, № 6, pp. 70-78.

Bondur V.G., Savin A.I. Scientific basis for the creation and diversification of global aerospace systems // Optics of Atmosphere and Ocean, №1, 2000, 27 p.

Bondur V.G., Savin A.I. Principles of signal field modeling at input into remote sensing equipment of aerospace environmental monitoring systems // Research of Earth from Space. 1995, № 4, pp. 24-33.

Bondur V.G., Starchenkov P.A. Methods and programs for processing and classification of aerospace images // Bulletin of Universities, Series: Geodesy and Aerophotography, №3, 2001, pp. 118-143.

Bondur V.G., Sharkov E.A. Statistical characteristics of foaming formations on the perturbed sea surface // Oceanology, 1982, Vol. 29, №3, pp.372-379.

Bondur V.G., Sharkov E.A. Statistical characteristics of foaming structures on the sea surface from optical sensing data // Research of Earth from Space, 1986, № 4, pp. 21-31.

Brehovskih L.M. (Ed.) Ocean acoustics. M.: Nauka, 1974, 694 p.

Bulatov M.G. et al., Physical mechanisms for formation of aerospace radar ocean images // Uspekhi Fizicheskikh Nauk, 2003, Vol. 173, № 1, pp. 69-87.

Bukin O.A., Permiakov M.P., Zenkin O.L., Hovanets V.A., Puzankov K.A., Burov D.V., Saluk P.A. Comparative analysis of results from measurements of Chlorophyll "a" concentration received using data from a scanner of sea surface color "SeaWiFS" and using the method of laser induced fluorescence in the Ohotsk Sea // Research of Earth from Space, № 4, 2003, pp. 84-90.

Bunkin A.F., Vlasov D.V., Mirkamilov D.M. Physical basis of aero-sensing of the earth's surface // Tashkent, FAN, 1987, 272 p.

Burenkov B.И., Vedernikov V.I., Ershova P.V. et al., Using data from the satellite ocean color scanner SeaWiFS for evaluating bio-optical characteristics of the Barents Sea // Oceanology, 2001, Vol. 41, № 4, pp. 485-492.

Burenkov V.I., Ershova P.V., Kopelevich O.V. et al., Evaluation of spatial distribution of suspended material in the waters of the Barents Sea using data from ocean color scanner SeaWiFS // Oceanology, 2001, Vol. 41, № 5, pp. 653-659.

Burenkov V.I., Kopelevich, O.V., Sheberstov P.V. Optical monitoring of the biological and ecological condition of the Black Sea // Complex research of the northeastern portion of the Black Sea. Eds. Zatsepin A.G., and Flint M.V., Nauka, 2002, 480 p.

Burenkov V.I., Kopelevich, O.V., Sheberstov P.V., Vedernikov V.I. Ground truth measurements of ocean color, verification of satellite data from color scanner SeaWiFS // Oceanology, 2000, Vol. 40, № 3, pp. 357-362.

Vasilkov A.P., Kondranin T.V., Miasnikov E.V. Determining the profile of the light refraction indicator based on the polarization characteristics of backscattered radiation during impulse sensing of the ocean //Bulletin USSR Academy of Sciences. Physics of Atmosphere and Ocean. 1990, Vol. 26, № 3, pp. 307-312.

Vedenkov V.E., Smirnov G.V., Borisov T.N. Dynamics of surface and internal ship waves. Vladivostok: Dalnauka, 1999, 224 p.

Wind, waves, and ocean ports. *Ed*. Krilov Yu..M., L.: Gidrometeoizdat, 1986, 264 p.

Vinogradov M.E. Research of pelagian biogeocenosis// Nature, 1971, № 4, pp. 35-41.

Vinogradov M.E. The role of the ocean in life and conservation of the earth's biosphere. In: Global ecological problems at the threshold of the 21st century. M.: Nauka, 1998, pp. 99-118.

Vinogradov M.E. (chief Ed.) Modern methods of numerical estimation of sea plankton distribution. M.: Nauka, 1983, 279 p.

Vinogradov M.E. Function of pelagian communities in tropical ocean regions. M.: Nauka, 1971, 272 p.

Viter V.A., Efremov G.A., Ivanov A.I. et al., Spacecraft "Almaz-1" - "Ocean-E" program: Initial results from high resolution radar monitoring of the ocean surface, currents and other phenomena, as well as bottom topography // Research of Earth from Space, 1994, № 1, pp. 54-63.

Vladimirov A.M., Liahin Yu. I., Matveev L.T., Orlov V.G. Protection of the environment // L.: Gidrometeoizdat, 1991, 424 p.

Garbuk P.V., Gershenzon V.E. Space systems for remote sensing. M.: Volumes A and B, 1997, 296 p.

Ginzburg A.I., Kostianoi A.G., Shweremet N.A. Mid-scale variability of the black sea using altimetry data from TOPEX/POSEIDON and ERS-2 // Research of Earth from Space, 2003, № 3, pp. 34-46.

Golitsin G.P. Changes in climate during the 20th and 21st centuries. Physics of the Atmosphere and Ocean, Vol. 22, № 12, 1986, pp. 1235-1252.

*Gramberg I.*P. Comparative geology and mineralogy of the oceans and their continental surroundings for the aim of stable ocean development In: Russian arctic: geological history, mineralogy, and geo-ecology. St. Petersburg, All-union scientific research institute in Oceanology, 2002, pp. 17-34.

*Grankov A.*G., *Milshin A.A.* Usage of many year radiometry data from radiometer SSMI of the DMSP satellite for study of climate parameters of the ocean and atmosphere in the northern Atlantic // Research of Earth from Space, 2001, № 5, pp. 70-78.

Davidan I.N., Lopatuhin L.I., Rozkov V.A. Wind waving the global ocean. L.: Gidrometeoizdat, 1985, 256 p.

Dianski N.A., *Bagno A.V., Zalesni V.B.* // Bulletin Russian Academy of Sciences, ФАО. 2002, Vol.38, № 4, pp. 537-556.

Dynamics of waves on the surface of liquids. *Ed.* K.I.Voliak, Transactions of Institute of Optical Physics, Russian Academy of Sciences, Vol. 56. M.: Nauka. Fizmatlit, 1999, 176 p.

Remote sensing in meteorology, oceanography and hydrology / *Ed*. A.P.Krankell. M.: Mir, 1984, 535 p.

Remote sensing of the earth. Vol. 1. Conditions and near-term perspectives for the advancement of space methods for remote sensing of the earth abroad. St. Petersburg Gidrometeoizdat, 2000, 82 p.

Dolotov Yu.P. Issues of rational use and protection of the coastal areas of the global ocean. Moscow: Nauchni Mir, 1996, 30 p.

Ermakov P.A., Pelinovski E.N., Talipova T.G. Film mechanism for the effect of internal waves on surface ripples. // In.: Effects of large-scale internal waves on the ocean surface *Ed*. Pelinovski E.N., Gorki, Applied Mechanics Institute, USSR Academy of Sciences, 1982, pp. 31-51.

Zidko Yu.M., Kalmikov A.I., Kanevski M.B., Pichugin A.P., Tsimbal V.N. Radar sensing of the ocean// Remote methods of ocean research. Gorkii. Institute of Applied Physics, Russian Academy of Sciences, 1987, pp. 5-53.

Zurbas V.M. Trajectories of turbulent streams of contaminants in stably-stratified medium. // Water resources, 1977, № 4, 165-172.

Zagorodnikov A.A. Radar imaging of sea waving from aerial equipment. L.: Gidrometeoizdat. 1978, 324 p.

Zubkovich P.G. Statistical characteristics of radio signals reflected from the earth's surface. M.: Sovetskoe Radio, 1968, 356 p.

Ibraev P.A., Sarkisian A.P., Truhachev D.I. Seasonal variability in circulation of water in the Caspian sea, reconstructed from average multi-year hydrological data // Bulletin of the academy of science, physics of atmosphere and ocean. 2001, Vol. 37, № 1, pp. 103-111.

Ivanov A.P. Physical basis of hydrooptics. Minsk, Nauka and Technika, 1975, 504 p.

Ivanov V.V. Interpretation of satellite measurements of the variation in sea levels // Research of Earth from Space, 2003, № 3, pp. 85-92.

Changes in climate and their consequences. *Chief Ed.* Menzulin, G.A., St. Petersburg., Nauka, 2002, 272 p.

Israel Yu.A. (Ed.) Works of National conference "Scientific aspects of ecological problems of Russia", Vol.1, 625 p.; Vol.2, 412 p. M.: Nauka, 2002.

Israel Yu.A. Ecology and control of environmental conditions. M.: Gidrometeoizdat, 1984, 560 p.

Israel Yu.A. Tsiban A.V. Anthropogenic ecology of the ocean. L.: Gidrometeoizdat, 1989, 528 p.

Irisov V.G., Trohimovski Yu.G., Etkin V.S. Radiometric diagnostics of the ocean // Remote methods of ocean research. Gorki: Institute of Applied Physics, Russian Academy of Sciences, 1987, pp. 34-58.

Kalmikov A.I., Ostrovski I.E., Fuks I.N., Rosenberg A.D. Scattering of UHF signals by perturbed surface. TIIER, Vol.16, №15, 1968.

Karabishev G.P., Evdoshenko M.A., Sheberstov P.V. Manifestation of vortex dipoles on satellite images of the surface of the Black Sea in the IR and visible ranges// Research of Earth from Space, 2003, № 1, pp. 74-81.

Karaev V.Yu., Balandina G.N. Modified waving spectrum and remote ocean sensing // Research of Earth from Space, 2000, № 5, pp. 45-56.

Kienko Yu.P. Introduction to space-based environmental science and cartography. M.: Cartogeocenter, Geoizdat, 1994, 214 p.

Klishko D.N., Fadeev V.V. Remote determination of the concentration of contaminants in water, using the laser spectroscopy method with calibration based on combination scattering // Reports of USSR Academy of Sciences, 1978, Vol. 238, № 2, p. 320.

Kozoderov V.V., Kosolapov, V.P., Sadovnichi V.A. et al., Space-based earth science: Information-mathematical foundations / Ed. Acad. V.A. Sadovnichi, M.: Moscow State University, 1998, 571 p.

Kozoderov V.V., Sadovnichi V.A. et al., Space-based earth science: Dialogue of nature and society. Stable development / *Ed.* Acad. V.A. Sadovnichi. M.: Moscow State University, 2000. 640 p.

Complex research of the northeast Black Sea. *Eds*. Zatsepin, A. G. and Flint, M.V., M.: Nauka, 2002, 480 p.

Kondratiev K.Ya. Global ecology and requirements for monitoring data, S. Petersburg. Nauka, 1992, 98 p.

Kondratiev K.Ya. Global Climate, L.: Nauka, 1992, 359 p.

*Kondratiev K.*Ya. Research of Earth from Space: Scientific plan for the EOS system // Research of Earth from Space, 2000, № 1, pp. 82-91.

Kondratiev K.Ya., Buznikov A.A., Pokrovski O.N. Atmosphere, Ocean and Space. "Rozeri" program, Global ecology: remote sensing, conclusions of science and technology. VINITI, Moscow, 1992, 240 p.

Kondratiev K.Ya., Krapivin V.F. The carbon cycle and climate // Research of Earth from Space, 2003, № 1, pp. 3-15.

Kopelevich O.V., Burenkov V.I., Ershova P.V., Sheberstov P.V., Evdoshenko M.A., Lukianova E.A. Bio-optical characteristics of Russia's seas based on data from the SeaWiFS scanner. Moscow, Institute of Oceanography, Russian Academy of Science, 2002.

Koptev Yu. N. Remote sensing of the earth. Radiotechnika. 1995, №10, pp. 83-90.

Korver K.P., Elashi Sh., Halbi F.T. Remote sensing from the space in the ultra-high-frequency range. TEEAR, 1979, Vol.73, № 6, pp.30-56.

Korotaev G.K. et al., Dynamics of anticyclones in the black sea from satellite altimetry measurement data // Research of Earth from Space, 2002, № 6, pp. 60-69.

Space imaging of the earth. Satellite optical imaging of the earth with high resolution. M.: EPRGR, 2001, 136 p.

Space methods of geo-ecology / *Ed.* V.I. Kravtsov. M.: Geographical department of Moscow State University, 1998, 108 p.

Kudriavtsev V.N.., Akimov D.B., Iohannessen O.M. Manifestation of mid-scale variability of the ocean in radar images of its surface // Research of Earth from Space, 2003, № 2, pp. 27-46.

Laverov N.P., Vedeshin L.A. Russian-American cooperation in research of the earth from Space // Research of Earth from Space, 2002, № 1, pp. 81-89.

Lazarev A.I., Bondur V.G., Koptev Yu.I., Savin A.I., Sevastianov V.I. Space reveals the secrets of the earth. // S. Petersburg., Gidrometeoizdat, 1993, 240 p.

Lappo P.P. Climate of the earth and ocean (a later chapter in this book; *"New Approaches to Oceanology and Marine Geology"*, A.P. Lisitsin, ed., Nauka, 2003, 648 pp. (in Russian)).

Lappo P. Mid-scale dynamic processes of the ocean evoked by the atmosphere. M.: Nauka, 1979, 181 p.

Lisitsin A.P. Bio differentiation of substances in the ocean and the sedimentary process // Bio differentiation of sedimentary matter in the oceans and seas. Rostov-na-Donu: Rostov State University, 1986, pp. 3-66.

Lisitsin A.P. Geology of the global ocean in the third millennium – achievements and perspectives (in this book).

Lisitsin A.P. Avalanche sedimentation and pauses in the accumulation of sediments in oceans and seas. M.: Nauka, 1988, 309 p.

Lisitsin A.P. Ice sedimentation in the global ocean. M.: Nauka. 1994. 448 p.

Lisitsin A.P. Lithology of lithosphere plates//Geology and Geophysics, 2001, Vol.42. №4, pp. 522-559.

Lisitsin A.P. Marginal filtering of the ocean// Oceanology, 1994, Vol.34, № 5, pp. 735-747.

Lisitsin A.P. Unsolved problems of arctic Oceanology // In: Experience of system oceanological research in the arctic. M.: Nauchni Mir, 2001, pp. 31-74.

Lisitsin A.P. Sediment formation in the ocean. M.: Nauka, 1974, 438 p.

Lisitsin A.P. Primary concepts of ocean bio-geo-chemistry /In: Ocean bio-geo-chemistry Eds. A.P. Monin and A.P. Lisitsin. M.: Nauka, 1983, pp. 9-32.

Lisitsin A.P. Currents of matter and energy in internal and external spheres of the earth. Global changes of the natural environment. Novosibirsk, 2001, pp. 163-248.

Lisitsin A.P. Ocean sedimentation processes. M.: Nauka, 1978, 392 p.

Lisitsin A.P. Processes of terragenic sedimentation in oceans and seas M.: Nauka, 1991, 271 p.

Marchuk G.I., Dimnikov V.P., Zalesni V.B. et al., Mathematical modeling of the overall circulation in the atmosphere and ocean. L.: Gidrometeoizdat, 1984, 320 p.

Marchuk G.I., Kondratiev K.Ya. Priorities of global ecology. M.: Nauka, 1992, 264 p.

Matishov G.G. Anthropogenic destruction of ecosystems in the Barents and Norwegian seas: Kolsk Scientific Center, Russian Academy of Sciences, 1992, 112 p.

Matishov G.G. (chief Ed*.)* Centennial changes of ocean ecosystems in the arctic. Climate, sea glacialization, and bio-productivity. Compilation of the scientific work of Apatiti: 2001, 320 p.

Matishov G.G. (chief Ed.). Patterns in oceanographic and biological processes of the Azov sea. Apatiti: Kolsk Scientific Center, Russian Academy of Sciences, 2000, 434 p.

Matishov G.G.(Ed.) Plankton of western arctic seas. Appatiti, 1997, 352 p.

Matishov D.G., Matishov G.G. Radiational ecological Oceanology. Apatiti: Kolsc Scientific Center, Russian Academy of Sciences, 2001, 417 p.

Mezeris A. Laser remote sensing. M.: Mir, 1987, 552 p.

Melentiev V.V., *Bobilev L.P.* Fourth ERS-"Envisat" – Symposium «View of the earth in a new millennium» (16-20 October, 2000, Geterberg, Sweden): short review // Research of Earth from Space, 2001, № 4, pp. 81-90.

Melentiev V.V., Chernook V.I. Multifrequency radar airplane imaging: new capabilities for diagnostics of ice covering in arctic seas // Research of Earth from Space, 2002, № 6, pp. 49-59.

Methods, procedures, and means of aerospace computer radiotomography in near-surface areas of the earth. Eds. Nesterov P.V., Shamaev A.P., and Shamaeva P.I. M., Nauchni Mir, 1996, 272 p.

Mitnik L.M., Dubina V.A., M.L.Mitnik. Usage of satellite radar with real and synthetic aperture for cartography of wind fields in coastal areas // Research of Earth from Space, 2003, № 2, pp. 47-58.

Mishev D. Remote Research of Earth from Space. M.: Mir, 1985, 232 p.

Moiseenko A.E. Current condition and perspectives for the use of space-based earth remote sensing means for study of natural resources and ecology M.: 1994, 80 p.

Monin A.P. Introduction to climate theory. S. Petersburg.: Gidrometeoizdat, 1992, 246 p.

Monin A.P. Theoretical basis of geophysical hydrodynamics. L.: Gidrometeoizdat, 1988.

Monin A.P., Krasitski V.G. Effects on ocean surface.// L.: Gidrometeoizdat. 1985, 371p.

Moore T., *Bridge G.* Evolution of integral global system of Earth observations // Research of Earth from Space, 2003, № 1, pp. 64-73.

Mur P.K., Fan A.K. Radar determination of wind parameters above the sea // ТИИЭР, 1973, Vol. 67, №11, pp. 40-63.

Neshiba P.P. Oceanology. Modern representation of liquid envelope of the Earth. // M.: Mir, 1991, 414 p.

Ozmidov P.V. Diffusion of impurities in ocean. M: Gidrometeoizdat, 1986, 280 p.

Oceanology. Ocean Biology. Vol.1. Biological structure of ocean. *Ed*. M.E.Vinogradov // M.: Nauka, 1977, 424 p.

Oceanology. Ocean Physics. Vol. 1. Hydrophysics of Ocean. 456 p; Vol.2. Ocean Hydrophysics. 456 p. *Eds*. Kamenkovich V.M. and Monin A.P., M.: Nauka, 1978.

Experience of systematic oceanological research in the arctic. *Eds*. Lisitsin A.P., Vinogradov M.E., Romankevich E.A. M.: Nauchni Mir, 2001, 644 p.

Pozdniakov D.V. et al., Numeric modeling of trans-spectral process (TSP) of light's interaction with the water environment. Effects of TSP on spectral composition of input radiation // Research of Earth from Space, 2000, № 5, pp. 3-15.

Pokazeev K.V., Filatov N.N. Hydrophysics and ecology of lakes. Vol 1. Hydrophysics. M.: Physical department of Moscow State University, 2002.

Problems of chemical contamination of World Ocean. Volumes 1-9 // L.: Gidrometeoizdat, 1985.

Radiolocation of Earth surface from space. *Eds*. Mitnik L.M. and Vinogradov P.V. L.: Gidrometeoizdat, 1990, 200 p.

Raizer V.Yu., Cherni I.V. Microwave diagnostics of ocean surface layer. S. Petersburg., Gidrometeoizdat, 1994, 232 p.

Rozkov V.A. Methods probabilistic analysis of ocean processes, L.: Gidrometeoizdat, 1979, 280 p.

Romankevich E.A., Vetrov A.A. Carbon cycle in the arctic seas of Russia. M.: Nauka, 2001, 302 p.

Savin A.I. Experience in and technologies for creation of global information-control systems // In: "Aerospace information systems", Vol.1, "Technologies for creation and diversification of space systems", Eds. Bondur V.G. and Savin A.I., M.: Nauka, 2000, 486 p.

Savin A.I. Principles of development for space systems of global monitoring // Research of Earth from Space, 1993, № 1, pp. 40-47.

Savinih V.P., Solomatin V.A. Optic-electronic systems for remote sounding of Earth. M.: Nauka, 1995, 349 p.

Sarkisian A.P. Accounting of net-scale turbulent pulsations in modeling of ocean dynamics // Oceanology, 2003, Vol. 388, № 4, pp. 545-548.

*Sarkisian A.*P., Zunderman Yu. // Bulletin of Russian Academy of Sciences, FAO. 1995, Vol. 31. № 3, pp. 427-454.

Satellites of earth radar sensing. *Ed.* Kucheiko A.L., Addition № 1 to the Annual publication «Satellite systems of communications and transmission», 2001, 86 p.

Fedorov K.N. Thin structure of ocean hydrophysical fields. In: Oceanology, Vol.1, M:, Nauka, 1978, pp. 113-147.

Fedorov K.N., Ginzburg A.I. Near-surface layer of the ocean. L.: Gidrometeoizdat, 1988, 304 p.

Filatov N.N. Lake hydrodynamics. С-Пб.: Nauka, 1991, 191 p.

*Hain V.*E. Tektonics of continents and oceans (year 2000). M.: 2001, 606 p.

Shamaev P.I. Multi-frequency computer radio-topography of the ocean // Issues of Radioelectronics, M.: 1994, № 2, pp. 3-12.

Shutko A.M. Super high frequency radiometry of water surface and soils/grounds. M.: Nauka, 1986, 192 p.

Advanced Airborne Hyperspectral Imaging System (AAHIS): an imaging spectrometer for maritime application. Pfeiffer, et al. 2002, See reference 40 in Keeler, 181.

Atlas D., Beal R.C., Browm R.A. et al. Problems and future direction in remote sensing of the ocean and troposphere: a workshop report. - J.Geophys. Res. 1986, Vol. 91, №c2, pp. 2525-2548.

ATSR-2: The evolution in its design from ERS-1 to ERS-2/Stricker N.C. e.a.//ESA Bull. 1995. №83, pp. 32-37.

Baldrige M, Byrne J., McElroy J. NOAA Satellite Programs Briefing / NOAA. January 1984. 203 p. Ocean Color from Space. Ocean Processes Program. NASA Headquarters 600 Independence Avenue. S.W.Washington, D.C. 20546, 1980.

Bidigare R.R., Trees C.C. HPLC phytoplankton pigments: Sampling, laboratory methods and quality assurance procedures. In: Ocean Optics Protocols for Satellite Ocean Color Sensor Validation: Version 2.0. Mueller J., Fargion G. (eds.), NASA Technical Memorandum, 2000.

Bolin B. (Ed.) An assessment of the role of carbon dioxide and of other radioactively active constituents in climate variation and associated impacts/ SCOPE Publ. John Wiley, 1996, №29, 540 p.

Bondur V.G. Conception of the development of the global environmental monitoring system based on dual use and civilian space means. Gore-Chernomyrdin Environmental Working Group Initiative. Proceedings of the Global Environmental Disaster Monitoring Subgroup Meeting. Rosslyn, Virginia, 5-7 December, 1995, 32 p.

Bondur V.G. Techniques and systems of monitoring of anthropogenic impact on coastal ecosystems. Gore-Chernomyrdin Environmental Working Group Initiative. Proceedings of the Global Environmental Disaster Monitoring Subgroup Meeting. Rosslyn, Virginia, 16-17 September, 1995, 24 p.

Bondur V.G., Kulakov V.V., Murinin A.B. Numerical Simulation of Spatial Nonuniform Sea Surface Optical Images // Thesis's of 14-th International Conference on Coherent and Nonlinear Optics, Leningrad, 1991. Vol.3, p. 27.

Bondur V.G., Murinin A.B. Restoration of Surface Wave Spectra from the Spectra of Images with the Account for Nonlinear Modulation of the Brightness Field // Atmospheric optics, 1991, Vol.4, №4, pp. 387-393.

*Crawford W.*R*., Cherniawsky J.Y., Foreman M.G.* Multi-year meanders and eddies in the Alaskan Stream as observed by TOPEX/Poseidon altimeter // Geophys. Res. Letters. 2000. Vol. 27. № 7. pp. 1025-1028.

Ducet N., *Le Traon P.Y.* Global high-resolution mapping of ocean circulation from Topex/Poseidon and ERS-1 and –2 // J. Geophys. Res. 2000. Vol. 105. № C8. pp. 19477-19498.

DYNAMO Group, Dynamics of North Atlantic Models. Ber. Inst. Meereskunde Kiel, 1997. Vol. 294. 333 p.

Elachi C., Brown W.E. Models of radar imaging of the ocean surface waves // IEEE, Trans, Antennas and Propag., 1977, Apr.25, №1, pp. 84-95.

Ers-1/Ers-2. ESA Bulletin-83. 1995, pp. 9-52.

Ezer T., Mellor G.L. // J. Geophys. Res. 1994, Vol.99, pp. 14159-14171.

Gairola R.M., Basu S., Pandey P.C. Eddy Detection over Southern Indian Ocean Using TOPEX/Poseidon altimeter data // Marine Geodesy, 2001, Vol. 24, pp. 107-121.

Indian Earth Remote Sensing Satellites IRS-1C/ID//Int. J. Remote Sensing, 1995. Vol. 16, №3, pp. 791-799.

Iudicone D., Santoleri R., Marullo S., Gerosa P. Sea level variability and surface eddy statistics in the Mediterranean Sea from TOPEX/Poseidon data // J. Geophys. Res. 1998, Vol. 103, № C2, pp. 2995-3011.

Johnson N, Rodvald D. "1993-94 Europe and Asia in Space". Kaman Sciences Corp., 1994.

Keeler R.N. Ulich B.L. Some aspects of wide beam imaging lidar performance. // Society of Photo-Optical Instrumentation Engineers, Vol.2258. Ocean Optics XII, 1997, pp. 480-501.

Levitus S. World Ocean Atlas – CD-ROM. Wash. (D.C.) US Department of Commerce; NOAA; NESDIS; NODC; Ocean Climate Laboratory, 1994.

Lutomirsky, R. F, Lidar remote sensing of ocean waters, SPIE v 2222, 12-19, 1994

Keeler R.N. Ocean Optics – Airborne systems for seeing into the water. // Encyclopedia of Optical Engineering, Marcel Dekker, New York, 2003, pp.1543-

Merrifield M.A. Holloway P.E. Model estimates of M2 internal tide energetic at the Hawaiian Ridge. Journal of Geophysical Research, 2002, Vol. 107, № 10.

MODIS. Moderate Resolution Imaging Spectroradiometer. NASA's Earth Observing System. Goddard Space Flight Center. Greenbelt, Maryland, 20771, USA, NP-2002-1-423GSPC, 2002, 21 p.

National Environmental Satellite, Data, and Information Service, NOAA, 1998, 54 p.

Paiva A.M., Hargrrov J.T., Chassignet E.P., Bleck R. // J. Mar. Syst., 1999, Vol. 21, pp. 307-320.

Remote sensing of environment. Elsevier, 2002. Vol. 83, 362 p.

R.D., Maltrud M.E., Bryan F.O., Hecht M.W. // J. Phys. Oceanogr. 2000. Vol. 30, № 7. pp. 1532-1561.

The special issue on Seasat A // J.Geophys. Res. 1982, Vol.87, № C5.

The special issue on Seasat A // J.Geophys. Res. 1983, Vol.88, № C3.

Viktorov S.V. Regional Satellite Oceanography. Taylor & Francis, UK, London, 1996, 306 p.

Zubkov E.V., Bunkin A.F. Recording vertical structure of optical characteristics of the upper ocean by a method of local gradient extrema of lidar return. // Bulletin of Russian Academy of Sciences (BRAS) /Supplements Physics of Vibrations. 1995, Vol.59, № 3, pp. 165-172.